AN EXPLORATION OF THE VIABILITY OF SPARK PLASMA SINTERING FOR THE COMMERCIAL FABRICATION OF NUCLEAR FUEL PELLETS

By

TIMOTHY IRONMAN

A DISSERTATION PRESENTED TO THE GRADUATE SCHOOL
OF THE UNIVERSITY OF FLORIDA IN PARTIAL FULFILLMENT
OF THE REQUIREMENTS FOR THE DEGREE OF
DOCTOR OF PHILOSOPHY

UNIVERSITY OF FLORIDA

2017

To my friends and family, who expect more out of me then I expect out of myself

ACKNOWLEDGMENTS

I would like to thank my friends and family for their unwavering support. I would like to thank Professor Tulenko for giving me the opportunity and for entrusting me with all the duties and responsibilities of a laboratory manager. The experience has led to immeasurable personal growth. I would like to thank Professor Subhash for all of his assistance and his honest critiques of myself and my work. I would like to thank Professor Lear and Professor Yang for sitting on my committee and having patience with me. I would like to thank all of the members of the Laboratory for the Development of Advanced Nuclear Fuels and Materials for their assistance and support over the past four years. I would like to give a special thanks to Patrick Moo and Jitesh Kuntawala.

TABLE OF CONTENTS

page

ACKNOWLEDGMENTS 4

LIST OF TABLES 7

LIST OF FIGURES 8

ABSTRACT 10

CHAPTER

1 MOTIVATION AND SIGNIFICANCE 11

2 LITERATURE REVIEW 14

2.1 Commercial UO2 Pellet Production 14
2.2 Spark Plasma Sintering 15
2.3 SPS of UO2 19
2.4 Graphite SPS Tooling 21
2.5 Commercial SPS Capabilities 22

3 METHODOLOGY REVIEW 25

3.1 Spark Plasma Sintering 25
3.2 Commercial Pellet Qualification 26
3.3 Pellet Loadability Tester 28
3.4 Laser Profilometer 29

4 FABRICATION OF COMMERCIAL UO2 PELLETS 34

4.1 Introduction 34
4.2 Experimental Procedure 34
4.3 Results and Discussion 36
4.4 Conclusions 39

5 COMPOSITE PELLETS 44

5.1 Introduction 44
5.2 Experimental Procedures 44
5.3 Results and Discussion 47
5.4 Conclusions 50

6 SPS TOOLING 55

6.1 Introduction 55
6.2 Tooling Considerations 56

6.3 Conclusions 67

7 SCALING UP PRODUCTION 77

7.1 Introduction 77
7.2 Experimental Procedures 78
7.3 Results and Discussion 82
7.4 Conclusions 88

8 ATR PELLET PRODUCTION 100

8.1 Introduction 100
8.2 Experimental Procedures 101
8.3 Results and Discussion 103
8.4 Conclusions 105

9 ECONOMIC CONSIDERATIONS 111

9.1 Introduction 111
9.2 Capital Costs 112
9.3 Production Costs 114
9.4 Conclusions 117

10 CONCLUSIONS AND FUTURE WORK 120

REFERENCES 122

BIOGRAPHICAL SKETCH 125

LIST OF TABLES

Table		page
4-1	Dimensions and density of single pellets produced via SPS	43
4-2	Pellet grain size versus position as measured	43
4-3	Dimensions of UO_2 pellets fabricated in two runs	43
4-4	Pellet end geometry measurement statistics	43
5-1	Diamond physical dimensions	52
5-2	SiC physical dimensions	52
5-3	Comparison of dish depth in composite and pure UO2 pellets	54
6-1	Pellet density with varying die outer diameter	69
6-2	Comparison of dish depth in a five pellet run with graphite punches	69
6-3	Comparison of dish depth in a four pellet run with YZX punches	69
6-4	Comparison of dish depth in a three pellet run with B4C punches	69
7-1	Statistics of pellets produced as stacked doubles	90
7-2	Density and dimensions of parallel produced pellets	90
7-3	Pellets produced by combining series and parallel setup	91
7-4	Pellets produced by 19 pellet die	91
8-1	Planned ATR pellet sintering parameters.	106
8-2	ATR Blanket pellet results	107
8-3	ATR Base pellet results	108
8-4	ATR Diamond pellet results	109
8-5	ATR SiC pellet results	110

LIST OF FIGURES

Figure		page
2-1	Example SPS die setup	23
2-2	Diagram showing heating at particle contacts during SPS.	23
2-3	Three stage commercial SPS machine.	24
3-1	An unloaded die with punches.	29
3-2	A loaded die with graphite feltr.	29
3-3	A representative temperature and pressure curve for the SPS process.	30
3-4	A die loaded in the SPS machine.	31
3-5	The pellet load tester.	32
3-6	The Bruker optical profilometer	33
4-1	Sintered UO_2 pellets.	40
4-2	Grain size measurements	41
4-3	Central ring artifact.	42
4-4	Profilometer measurement of the dish geometry	42
5-1	Diamond composite pellet lot.	51
5-2	SiC composite pellet lot.	52
5-3	Graphite on surface of SiC pellet	53
5-4	Diamond pellet showing surface chip	53
5-5	Fracture surface of diamond/UO2 pellet	54
5-6	Dish depth for SiC, diamond and UO2 pellet	54
6-1	Fracture surface of pellet fabricated with Al_2O_3 spray	70
6-2	SEM image showing UO_2 powder inclusions	70
6-3	Images of the punch wear with usage	71
6-4	Comparison of dish depth for graphite tooling	71

6-5 Pellets produced with YZX punch tip 72
6-6 YSZ punch tips after use 73
6-7 Comparison of dish depth using YSZ punches 74
6-8 Comparison of dish depth using B4C punches 74
6-9 Profiles of SPS run of YSZ punch tips vs graphite punch tips 75
6-10 Profiles of SPS run of YSZ punch tips at 1050 C vs 900 C 76
7-1 Schematic showing stacking powder samples in two pellet die 92
7-2 Schematic of the die geometry used to fabricate multiple pellets 92
7-3 Die used to fabricate 19 pellets 93
7-4 Sintering of 19 pellet die 94
7-5 Stacked pellets as fabricated 95
7-6 Temperature profiles for dies fabricating multiple pellets I 95
7-7 Voltage profiles for dies fabricating multiple pellets I 96
7-8 Electrical power profiles for dies fabricating multiple pellets I 96
7-9 Z-axis displacement profiles for dies fabricating multiple pellets I 97
7-10 Temperature profiles for dies fabricating multiple pellets II 97
7-11 Electrical power profiles for dies fabricating multiple pellets II 98
7-12 Voltage profiles for dies fabricating multiple pellets II 98
7-13 Z-axis displacement profiles for dies fabricating multiple pellets II 99
9-1 Dr. Fuji Dr. Sinter largest standard furnace. 118
9-2 Dr. Fuji Dr. Sinter example tunnel furnace 119

Abstract of Dissertation Presented to the Graduate School
of the University of Florida in Partial Fulfillment of the
Requirements for the Degree of Doctor of Philosophy

AN EXPLORATION OF THE VIABILITY OF SPARK PLASMA SINTERING FOR THE COMMERCIAL FABRICATION OF NUCLEAR FUEL PELLETS

By

Timothy Ironman

December 2017

Chair: James Tulenko
Major: Nuclear Engineering Sciences

The viability of spark plasma sintering (SPS) for fabrication of industrial-grade nuclear fuel pellets is explored by utilizing die designs for single and multiple pellet manufacturing. Traditional UO2 pellets were also manufactured by systematically varying processing temperature and pressure as needed for single- and multi-pellet fabrication. The pellets were then qualified against commercial fuel specifications for density, shape, microstructure and surface flaws. Pellets produced one at a time met all commercial specifications except for grain size. Pellets produced in batches of 2, 4 and 8 pellets showed sub-optimal density indicating that further changes to sintering conditions are warranted. Additionally, commonly used graphite tooling for pellet fabrication was shown to be ineffective in producing large numbers of fuel pellets, as the die and punches were shown to undergo severe wear in each run thus decreasing the reliability of the tooling for production of pellets as per the specification. Finally, additional discussion is provided for identifying the avenues for scale-up of SPS to meet the current commercial demand of 400 million pellets per year. These studies are viewed as a first step towards assessing the ability of SPS technology to meet the quality specifications and quantity demands of the production of nuclear fuel pellets.

CHAPTER 1
MOTIVATION AND SIGNIFICANCE

The primary material for nuclear fuel, worldwide, is uranium oxide (UO_2). Compared to its metal counterpart (Uranium), UO_2 has higher melting point (2865 C vs 1132 C for U), which allows nuclear reactors to run much hotter. UO_2 also is chemically and physically more stable in reactor environments [1]. It has been used and extensively researched for over the 70 year history of commercial nuclear power. However, a key drawback of UO_2 is its low thermal conductivity (3.5 W/mK at 1000 C for UO_2 vs 38.7 W/mK at 1000 C for U). The negative effects of the low thermal conductivity of UO_2 include a large radial temperature gradient (in excess of 500 C° over a radial distance of 4 mm) in the fuel pellets and reduced operating power (reactivity) of the reactor. These temperature gradients create high thermal stresses which cause cracks to develop in the pellets, which further reduce thermal conductivity and increases gaseous fission product diffusion out of the pellet.

Despite six decades of research and practice, there have been no major changes in pellet shape or its processing method [2]. Advances in enhancing either UO_2 thermal conductivity or microstructure and properties using the conventional sintering process are also limited. In recent years, doping UO_2 with chromia (Cr_2O_3) has been shown to increase the grain size of fuel pellets up to 45 microns [3].The increased grain size is expected to provide improved fission gas retention and decreased cracking in the pellet. Efforts to further increase thermal conductivity of UO_2 with 2nd phase particles and dopants have been met with limited success due to the extreme difficulty in sintering these powders in the conventional processing method.

While the conventional sintering method has remained unaltered in the past few decades, in recent years spark plasma sintering (SPS) has emerged as a promising alternate method for processing nuclear fuel pellets into desired shape and dimensions in significantly lower processing times (30-45 min) and at lower sintering temperatures (900 C) [4]. The SPS method also requires a significantly fewer number of steps, time, energy and provides net shaped pellets in a single step. The SPS process has also been shown to be capable of successfully sintering UO2 powders with 2nd phase particles such as diamond, SiC and even carbon nanotubes (CNTs) [5].

SPS has many other benefits over conventional sintering. It can sinter novel materials and hard to sinter materials [3] to a desired density in a significantly reduced processing time. The SPS heating rates allow for reduced sintering times and minimize formation of undesirable chemical by products. There have been numerous instances of SPS being used to produce precise ceramics that may be cost prohibitive to machine to desired shape [3].

SPS has been successfully used by the University of Florida to consolidate commercial UO2 powder into pellet form. Ge et al [4] achieved over 96% theoretical density at a peak temperature of 1050 C for just 0.5 minutes of sintering time. Novel composite materials, with high thermal conductivity, such as UO2-SiC [5], UO2-diamond [6] and UO2-CNT [7] have been successfully fabricated by UF via SPS.

The above studies have unequivocally demonstrated the ability of SPS to fabricate UO2 fuel pellets rapidly and at lower sintering temperatures than conventional methods. However, the method has previously been shown to be effective only for fabricating a single pellet each time, thus questioning the utility of SPS for a scale-up to

multi-pellet batch manufacturing and, eventually, for industrialization of the technique for fabrication of hundreds of millions of pellets per year. Towards this end, this current study intends to explore the following features to determine the viability of commercial SPS manufacturing UO2 pellets.

1. Can the SPS process be used to fabricate commercial grade nuclear pellets with strict dimensional control, pellet density, microstructural homogeneity, and surface quality?

2. Can the SPS process be scaled-up to make multiple pellets in each production run?

3. Are there manufacturing defects in SSP produced pellets and what is the potential rejection rate?

4. What are the tooling failure modes and wear rate? How does tooling affect the pellet surface quality?

5. Can the pellets produced by the SPS process pass a screening test for loading into a cladding for evaluation of their performance in the Advanced Test Reactor?

6. Finally, can SPS be used to fabricate commercial scale pellet quantities at equal or cheaper cost than the conventional sintering process?

It is vital to seek answers to these questions before one can make sound judgments about the feasibility of SPS for scale-up fabrication and its potential for industrialization.

CHAPTER 2
LITERATURE REVIEW

2.1 Commercial UO2 Pellet Production

Commercial UO2 pellet production can be broken up into three parts: the production of UO2 powder from the UF6 feedstock, the fabrication of dense pellets from UO2 powder and the production of the metal assembly framework along with loading the pellets into the assembly framework [8]. The only aspect that concerns this process is step two, the fabrication of dense pellets from UO2 powder. After the raw UO2 powder is produced, the powder is conditioned. Conditioning involves blending powders together to ensure the required particle size distribution and specific surface area. U3O8 may be added to reduce the required sintering temperature and improve the sinterability of the powder overall. Additionally pore formers, lubricants and burnable poisons may be added in the powder conditioning stage.

The powder is then placed in a metallic die and pressed with hundreds of MPa into 50-60% dense green pellets. The pressing of pellets is done individually in high speed pressing machines. The axial edges of the green pellets are produced with a desired end geometry through the use of a machined punch tip, which is made of a highly wear resistant material. The green pellet is then removed from the die and placed in large trays and sent to the sintering furnaces. The furnaces heat the green pellets to temperatures in excess of 1750 C to densify the pellet from 50-60% dense to above 95% dense. The heating process requires in excess of 15 hours [9].

The fully dense pellet is not yet in the engineered shape. The sintering process deforms the pellets, so they are not perfectly cylindrical. The pellet are centerless grounded into the desired shape. This process also produces a very smooth outer pellet

surface along with a carefully controlled outer diameter. The UO2 ground off is then recycled back to the beginning of the process. Typical throughput for a commercial facility is 45000 pellets per hour. A representative sample size is removed from the line and tested for quality every hour.

2.2 Spark Plasma Sintering

Spark Plasma Sintering Spark Plasma Sintering (SPS) is a field-assisted sintering technique. SPS uses a low voltage, pulsed DC current and an applied pressure to activate sintering mechanisms for material synthesis. SPS is capable of synthesizing new materials, difficult to sinter materials and conventional materials all at a faster rate [10]. SPS also allows for sintering near net shape components. SPS is similar to hot-pressing, in that heat is applied and a pressure assists sintering. The major differences are the method of heating, Joule Heating, and the current activates other sintering mechanisms in conducting and semi-conducting samples.

The most common SPS setup uses a graphite die, a pair of graphite punches, graphite foil separating the powder sample for the die and graphite felt exterior to the die as a thermal insulator. An example is shown in Figure 2-1 below. Due to using the pulsed current, extremely high heating rates (>1000C/min) can be used.

This offers numerous advantages including both material advantages and economic advantages. The process begins by loading the die compact. The compact is placed in a furnace and set between two conducting steel rams. The rams apply the force to compress the powder and pressurize the powder, along with ensuring electrical contact. A pulsed DC current is run through the compact leading to Joule heating which quickly heats the sample and die. Depending on the conductivity of the powder sample and the specific tooling used, the current can be driven through the sample or the die

allowing for process control. When using purely insulating materials, such as Al2O3, the technique is comparable to hot pressing with high heating rates. The SPS technique dates all the way to 1906 with a patent for a current assisted sintering arrangement [11]. The process matured slowly until the 1960s when Inoue designed the modern form of SPS [11]. The maturation of the technology stalled while Inoue's patents were intact, but after they expired the technology was spread worldwide. Currently there are three major producers of SPS machines for research and commercial needs. These are Fuji Electronic Industrial Co., Ltd in Japan, FCT Systeme GmbH in Germany and Thermal Technology LLC, INC in the United States. The commercialization of SPS machines has led to a worldwide increase in patents and academic literature. The technology has exploded with over 400 patents between 2000 and 2008 compared to under 80 before 1990.

The exact mechanisms involved in SPS are still under discussion [12]. Many of the recent works have treated SPS as a black box. Researchers tend to just report mechanical properties and microstructure of various materials sintered without concrete mechanistic explanations [13-22]. SPS does feature three classes of effects: mechanical, thermal and electrical effects [23]. These effects work in tandem and are not truly separable. The mechanical effects originate from the compressive force applied by the furnace rams. This effect increases the contact between powder particles and modifies the morphology of particle contact areas. The applied pressure enhances conventional sintering mechanisms while activating other mechanisms. Plastic deformation allows for increased densification at high temperatures and densities. Typical pressures are limited to 80 -150 MPa due to the strength of the graphite tooling;

however, alternative tooling including Tungsten Carbide and Silicon Carbide have allowed for pressure up to 1 GPa.

The thermal effects are primarily due to the heating rate. The high heating rates allow for minimizing unfavorable densification mechanisms such as coarsening. The high heating rates make high activation energy mechanisms, such as grain boundary diffusion, dominant. These effects increases densification rates, decreasing processing times. The small processing times further discourage grain growth. The high heating rate therefor, allows for high densification rates without significant grain growth. There are detrimental thermal effects due to the high heating rates, such as both axial and radial thermal gradients within the sample and the tooling. This may lead to non-uniform microstructure or even localized melting. These can be avoided with tooling design [24].

The electrical effects involve both field effects and current effects. This is further complicated by the variable conductance of the sample. Conducting and non-conducting samples obviously behave differently, but individual samples have a variable effective electrical conductivity due to densification and temperature.

In conducting samples, a significant portion of the current flows directly through the sample. In non-conducting samples, the current runs essentially exclusively through the tooling. In nonconductors, such as Al2O3, sintering behavior is similar to hot pressing. In conducting samples there are numerous effects including the Peltier effect between the powder and the tooling, percolation effects, electrochemical reactions and electromigration. When the current flows through the sample, joule heating leads to local temperature gradients at particle contacts as shown in Figure 2-2. This creates very large differences from local to global temperature. These junctions sinter first

further increasing conductivity. These current pathways can be traced all the way through the process. Tooling design can control the current path [25].

By using conducting and non-conducting tooling or coatings, current can be driven into low conductance samples or driven away from conducting samples. This makes SPS complicated but quite malleable.

The Peltier effect which is directional heating due to electrons travelling across a junction, leads to anisotropic temperature gradients at the tooling powder interfaces [26]. This is particularly detrimental when making complicated shapes. This can be minimized by further tooling design. Electrochemical reactions can be manipulated for fabrication benefits or can lead to detrimental material properties but must be considered when designing a particular component process. Electric fields effects are typically discarded due to the low voltage in SPS, but may be important in certain systems. SPS has been used to fabricate numerous materials that are either difficult or impossible to sinter through other means. Materials that have been investigated include refractories, high temperature ceramics, nanostructured materials, functionally graded materials, transparent ceramics, and metastable materials [27, 28]. High temperature ceramics such as ZrB2 and B4C are materials which SPS provides numerous advantages.

Very high melting temperatures lead to high sintering temperatures which makes fabrication through other means difficult without extended grain growth. SPS allows for the production of these materials without that grain growth. Refractories have very high sintering temperatures and tend to oxidize. They require applied pressure to reach high density. SPS allows for atmospheric control, along with applied pressure to reduce

oxidation and short sintering times to minimize grain growth. A comparative study sintering ruthenium via SPS and hot pressing showed SPS produced sintered material with lower residual stress [29].

Non-equilibrium materials cannot be fabricated through conventional sintering or other alternatives due to chemical reactions or phase transitions that would occur. SPS allows for the fabrication of these materials due to the low time at temperature and the applied pressure. These materials include composite materials with various enhance thermal, electrical and mechanical properties. SPS provides unique advantages in fabricating functionally graded materials. The temperature gradients inherent in SPS setups can be manipulated to create variable environments in different area of a sample. Simply modifying the OD of a die enables controlling the amount of joule heat generated in various parts of the die. This enables variable environments for different sections of the sample. Also, the temperature gradients are continuous, reducing failure origins and delamination.

2.3 SPS of UO2

The University of Florida has pioneered processing UO2 via SPS. Ge et al [4] successfully sintered UO2 with an SPS sintering temperature of only 1050 C for 30 seconds. He produced 96% TD pellets with hardness and Young's modulus values consistent with conventionally produced UO2. The total run time was only 10 minutes. This is a large improvement over the many hours required to sinter UO2 conventionally. Chen et al [30] continued this work and produced the master sintering curve for UO2 via SPS. Chen determined the apparent activation energy for SP was lower than the conventional sintering process, which he attributed to the coupled current field and

pressure field in SPS. SPS leads to an increased diffusional transport rate and the pressure allows for more grain boundary contact. Chen does state that more study would be required to quantify the basis for the reduce activation energy. The master sintering curve allows for the designed path to achieve high density. Chen determined which temperatures and hold times are required for densification. Yeo, Chen and Cartas sintered UO2 with high thermal conductivity additives to produce ceramic matrix composites with improve thermal performance. Yeo produced UO2/SiC composites with both SiC whiskers and particles. The SiC/UO2 composites improved thermal conductivity consistently without undesired reaction products. The above study showed that UO2/ SiC composites could not reach high density and unfavorable chemical reactions occurred in conventional sintering, but in SPS high density and pure materials were produced. Chen produced UO2/diamond composites with improved thermal and mechanical performance. UO2/diamond composites did exhibit diamond graphitization above 1500 C. Cartas produced UO2/ CNT composites with high thermal conductivity. Cartas determined the material could be densified well as long as the CNTs were well distributed in the UO2 matrix.

Other more exotic nuclear fuels have also been explored via SPS fabrication. These include simulated UO2 fuel containing CsI [31], Tungsten-UO2 Cerments [32], and Uranium Nitride [33]. These materials have a wide variety of applications. The studies performed on these materials tend to focus on making laboratory quality samples and not with the geometry of the various applications.

2.4 Graphite SPS Tooling

There are two elements to the graphite tooling used in SPS that may negatively impact the sintering of UO2 fuel pellets. These two issues are the reaction of UO2 with graphite and the localized overheating problem. UO2 is known to chemically react with Carbon. This reaction is useful for the reduction of the UO2 powder to stoichiometric $UO_{2.00}$ without the need for extra steps in processing.

Various studies have claimed this reaction starts between 1000 C and 1300[34-37]. The reaction products are UC, UC_2 or $UC_{1-x}O_x$ depending on the amount of the residual oxygen in the UC lattice [35, 37]. Gosse [36] found for hyper-stoichiometric UO_2 powder, the reaction starting temperature could be as low as ~700℃ and in this reaction, UO_{2+x} is reduced into $UO_{2.00}$ without the formation of carbides. The reaction between graphite and UO_2 is more likely to happen on the surface contact between the UO2 and graphite punch because of the higher temperature on this surface. The following sequence of reactions are possible in the surface layer [38].

$UO_{2+x} + xC \rightarrow UO_2 + xCO$
$UO_2 + 4C \rightarrow UC_2 + 2CO$
$3UC_2 + UO_2 \rightarrow 4UC + 2CO$

The localized overheating problem occurs in many SPS experiments. This phenomena involves undesired extreme temperature gradients forming in the SPS tooling. This typically present in the punches. Giuntini [39] showed the difference in temperature between the punch and the powder may be as high as 1000 C. The origin of this phenomena may be related to the resistance associated with contact points in the SPS setup. Wei [40] showed electrical contact resistance dominates the

temperature evolution in SPS tooling compacts. The combination of these two issues may present problems at higher temperatures.

2.5 Commercial SPS Capabilities

Currently the commercial capabilities of SPS are limited. There is no published material describing commercial use but there are vendors producing large scale SPS machines. Any knowledge on the commercial use of SPS is protected tightly by for profit companies. There are three main companies producing SPS machines, they are FCT in Germany, Thermal Technologies in the USA, and Fuji electronic company in Japan. The commercial type machines (Figure 2-3) have three compartments. The first compartment is pre-sintering and accomplishes all tasks required before the high heating rate is applied. These tasks include loading powder into dies and preheating dies to an elevated temperature before sintering occurs. The second stage is the actual SPS sintering. In this stage the powder is heated with the electrical current and consolidates. In the third stage, the tooling and sintered pellet is cooled naturally to room temperature and the pellets are removed.

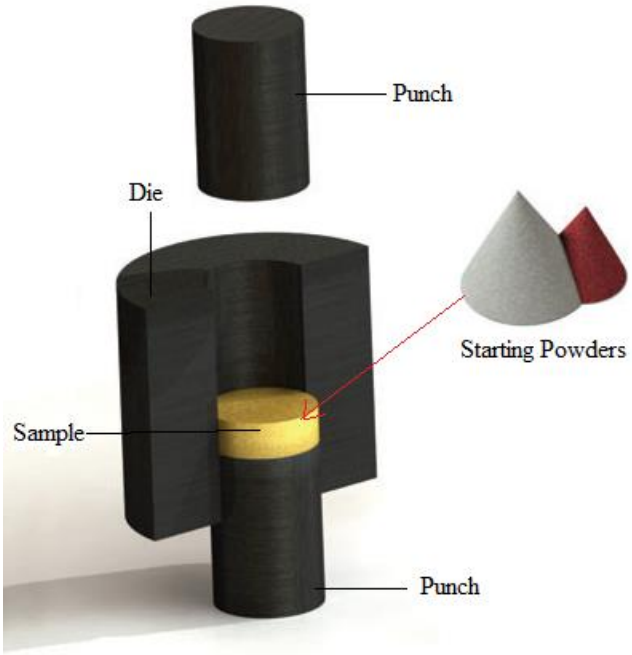

Figure 2-1. Example SPS die setup

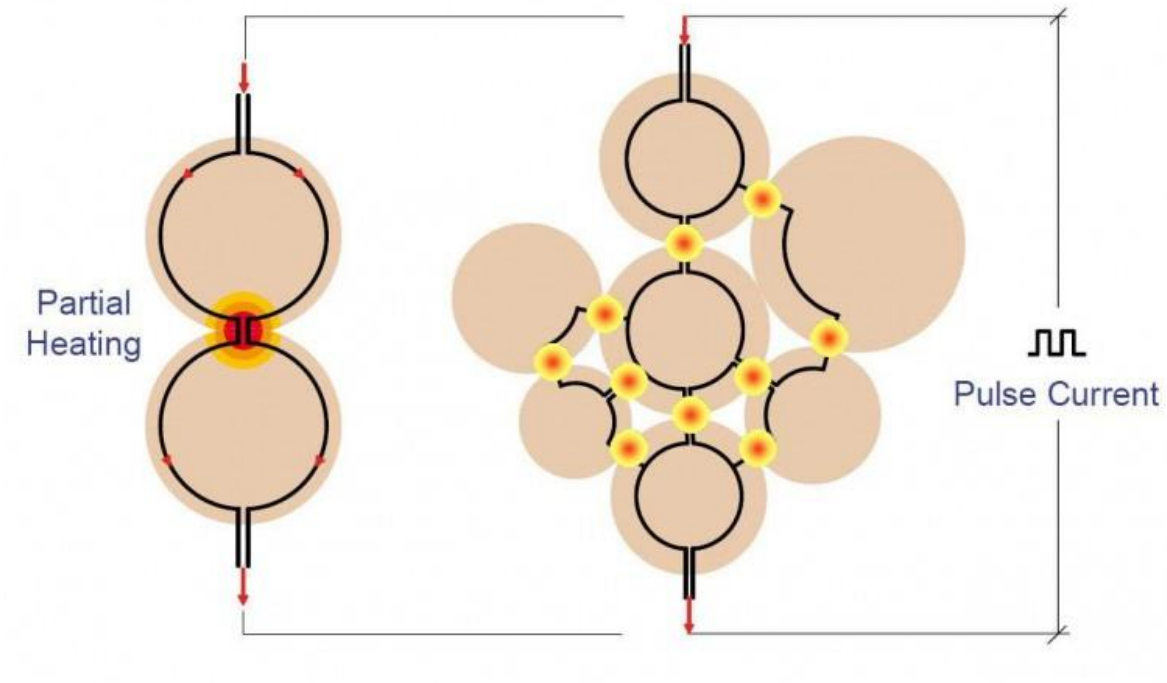

Figure 2-2. Diagram showing heating at particle contacts during SPS [10].

Figure 2-3. Three stage commercial SPS machine from Fuji Electric, Japan. Reproduced with permission from FUJI ELECTRONIC INDUSTRIAL CO., LTD. (Kawasaka, Japan, 2010).

CHAPTER 3
METHODOLOGY REVIEW

3.1 Spark Plasma Sintering

SPS is a field assisted sintering technique utilizing a large pulsed current to quickly heat graphite tooling, leading to high sintering rates in the powder loaded in that tooling. Heating rates can be as large as 1000 C/min. In addition to the current, SPS features an applied pressure which compresses the powder body, increasing particle contact and enhancing densification. This method allows for minimal powder preparation and sintering is accomplished in a single step. Applied pressure is limited by either the capacity of the SPS machine or by the tooling. In this study, a pressure limit of 80 MPA is set because this value is the fracture strength of the graphite tooling used.

All samples are loaded into a graphite die by hand by pouring the powder into the die. The tooling is shown in Figure 3-1. The powder is slightly compressed in between two punches with the pressure simply applied by hand. Typically the powder is physically separated from the die via a thin layer of graphite. This layer of graphite comes in two forms: a thin yet rigid graphite foil or a graphite spray. The graphite foil is the standard used in SPS research but is not viable for large scale industrial production. The graphite foil may act as a lubricant and/or current pathway. After the powder is loaded, a thick graphite felt is then wrapped around the die for insulation purposes. A loaded die, ready for sintering, is shown in Figure 3-2. A small hole is cut into the felt to allow for measuring the temperature of the die.

The die is loaded into the SPS machine in between two graphite spacers which are in physical contact with steel rams at the top and bottom of the machine. This completes the circuit for the current to flow. The complete die compact, ready for

sintering, is shown in Figure 3-3. A pyrometer, which measures the temperature of the die, focuses on the axial center of the die. The pyrometer is synced with the SPS controller. This controller modifies the current to achieve a preprogrammed temperature profile. A typical temperature profile is shown in Figure 3-4. The pyrometer has a minimum temperature it can read, which is 600 C. Typically there is a dwell time of 5-7 minutes at which the die set temperature is held at 600 C to allow the pyrometer to take a consistent reading. The temperature profile includes setting the heating rate to the maximum temperature. At the maximum temperature, the compact is held at temperature for a set time. During this time, an external pressure is applied via the pressure controller which requires manual input. The die may migrate slightly (on the order of 5 mm) vertically during sintering. This means the spot the pyrometer is measuring may slightly change during the process. After sintering, the consolidated pellet is removed by hand pressing the punch through the die. If the pellet cannot be removed by hand, a carver press is used to force the pellet out of the die. Then the die is cleaned and reused.

3.2 Commercial Pellet Qualification

Typical commercial pellet qualification requires a sample of 20 pellets, out of millions, to be randomly tested against the requirements stated below.

Pellet diameter is measured via a digital micrometer three times and the average of these three measurements is used to calculated density. The three measurements are taken at 120 degree azimuths to provide further insight into pellet shape. The diameter of the pellets shall be 8.1915 ± 0.0254 mm, with a goal of meeting a tolerance that is reduced by 1/2, i.e. ± 0.0127 mm.

The length of each pellet is taken as a single measurement. The length of the pellets shall be 10.16 ± 1.27 mm, with a goal of meeting a tolerance that is reduced by approximately 1/3, i.e. ± 0.423 mm Mass is a single measurement.

Density is then calculated using the calculated pellet volume and measured mass. A correction factor of 0.9909 used to correct the volume due to the missing volume of the dish and chamfer. For each pellet type, the average pellet density shall be greater than or equal to 96.5% of theoretical density and individual pellet densities shall be ± 2.0 % of that average.

The pellets shall have a spherical dish and chamfer on each end. The width of each dish shall be 4.52 mm and the depth shall be 0.0254 mm. The target width (radial dimension) and depth (axial dimension) of each chamfer shall be 0.381 mm and .127 mm, respectively. Pellet end geometry is measured via the profilometer described below.

Surface quality is determined by visual inspection. Any chip or crack that may be larger than the allowable size are further examined with a magnifying lens with a built in scale. Each pellet shall be inspected at 1× magnification for cracks and chips. The length of any individual axial crack shall not exceed 1/3 of the pellet length. The length of any individual circumferential crack shall not exceed 1/3 of the pellet circumference.

The total area of all chips on the cylindrical surface of a pellet shall not exceed 5% of the area of the cylindrical surface. Chips on the cylindrical surface that exceed a circumferential width of 1.5 mm or larger shall be recorded. The total area of all chips on any end surface of a pellet shall not exceed 1/3 of the area of the end surface.

Each pellet type shall be subjected to a loadability test. A minimum of two test samples of each pellet type shall be tested. A test sample consists of a “stack” of ten sintered pellets. Each test stack shall be loaded axially in compression to a maximum of 100 lb. The load at which a 1.5 mm (maximum dimension) chip or larger is produced shall be recorded. If the sample withstands a 100 lb load without chipping, the chip loading for the sample shall be recorded as 100 lb. The expectation is that pellets can withstand a 40 lb load without producing a 1.5 mm (maximum dimension) chip.

Grain size is measured via thermal etching following by the linear intercept method [41]. The pellet grain size measured at three representative points (edge, midway and center) shall be greater than or equal to 10 µm, with a goal of 20 µm or larger. The pellet porosity greater than 20 µm shall be less than or equal to 0.5% by volume.

3.3 Pellet Loadability Tester

Pellets must be able to survive an axial force of 100 pounds without chipping or cracking, to ensure they would survive insertion into the clad. The pellet loadability tester, provided by Areva, was used to accomplish this. The standard loadability test was performed on all the pellets [42]. In this test, a pre-inspected stack of ten pellets were laid horizontally in between the space provided by the four rods in the tester shown in Figure 3-5, and the tester slowly exerted 100 pounds of force on the stack. The force was then removed and the pellet inspected for chips and cracks.

3.4 Laser Profilometer

The Contour GT-I Bruker Optical Profilometer is a benchtop instrument used to measure the profile and surface roughness of a sample. The device uses a laser to measure the vertical location of the focused spot to a resolution of 0.1 nm. The device can automatically make a map of the vertical locations of the laser as it moves across the sample surface. Post processing can remove any intrinsic tilt in the sample. The profilometer is shown in Figure 3-6.

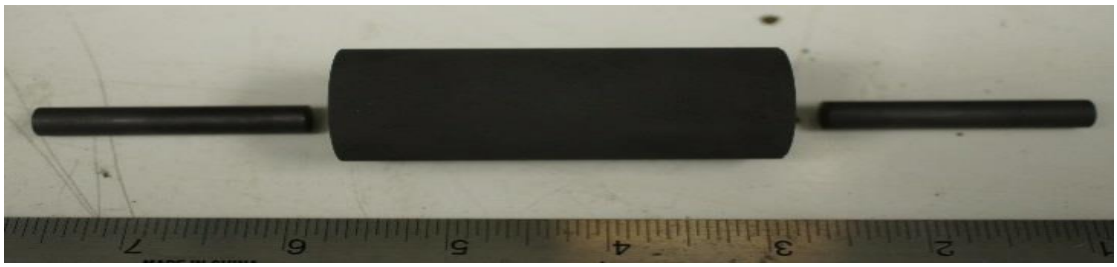

Figure 3-1. An unloaded die with punches. Photo courtesy of the author.

Figure 3-2. A loaded die with graphite felt. Photo courtesy of the author.

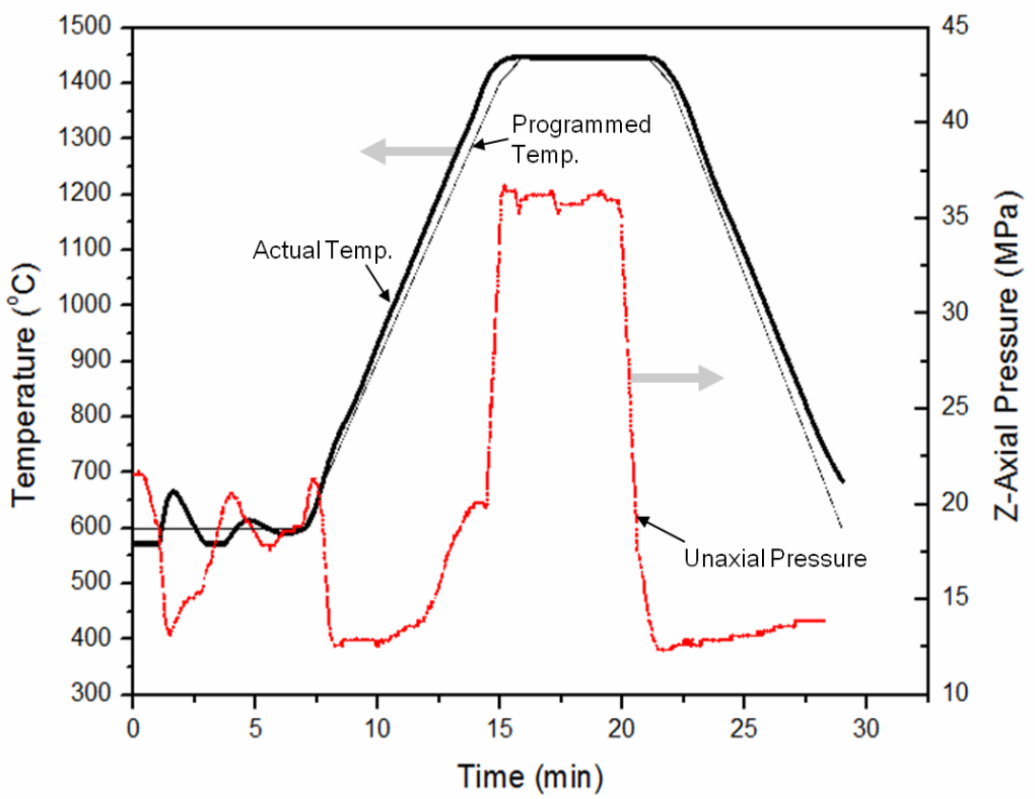

Figure 3-3. A representative temperature and pressure curve for the SPS process.

Figure 3-4. A die loaded in the SPS machine. Photo courtesy of the author.

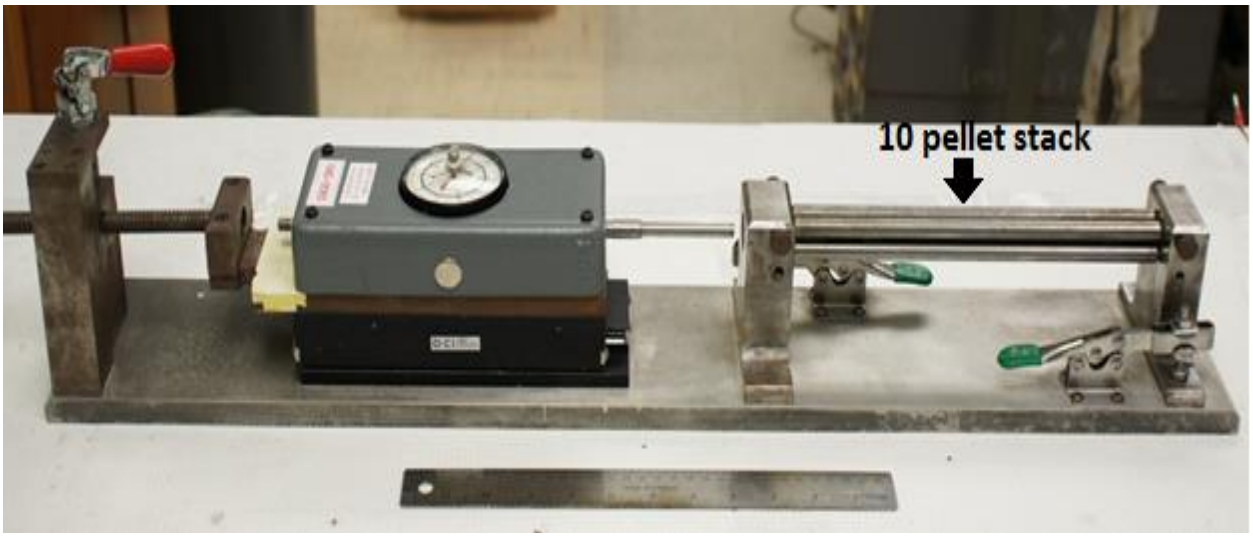

Figure 3-5. The pellet load tester which is used to measure pellet strength. Photo courtesy of the author.

Figure 3-6. The Bruker optical profilometer being used to measure pellet end geometry. Photo courtesy of the author.

CHAPTER 4
FABRICATION OF COMMERCIAL UO2 PELLETS

4.1 Introduction

Commercial grade nuclear fuel pellets are specifically engineered parts, with tight tolerances and precise dimensional requirements. Previous SPS work at UF focused on producing dense UO_2 samples from feedstock powder without concern for the size and shape of the sample. These previous samples were flat disks with a length of 4-8 mm and a diameter matching Mark B fuel pellets (12.5 mm). Thin disks are both easier to fabricate and easier to characterize. The commercialization of this process requires pellets to be fabricated according to the industry standards described in Chapter 3. The major changes are the modification of the diameter from 12.5 mm to 8.19 mm, the change in L/D ratio of the pellets and the shape change from a flat disk to a modified cylinder with a dish and chamfer. As stated in Chapter 2, the current standard for achieving the desired pellet shape is a combination of prepressing the UO2 powder and using centerless grinding. SPS has been used previously to make various shapes while not requiring these other processing steps.

4.2 Experimental Procedure

Initially, 20 single pellets were produced to meet the requirements set in the pellet qualification plan described in Chapter 3. The powder used was feedstock powder supplied by AREVA Federal Services. This powder was raw UO2 which was not modified with any additives or prepared in any special way. The O/M ratio of the powder is approximate 2.11. The average grain size of the raw powder is 0.1 µm to 0.4 µm. The pellets were sintered at 1050 C for 5 minutes with a heating rate of 100C/ min and an

applied pressure of 40 MPa. The initial dwell time was 6 minutes, leading to a total run time of 22 minutes.

All pellet dimensions were measured to determine dimensional consistency and process reliability. These 20 pellets used a variety of freshly machined punches and dies. The tooling was replaced as often as deemed necessary after visual examinations of the tooling, to maximize the quality of the pellets. Most punches were used 2-3 times, with 5 dies making the 20 pellet batch.

Pellet surfaces were cleaned with alcohol and visually inspected with both a 1X magnified lens and a 10X magnified lens for defects, chips, cracks and inclusions. Typical industrial specification is that the total chip area is required to be less than 5% of the total surface area. Any cracks must be less than a third of the pellet circumference. The pellet ends were inspected for the characteristic dish and chamfer shape.

To ensure pellets were fabricated with the required end geometry, a laser profilometer (Bruker Contour GTI) was used. The instrument had a vertical resolution of 3 nm and a horizontal resolution of 0.15 microns. The laser was focused on the pellet land area and the measurement was taken toward the center of the pellet creating a profile showing the dish dimension and then on the other side measuring the chamfer dimensions.

The pellet density was calculated from mass and dimensional measurements. The length of each pellet was measured once, while the pellet diameter was measured at three orientations separated by 120 degree. The pellet volume was calculated from the average diameter and length, while accounting for missing material from the dish and chamfer. A pellet was cut at three axial locations and the cut surfaces were

polished. These segments were then thermally etched for ten minutes at 1100 °C in a CO2 atmosphere to reveal grain structure. The grain size was measured via the linear intercept method.

A standard loadability test was performed on all the pellets [42]. In this test, a pre-inspected stack of ten pellets were laid horizontally and a force of 100 pounds was slowly applied to the stack. Then, the force was removed and the pellet inspected for chips and cracks. This test checks if pellets would survive loading into cladding without chipping or cracking.

Additionally, a second round of ten additional pellets were produced to determine the relationship between tooling reliability and pellet reliability. In each of two runs, 5 pellets were fabricated with the die and punches being reused for all five pellets, consecutively. The tooling and pellets were then examined for any sign of tooling wear or degradation.

4.3 Results and Discussion

Table 4-1 shows the compiled results for the 20 pellets initially produced. It reveals that the pellets were successfully fabricated to the specified (goal) dimensions. In SPS, the die inner diameter confines the pellets, so the diameter of all pellets was consistent. The pellet length was shorter than required, as this may be due to incorrect estimation of powder weight required for correct length of pellet. However, the resulting length of the pellet was consistent. Also, measured pellet density was consistently acceptable.

Figure 4-1 shows 19 of the 20 produced pellets. The excluded pellet was removed and processed for the grain size measurements. The surface of all the pellets appeared smooth and clean. However, there was an obvious gray ring in the center of all pellets, (Figure 4-1a). The origin of this artifact was unknown but was smooth to the touch. All pellets were produced with a clear dish as shown in Figure 4-1 (b). Some pellets had light chipping along the pellet edges, as indicated. The chipping was within the 5% of surface area allowed in the specification.

To observe the microstructural homogeneity throughout the pellet, one of the pellets from the above batch was cut at ¼, ½, and ¾ length, as shown in Figure 4-2. Using the linear intercept method, the grain size on each cross section was measured at locations near the circumference and at the center.

The pellet average grain size at each position are shown in Table 4-2. It is clear that the smallest grains are in the center of the pellet and the largest grains are near the edges of the pellet. This is consistent with previous SPS studies [4]. The average grain size at the center of the pellet was 5.52 ± 0.6 microns. Average grain size at all points was 6.37 ± 0.9 microns

The second batch of pellet production, featuring two runs of 5 pellets each, is described in Table 4-3. Pellets 1-5 were fabricated one at a time using a single die and set of punches as run 1, while pellets 6-10 were fabricated in another die and utilizing another set of punches as run 2. From Table 4-3, it is seen that the diameter and standard deviation of the pellets increased from 1st pellet to 5th pellet in each run. Pellet #1 was very symmetric and had the smallest OD. Pellet #5 showed a noteworthy increase in OD and was the least symmetric. This increase is attributed to wear of the

inner diameter of the die in each run, which will be discussed separately later in Chapter 6. Despite this wear, all pellets achieved a density above 96.5 % theoretical density and all ten pellets survived axial loading up to 100 pounds.

Figure 4-3 shows the central circumferential ring that appears on all pellets fabricated (Fig 4-1(a)). A laser profilometer scan of the surface near this ring, shown in Figure 4-3(b), revealed a localized increase in surface roughness. This artifact consistently appeared at halfway of each pellet length. At this point, we are unable to identify its origin. This artifact is not an indention but only surface roughness

Some pellets showed slight chipping around their edges (Figure 4-1(b)). This may be due to a mismatch in the punch diameter and die inner diameter. If the gap between the punch and the die is too large, upon sintering, some UO2 may form a sharp edge which can fracture during pellet removal. The chips may have occurred during the sintering process due to the axial load being applied or after sintering during removal.

The end surface of the first pellet produced in each run (with a new graphite punch) was measured with a profilometer to obtain the dish and chamfer profiles. This measurement length was taken from the land area (at the top of the chamfer) to the dish center on one side (as shown in the inset of Figure 4-4) and then from the land to the end of the chamfer on the other side. A summary of the results of these measurements are listed in Table 4-4. These parameters were within 10% of the goal confirming the acceptability of dimensions of the dish. The only parameter that deviated more than 10% was the chamfer depth. This is most likely because as the laser reaches the edge of the chamfer (close to the cylindrical surface), it goes out of focus and the rest of the

measurement becomes unreliable. Therefore, the measurement given here does not imply that the pellet chamfer was not to the specifications, but also does not confirm that it was to the specifications.

4.4 Conclusions

SPS has been shown to be capable of producing single fuel pellets meeting the specifications of the nuclear industry, with the exception of grain size. High density pellets, conforming to the nuclear industry qualification requirements, were fabricated and evaluated. These pellets met all required criteria except for grain size. The process is reproducible, over a 95% success rate, when pellets are produced under ideal conditions: one at a time and with fresh tooling. An unknown artifact, which may be surface roughness, is present in the form of a ring along the pellet axial center. This ring does not appear to have an impact on pellet density or the pellets' ability to stand up to 100 lbs of loading force. The quality of the pellets decreases as the tooling is reused. As tooling is reused, the surfaces of the pellets have a greater likelihood of a defect.

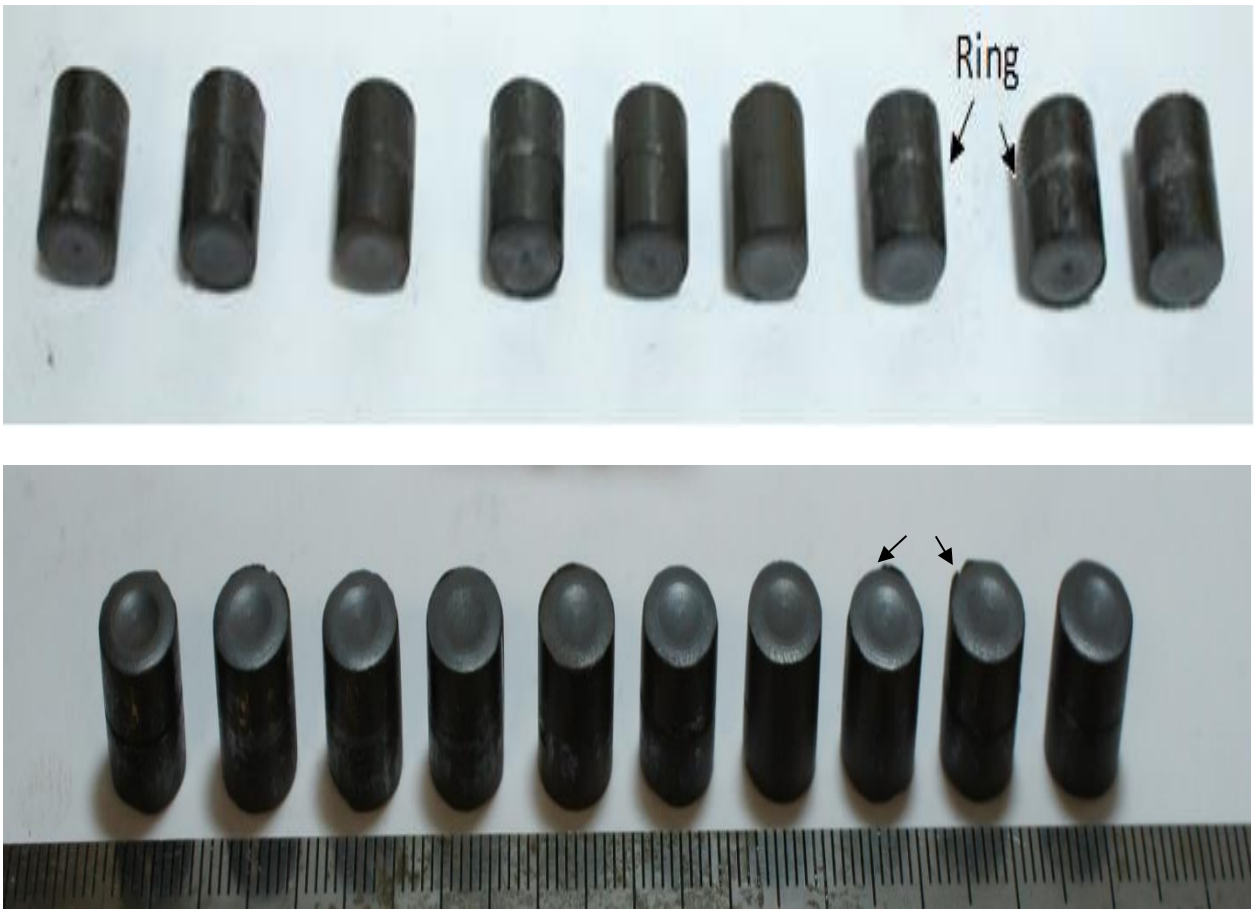

Figure 4-1. Sintered UO_2 pellets A) Pellet artifact (central ring on surface). B) Dish and chamfer along with slight chatter on chamfer edge. Photo courtesy of the author.

(a) (b)

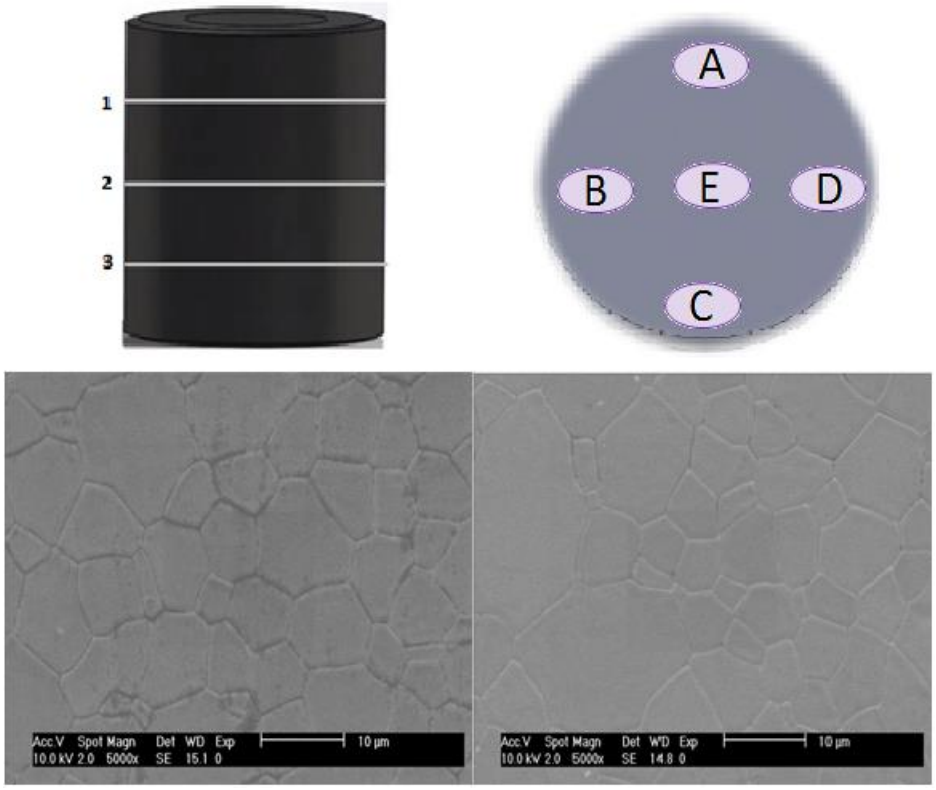

(c) (d)

Figure 4-2. Grain size measurements. A) Schematic of the grain size measurement cross section locations. B) Grain size measurement surface locations. C) Micrograph revealing grain structure of pellet edge. D) Micrograph of pellet center. Photo courtesy of the author.

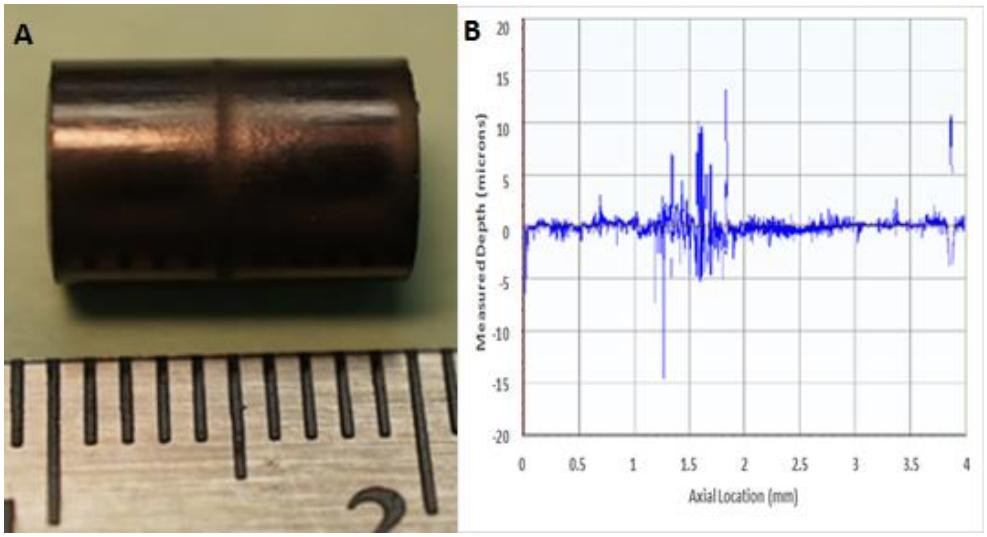

Figure 4-3. Central ring artifact A) Image of a pellet with central circumferential ring. B) Laser scan of the ring revealing high surface roughness. Photo courtesy of the author.

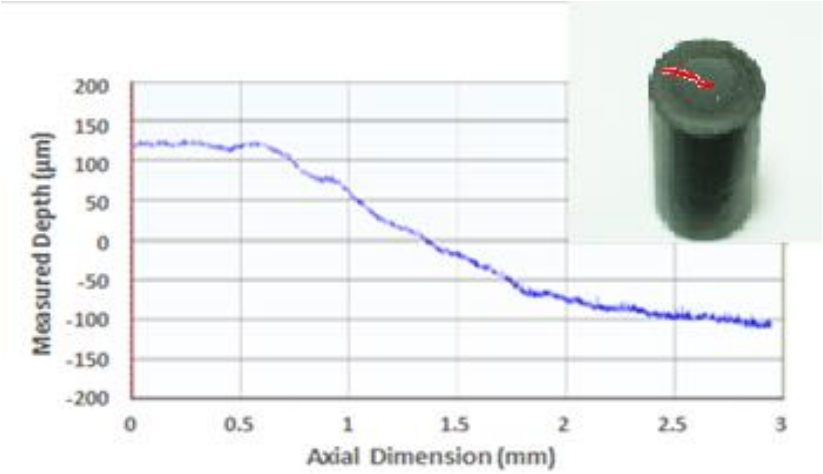

Figure 4-4. Profilometer measurement of the dish geometry. The inset reveals the measurement location. Photo courtesy of the author.

Table 4-1. Dimensions and density of single pellets produced via SPS

	Goal	Measured
Sample Size	20	20
Sample mean diameter (mm)	8.1915 ± 0.0254	8.194 ± 0.013
Sample mean length (mm)	10.16 ± 1.27	9.83 ± 0.26
Density (% TD)	96.5 ± 2.0	96.8 ± 0.056

Table 4-2. Pellet grain size versus position as measured

Position	Average Grain Size (µm)
1	6.3 ± 1.0
2	5.52 ± 0.6
3	7.28 ± 0.9
A	6.79 ± 1.3
B	6.15 ± 0.9
C	6.88 ± 1.1
D	6.33 ± 1.4
E	5.7 ± 0.9

Table 4-3. Dimensions of UO_2 pellets fabricated in two runs

Pellet	Density (%)TD	Length(mm)	Diameter (mm)
Goal	96.5 ± 2.0	10.16 ± 1.27	8.192 ± 0.0254
1	96.9	10.26	8.184 ± 0.0031
2	96.9	10.26	8.192 ± 0.0076
3	97.0	10.26	8.189 ± 0.0046
4	96.9	10.26	8.189 ± 0.0033
5	96.7	10.26	8.199 ± 0.0160
6	97.2	10.21	8.176 ± 0.0025
7	97.7	10.19	8.176 ± 0.0076
8	97.2	10.21	8.181 ± 0.0081
9	96.9	10.29	8.192 ± 0.0026
10	96.6	10.29	8.199 ± 0.0104
Avg	97.0 ± 0.3	10.24 ± 0.04	8.188 ± 0.0081

Table 4-4. Pellet end geometry measurement statistics

Parameter	Goal (mm)	Measured (mm)
Dish Depth	0.254	0.247
Dish Radius	2.260 ± 0.50	2.350
Chamfer Length	0.381 ± 0.17	0.400
Chamfer Depth	0.127 ± 0.05	0.075

CHAPTER 5
COMPOSITE PELLETS

5.1 Introduction

Previous research into composite pellets at UF had focused on the many facets of SPS including sintering parameters, optimal volume fraction of additives, optimal additive particle size, and dispersion techniques. None of these facets were extensively examined in this study. The focus of this study was producing commercial grade fuel pellets. This required the fabrication of composite pellets to net shape, while still meeting the density, cleanliness and other requirements of the pellet qualification plan described in Chapter 3. All previous studies were performed with thin flat disks with an L/D ratio of 0.32-0.75. The increase in L/D ratio may make achieving a high density more difficult. The addition of the pellet end geometry requires additional tooling modifications and adds stresses to the pellet. The composite pellets require greater temperatures than the pure UO2; fabrication may be more difficult than for pure UO2 and the behavior may be different than for the pure UO2 studies previously discussed. All previous studies have shown the additives prevent grain growth during SPS, so it is expected that large grain sizes will not be produced in this experiment. Sintering parameters were used as suggested by previous studies, which is a temperature around 1400 C.

5.2 Experimental Procedures

The UO_2 powder was the same powder used in the pure UO_2 experiments above and was obtained through AREVA. The powder had a bulk density of 2.3 g/cm^3, a mean diameter of 2.4 μm, and a starting O/M ratio of 2.11. The powder was depleted UO_2 with

an enrichment of less than 0.71%. The raw powder was stored at room temperature and pressure for period of time of over one year after being obtained from AREVA. The SiC whiskers used in these experiments was obtained from Advanced Composite Materials, Inc. The whiskers had an average length of 11 µm, an average diameter of 0.65 µm, an aspect ratio of 15:1, and were reported to be greater than 98% pure. The whiskers were found to have trace amounts of Carbon (0.1 wt %) and SiO_2 (0.43 wt %). The diamond particles used were purchased from Advanced Abrasives Corporation. The particles were single crystals with a reported average diameter of 3 µm and a standard deviation of 0.475 µm.

The constituent powders were mixed through the use of a vibrational ball mill acting as a mixer. Powder batches totaling 20 grams were produced by loading raw UO_2 powder and the requisite additive powder into a zirconia vial; a mixing aid, Decafluoropentane (DECA), was also added to enhance facilitate mixing. Deca is a stable organic compound that does not react with UO_2, SiC (w) or diamond. Additionally, Deca evaporates quickly at room temperature. Powders were mixed to attain a 10 % by volume fraction of the additive. The SiC (w) /UO_2 mixture contained 19.37 grams of UO_2 and .69 grams of SiC (w). The diamond/UO_2 mixture contained 19.31 grams of UO_2 and .63 grams of diamond particles. The zirconia vial was then sealed via a rubber O-ring and a generous amount of electrical tape. The SiC (w) and UO_2 were mixed in the mill for 60 minutes. Three steel balls were added to the UO_2/SiC (w) mix to break up SiC (w) agglomerates. The diamond and UO_2 powders were mixed for 60 minutes. Steel balls were not used to mix the diamond because the hard diamond particles led to iron contamination. After mixing, the mixed powders were removed and

placed in paper cups and dried in a dry keeper from 24 hours. Twenty four hours was enough time for the Deca to evaporate away.

The dried powders were loaded, by hand, into the graphite tooling. To prevent a reaction with the die wall, a thin graphite foil was placed between the powder and the die wall. This foil acted both as a barrier and as a lubricant. Additionally, the graphite foil facilitates the flow of current from the punches to the die. The punch tips were sprayed with a thin layer of graphite spray, to prevent the powder from reacting with the punches. The mass of powder was calculated by assuming the desired pellet volume and the desired 96.5 % theoretical density would be attained. The mass of a diamond/UO_2 powder body was 5.3 grams and the mass of the SiC/UO_2 powder body was 5.25 grams.

Ten pellets of both types were sintered according to the sintering conditions recommended by previous researchers. The sintering parameters used for both SiC/UO_2 and diamond/UO_2 composites were a peak temperature of 1400 degrees centigrade held for five minutes. The pressure at the hold for diamond/UO_2 composites was 40 MPa, while the SiC/UO_2 composites used 60 MPa. The difference was mainly due to a reluctance to increasing the temperature of the UO2/SiC (w) composites out of concern that the punches would react with the powder. The extra pressure should lead to a small increase in attained density. The heating rate was held at 100 degrees centigrade per minute during heating and cooling. After the sintering cycle was completed, the die compact was allowed to cool naturally for one hour. Then the die was removed and taken to the laboratory for pellet extraction.

Pellets were extracted through the use of a carver press. After removal from the die, pellets required light polishing to remove the graphite foil attached to the outer diameter of the pellets. After the foil was removed, pellets were cleaned with alcohol and stored. At a later time, pellets were weighed and measured to determine the actual diameter, length and density. The pellet end was visually inspected to determine if the dish and chamfer were present. Pellet 1 from both the diamond and SiC pellet lots were further inspected via the laser profilometer to determine if the dish was formed as designed.

5.3 Results and Discussion

The diamond pellet lot is shown in Figure 5-1. The pellet measurements are described in Table 5-1. The average density of 95.2% TD was below the 96.5% goal. These pellets had a larger standard deviation, than previous pure UO2 pellets, but it is within the requirements. Three pellets were below the 94.5% minimum. These pellets were longer than the specified goal. This implies these pellets did not shrink as desired. It is not clear why this occurred for these three pellets. Pellet number five was egregiously long and of poor density. It was 10% longer than desired and only 91.5% theoretical density. This pellet may simply be an outlier, perhaps due to human error. Pellet 3 was very short (8.8 mm). The pellet was dense (95%), so the pellet mass was too small. This is either due to human error when measuring out the powder or human error in loading the powder causing a significant portion of the powder to be lost.

These pellets did not have as clean an OD as UO_2 pellets. This result is primarily due to the use of graphite foil on the exterior. Light polishing was required to remove the graphite foil. On pure UO_2 pellets, graphite could be removed via sandblasting, but with

the composite pellets sandblasting was insufficient. Additionally, there was some chipping on the pellet edge. This is from the chamfering. The chipping is most likely caused by a size mismatch between the designed chamfer and the actual powder dimensions after pressing. The foil recoils a bit during pressing leaving the powder to expand further than the designed OD. This is a very small effect but enough to lead to some chipping (Figure 5-1). With the pure UO_2, the rigid die wall does not allow for the powder OD to expand. The pellets showed a visible dish and chamfer. A visual inspection indicated graphite from the punch adhered to the dish. Most of this graphite could be removed via sandblasting, but not entirely. Certainly these pellets required post-processing after removal, which is not ideal.

On the diamond pellets there was slight chipping. The largest chip, located on a diamond composite pellet, is shown below in Figure 5-4. The chipping may be due to tooling size mismatch or a localized flaw in microstructure. A mismatch in the punch tip creating the chamfer could cause the flaw shown. Figure 5-5 shows a micrograph of the fracture surface shown in Figure 5-4. The image shows a large amount of diamond particles on the fracture surface. The localization of diamond particles could have led to the chipping. This implies the mixing of diamond particles was not adequate.

The SiC (w) pellet batch appears respectable (Figure 5-2). The physical characteristics are described in Table 5-2. The pellet batch had an average density of 95.3 % TD. These pellets had a tighter standard deviation than the diamond pellets. Two pellets had densities under 94.5%, meaning 80% of the pellets met the required density. The pellets were shorter than desired. This mismatch is most likely due to powder lost during loading. A small amount of powder is lost in the loading procedure

since it is done by hand. The SiC (w) pellets did attain the desired diameter, this is of course constrained by the die inner diameter.

The SiC (w) pellet's required thorough polishing to remove the graphite foil from their exterior. The polishing required was significantly more arduous than for the diamond pellets. This is most likely due to the increased pressure applied during sintering. The larger pressure leads to a larger pressure on the pellet exterior exerted by the die wall. The foil is believed to include deeper into the pellet exterior which requires polishing more material to achieve a smooth surface. Most pellets had very clean surfaces. Some pellets had graphite foil adhesions as shown in Figure 5-3. This is due to graphite foil crunching up upon powder loading. This problem is exacerbated when decreasing the die ID. This produces a non-uniform pellet OD filled with residual graphite.

There was some light chipping and significant chatter on the pellet ends. The chipping present was less severe than on the diamond pellets. There was a dish present as indicated by the visual inspection. This dish was present, and was comparable to the dish in the diamond pellets. Fabricating both the diamond and the SiC (w) pellets led to punch failure in a single fabrication run. The dish surface on the punches is visibly reduced after a single run. It is unclear if this is due to the increased temperature or the composite material itself.

Figure 5-6 shows the dish depth of pellet 1 of the SiC (w) and diamond pellet lots as measured by the laser profilometer. A representative dish measurement for a UO2 pellet is also shown on Figure 5-6 for comparison. Table 5-3 compares the maximum depth achieved for the SiC (w), diamond and UO2 pellet. The composite pellets

achieve the desired depth, even attaining a deeper dish than the UO2 pellet. It should be remembered that the diamond and SiC (w) pellets were post processed; whereas, the UO2 pellet did not required this post-processing. The post-processing included a sandblaster removing graphite located in the dish. The effect the post-processing has on the dish geometry is unknown. It is obvious that the shape of the dish differed between the three pellets. The SiC dish was the smoothest and most spherical, but the SIC also required the greatest amount of post-processing. The diamond pellet had a flatter and more linear dish. This showed the composites did form a dish and at the depth desired, but the behavior is slightly different than for the pure UO2 pellets. Also the punches were essentially single use. No comparison of fabricated multiple composites pellets was performed. More work is required to guarantee composite pellets would pass qualification.

5.4 Conclusions

Fabricating 17x17 composite pellets proved to be more difficult than pure UO_2 pellets. It appears the 1400 C sintering temperature is nearing the capacity of the graphite tooling. There is not much leeway when working at these temperatures. Even a small increase to 1450 C may cause a reaction between the UO_2 and the graphite tooling. As it stands now, the tooling can only survive a single run before needing replacement. Even at 1400 C and the available applied pressures, the composite pellets were of significantly lower quality than the pure UO_2 pellets described previously. Only 70% of the diamond pellets passed the density requirements and even less passed the entire pellet qualification. The SiC pellets had superior density but graphite foil inclusions were seen on all pellets.

Currently a significant amount of post-processing is required to ensure pellets meet requirements. The graphite foil produces flaws that must be removed in the future. The best case scenario requires polishing off on graphite that bonds with the pellet. In the worst case scenario, the foil bunches up and then includes into the outer surface of the pellets. These inclusions may not be removable while still maintaining the required outer diameter.

Diamond pellets showed signs of particle agglomeration, hinting that the mixing was inadequate. These may exacerbate chipping near the pellet edge. Using steel or ceramic ball to break up agglomerates will introduce contaminates and still may not break up the hard diamond agglomerates. A longer mixing time than 60 minutes is suggested.

Pellets do approach 96.5 % TD, indicating studies could move forward fabricating multiple composite pellets in a single run. Pellets acquired a dish as deep as required but the shape of the dish was not as good as for pure UO2 pellets. More precise measurements of the pellet end geometry of composite pellets, including the effect of post-processing, should be performed. Using the information learned, optimized pellets were fabricated for insertion into the Advanced Test Reactor.

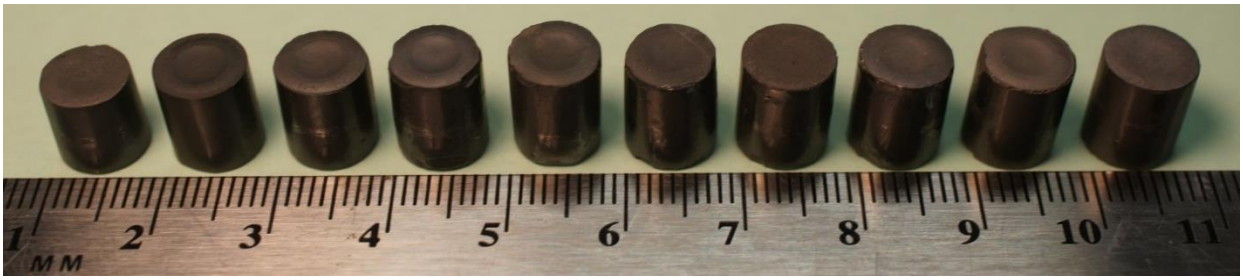

Figure 5-1. Diamond composite pellet lot. Photo courtesy of the author.

Table 5-1. Diamond physical dimensions

Pellet	Density	Length (mm)	Diameter (mm)	D_{stdev}
Goal	96.5 ± 2.0	10.16 ± 1.27	8.1915	0.0254
1	95.8	10.08	8.1940	0.0051
2	93.9	10.9	8.1915	0.0127
3	95.1	8.81	8.1839	0.0203
4	94.1	10.92	8.2093	0.0102
5	91.2	11.13	8.1813	0.0076
6	97.2	10.52	8.2067	0.0127
7	97.4	10.77	8.2093	0.0076
8	96.2	10.49	8.2093	0.0102
9	95.0	10.77	8.2144	0.0254
10	95.84	10.03	8.1712	0.0229
Avg	95.2 ± 1.8	10.44 ± 0.69	8.1966	0.0203

Table 5-2. SiC Physical Dimensions

Pellet	Density % TD	Length (mm)	Diameter (mm)	D_{stdev}
Goal	96.5 ± 2.0	10.16 ± 1.27	8.1915	0.0254
1	96.0	10.24	8.1737	0.0127
2	95.8	9.53	8.1483	0.0203
3	94.0	9.63	8.1788	0.0203
4	94.7	9.96	8.1610	0.0076
5	94.8	9.73	8.1636	0.0025
6	95.4	10.11	8.1661	0.0254
7	95.9	9.75	8.1594	0.0102
8	96.0	9.93	8.1407	0.0152
9	96.7	9.68	8.1788	0.0203
10	94.1	10.03	8.2931	0.0051
Avg	95.3 ± 1.0	9.86 ± 0.254	8.1661	0.0508

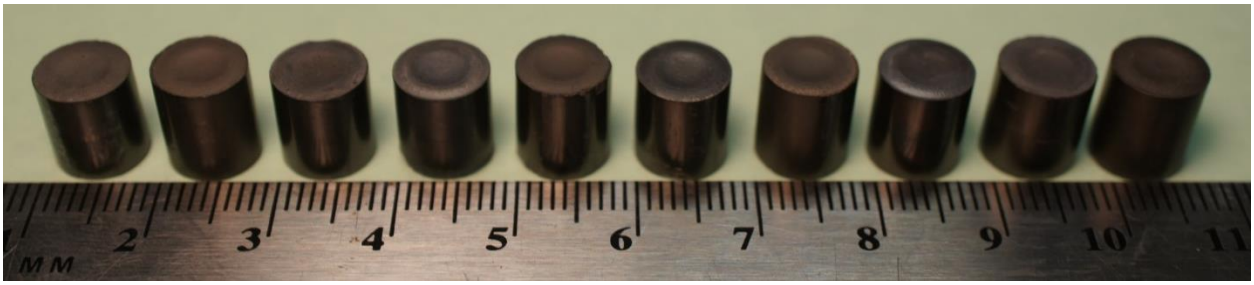

Figure 5-2. SiC Composite pellet lot. Photo courtesy of the author.

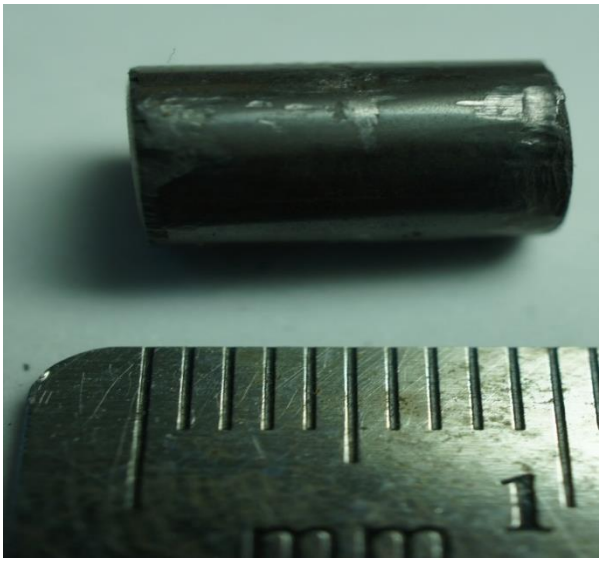

Figure 5-3. Graphite on surface of SiC pellet. Photo courtesy of the author.

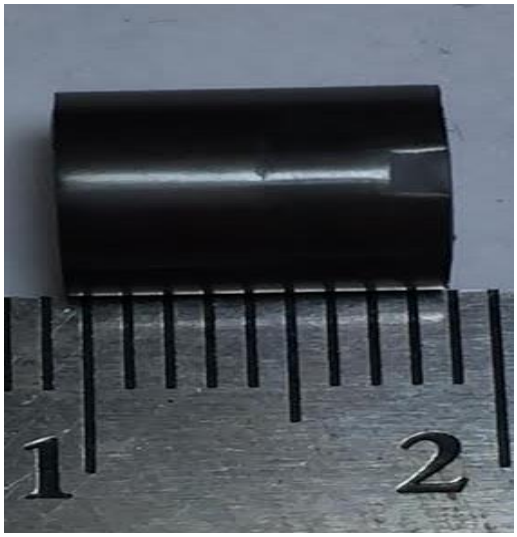

Figure 5-4. Diamond pellet showing surface chip. Photo courtesy of the author.

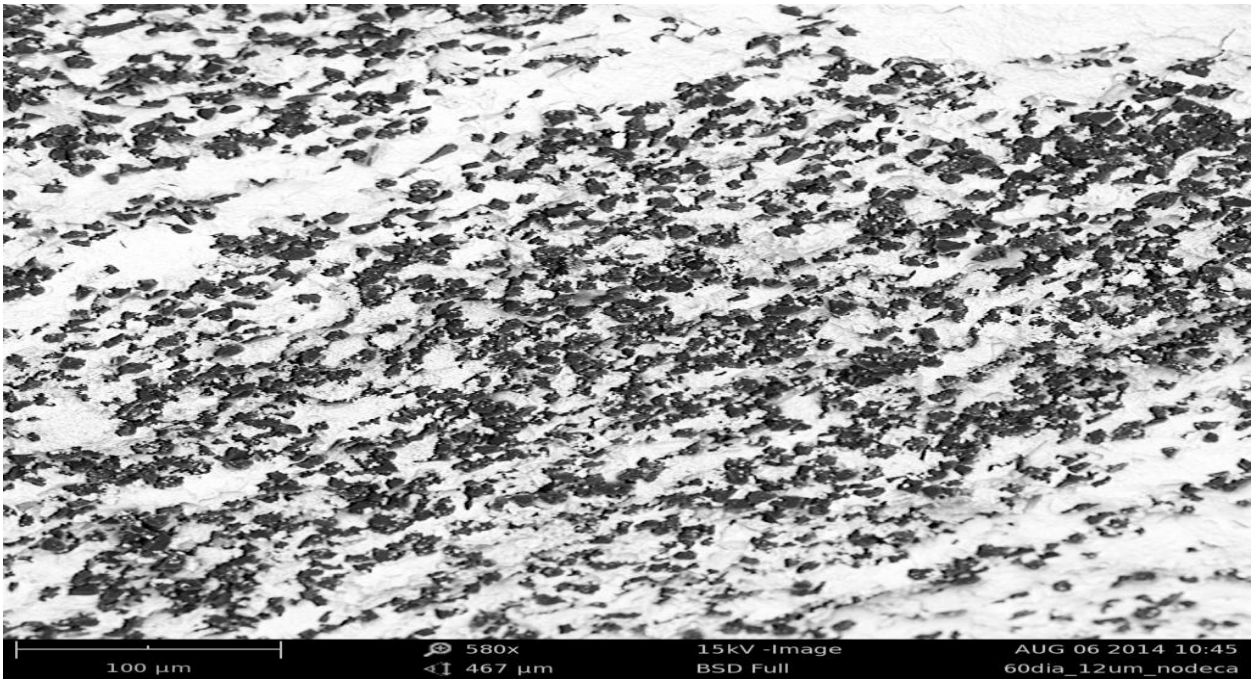

Figure 5-5. Fracture surface of diamond/UO2 Pellet. Photo courtesy of the author.

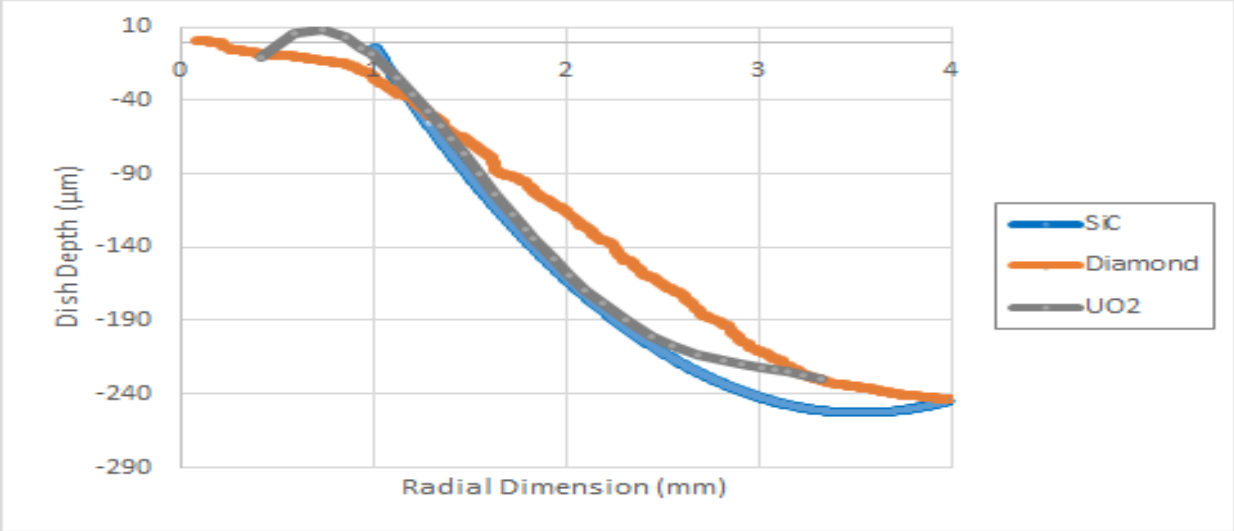

Figure 5-6. Dish depth for SiC, diamond and UO2 pellet

Table 5-3. Comparison of dish depth in composite and pure UO2 pellets

Parameter	Goal Depth (mm)	UO2 (mm)	Diamond (mm)	SiC (mm)
Dish Depth	0.254	0.237	0.255	0.263

CHAPTER 6
SPS TOOLING

6.1 Introduction

The SPS process is firmly tied to the tooling used in the process. The tooling considerations of SPS include the geometry of the tooling apparatus, the barrier between the powder and the die wall, and the actual tooling material.

The geometry of the tooling setup has large effects on the SPS process. This is in large part because the tooling actually creates the heat that is used to sinter the powder. The outer diameter of the die determines the diameter of the resultant pellets. The tips of the punches mirror the surface profile of the pellets. The size and shape of the punches and dies have a large effect on the power consumption of the process and on the temperature gradients within the tooling. During the SPS process, there is a small gap between the punches and the die. In the majority of SPS experimental work, a thin graphite foil fills this gap and prevents the powder body from coming in contact with the die wall. Furthermore, a thin graphite spray prevents the powder body from coming in direct contact with the punch tip. The graphite in the tooling reacts with oxygen freed from the powder forming carbon dioxide. The punch is also applying the pressure on the powder body. So the tooling provides the heat, the pressure and contributes to the gaseous environment the powder experiences.

The tooling material must have a high electrical and thermal conductivity so the current can pass through the tooling compact and thermal gradients are minimized. The primary method of heating comes from the resistive heating of the tooling material. The typical tooling material used is graphite. Graphite is unmatched in electrical conductivity, thermal conductivity and physical integrity at high temperatures. Graphite's

main drawback is that it is soft and has limited strength and poor wear resistance. Additionally, UO_2 does react with both graphite and Carbon Monoxide at temperatures over 1000 C, which is experienced during SPS. .

6.2 Tooling Considerations

Typically there is a graphite foil acting as a barrier between the powder and the die wall. This barrier prevents the powder from reacting with the die wall. It also prevent the powder from eroding the die wall. The barrier also directs current from the punch around the powder and into the rest of the tooling. Most SPS studies use a graphite foil as the barrier. For the contact point where the punch comes in contact with the powder, this is impossible. The punch end is a precisely machined surface, designed to imprint a shape onto the powder body. A rigid foil would prevent this. For the punch ends, a graphite spray has been used. The graphite spray was attained from ZYP coatings. A thin layer is sprayed onto the punch ends. This seems to do the trick; however, at high temperatures, the punch ends still react with the UO2 powder.

To determine if the graphite foil and graphite spray could be removed, preliminary studies were conducted with alternative coatings. A boron nitride coating, an alumina-based coating and a Yttria-based coating were explored. All of these were acquired from ZYP coatings.

The Alumina based coating consistently produced pellet failure. The pellets would continuously fracture immediately upon removal. After SEM examination, Figure 6-1, it was concluded that Al_2O_3 was coating the fracture surface. It is believed that the Al_2O_3, being an insulator, created a large temperature spike at the punch/powder

interface. This melted the Al_2O_3 and allowed it to find its way into the powder body interior leading to failure. The Al_2O_3 spray was scraped.

The Yttria based spray proved to be nearly indistinguishable from the graphite spray. Sometimes the Y_2O_3 spray outperformed the graphite spray but no conclusively. Additionally, the Y_2O_3 spray was significantly more difficult to remove form pellets during post processing.

The Boron Nitride spray prove to be unsafe to use. Other studies have used BN spray but on the single attempt made during this study, the die blew apart during sintering. For safety reasons, no more study were performed.

There was no barrier found to be adequate. For most studies, the powder was allowed to interact with the die directly. This had negative consequences described below.

There are six major factors to consider in the SPS tooling geometry: The outer diameter of the die, the inner diameter of the die, the length of the die, the diameter of the punches, the length of the punches, and shape of the punch tip. All of these can play a large difference in the results of pellet fabrication. Additionally, the gap between the punch and the die wall can actually prevent the process from even starting.

The most obvious factor to consider is die inner diameter. One of the key benefits of SPS is the ability to fabricate cylindrical pellets at a specific diameter; thus, removing the need for centerless grinding or other post processing. Is determined primarily by the inner diameter of the die. This surface acts as a physical barrier to the powder as it is being compressed upon startup. The ID continues to restrain any radial expansion of the pellet as pressure is applied during sintering. When fabricating pellets with a

diameter of 8.19 mm, the die ID was set at 8.20 mm as long as there was no graphite felt being used as a barrier. The graphite felt typically used in these experiments was .025 mm thick. So, an additional 0.05 mm would be required in the die ID making it 8.25 mm. In addition to acting as a physical barrier for the powder expansion, the die ID acts as a conduit, transferring current from the punch into the rest of the die. For this reason, if the die ID is too big or if there are inclusions on the die ID, then there will not be uniform current flow. Non-uniform current flow leads to temperature gradients and non-ideal sintering. For this reason, the die ID must be cleaned routinely with alcohol and/or a brush.

The die outer diameter plays more subtle roles in the SPS process. On first inspection, the die OD doesn't make contact with the powder, it doesn't make contact with the punch, and there should not be any wear on that surface. All the die OD does is provide a spot for the pyrometer to read the die temperature. On further inspection, the die OD has large effects on the process. The die OD determines the distance from the pyrometer measuring spot to the sample, it determines the mass of graphite that needs to be heated, it determines the resistance of the apparatus and thus the current required, and it is a contributing factor in the maximum force that can be applied to the pellet by the rams. This is due to the hooped stress placed on the die via the powder pressing into the die ID.

Recall that all temperature measurements are conducted via the optical pyrometer focused on the die OD. The larger the OD, the farther from the sample the pyrometer is reading. This also allows for the possibility of increased uncertainty in the measurement. Table 6-1 shows a simple study in which four dies of OD 2 in, 1.5 in, 1 in,

and 0.5 in were used to fabricate depleted UO_2 samples at a sintering temperature of 1100 C for 5 minutes, with a pressure of 40 MPa. The ID was kept constant. Three samples were fabricated in each die. As shown in Table 6-1, as the die OD decreased so did the average density of the pellets. It is notable that density decreased almost a full 2% purely by altering the die OD. Graphite has a high thermal conductivity, so it was surprising that the effect was so large. It is believed that the electrical consequences are at least as important as the thermal consequences of altering the die size.

The die OD also determines the total volume of the graphite and thus the total mass of the graphite tooling. The larger the die OD, the more energy is required to heat the whole apparatus. This is simply a matter of efficiency but, the total volume is highly dependent of the OD. The ID is set so as the OD begins to grow, the volume of the tooling grows quickly. The surface area to volume ratio increases with a decreased die OD, which would lead to higher energy loss due to radiative heat loss. This is neglected because the use of the graphite felt should minimize radiative heat loss. Also the larger the die, the more current is used to heat the die. This increases the current density in the punches and leads to localized overheating. For these reasons the die OD should be minimized. This may not be true if new materials were developed for the punch or dies tooling.

While minimizing the die OD is a good idea, there is a limiting factor in the strength of the die. While the powder compresses, the powder exerts a hoop stress on the die wall. Additionally, graphite is a brittle material. A larger die OD allows for a larger pressure to be applied to the sample while not leading to die fracture. For safety reasons, it was determined that the ID to wall thickness ratio should not drop below 2.0.

So the thickness of the die walls was set to be the same thickness of the sample and the OD of the die is 3 times the diameter of the sample to ensure the dies maintained structure integrity. By setting the die dimensions, the density of the pellets could be controlled by changing sintering parameters.

The final consideration for the die OD is the effect on the current and the current path. The resistance of a hollow cylinder to current flowing along its axis is proportional to the reciprocal of the difference of the squares of the radii. So decreasing the die OD, increases the resistance of the die. This requires a larger voltage to push the current through the die. The power of joule heating is proportional to resistance. Also, the current path is related to the relative resistance of the sample and die. This means the die OD may affect the amount of current that flows through the sample itself. In an insulator, this effect would be negligible. In a conductor, this effect could be large. Since, UO_2 is a semi-conductor, it is unclear the effect die OD had on current flow through the sample.

The specifics of the thermo-electrical effects of die size are beyond the scope of this study, but it is obvious that the die OD affects the thermo-electrical environment of the tooling and most likely the sample as well.

The final dimension of consequence on the die is its length. The die length has similar efficiency consequences as the die thickness but without many advantages of a long die. A longer die requires more energy to heat, may have larger temperature gradients, and is costlier to make. There are two factors creating a minimum die length. The limiting factor was found to be ability of this researcher loading powder into the die. The funnel density of the powder is about 10% TD and even with some pressure

applied by hand, the powder is about 20% TD before being placed in the SPS machine. With a powder mass of 5.5 g, the powder body is about 50 mm in length before consolidated in the SPS machine. Any die smaller than 65 mm proved to be either difficult or impossible to load. The other consideration is, the shorter the die, the smaller the interface between the punches at the die wall are. A larger die/punch interface optimizes heat and current transfer.

The dimensions of the punch affect the SPS process. The punch diameter is simply as large as possible while still freely moving in the die. For most processes, if the die ID was 8.20 mm, the punch diameter was set at 8.15 mm. A larger punch diameter was desired but it was found than a larger punch diameter prevented the punch from moving freely within the die. This was usually due to either powder being stuck between the punch and the die or due to flaws in machining either the punch or die.

The punch length is a major contributor to the condition of the final pellets, specifically the pellet end geometry. All of the current travels through the punches; this means the current density of the punches is much higher than the current density in the die. This leads to higher temperatures in the punches. The higher temperature in the punches may be mitigated by heat transfer to the die. Heat transfer to the die is a function of the contact area between the punches and die. Joule heating is also proportional to the length of the resistor. A longer punch attains a higher temperature during the sintering process. A longer punch is also more susceptible to buckling during the process. SPS studies at UF started with 40 mm long punches. When the first studies shifted to 17x17 pellets, the pellet ends were constantly being fabricated with poor quality. Reducing the punches to 30 mm prevented most of those problems. Any

reduction less than 30 mm doesn't allow the pressure to be continuously applied to the sample.

During the course of this project, four materials have been used as the material for the die. Overwhelmingly, graphite has been the material of choice from the die. This is the industry standard for SPS studies. Tungsten Carbide, Molybdenum, and Silicon Carbide were also used to machine typical single pellet dies. These three materials were chosen in attempt to prevent negative consequences of graphite tooling. In all materials, the punches were made from the same material as the die.

Graphite has great electrical properties, adequate thermal properties and high strength at elevated temperatures. Graphite (Hardness 15 MPa)) is much softer than UO_2 (Hardness 8.5 GPa) and hence it erodes easily. While not having a barrier between the powder and the die led to excellent surface finish on the pellets, it also led to surface erosion on the die interior wall. The UO_2 (white) wears away the graphite (grey) and then adheres to the die wall (Figure 6-2). This reduces the dimensional reliability of the pellets. As the die wall is progressively worn away, the pellets get slightly wider at these locations. This process may lead to pellet chipping, surface deformities or even fractures upon removal. As the UO_2 powder sticks to the graphite die, the dimensions of the pellet also get disturbed. The process is less severe compared to punch tip erosion discussed earlier, but still undesirable. The stuck UO_2 on the die surface may also cause scratches on the pellet while it is being removed from the die and contribute to poor surface quality of the pellet.

Of the 3 additional materials investigated, none made it through sintering a single UO_2 pellet. The SiC die fracture upon initiating startup. This die fractured radially. The

Molybdenum die failed to complete a circuit. The Tungsten Carbide die worked as planned but at a temperature around 900 C, the punches buckled and failed. These studies made it obvious that at this time, graphite would still be required. Other materials may be possible, but they must be capable of reaching very high temperatures while maintaining strength.

To test the repeatability of and wear properties of various punch materials, punch tips were machined out of three different materials, graphite, Yttria Stabilized Zirconia, and Boron Carbide. These punch tips were then used to consecutively fabricate five UO2 pellets each. After pellets runs began, this number was altered to 5 for graphite, 4 for YSZ and 3 for B_4C. The dimensions of the fabricated pellets were then measured and the profile of the pellet ends were measured via the profilometer. These results were compared to better understand the effects of using the various materials.

The graphite punches were machined with the same vendor used for the rest of the study. These are the standards used in every SPS study conducted at UF. The YSZ was pure tetragonal phase, fine grain material, machined into the desired punch tip shape. The Boron Carbide punch tips were fabricated here at UF via SPS. Punch tips with the mirror image of the desired profile were used to fabricate B4C parts with the desired end profile. The dies used in all pellets were new graphite dies with no barrier between the die wall and the powder.

The initial design was for all pellets to be sintered at a peak SPS temperature of 1050 C for 5minutes with a pressure of 40 MPa applied. This was altered for the YSZ pellets. These alterations are discussed below.

Many graphite pellets were fabricated during this project, but five were fabricated specifically for the purpose of evaluating tooling wear. After each pellet, the physical changes in the die and punches were observed. Figure 6-3 shows the erosion of the dish forming part of the punch. The punch to the far left was used 5 times. The one to the far right is a virgin punch, fresh from being machined. The dish forming region of the punch erodes as it is used multiple times. This is due to graphite being soft while UO_2 is very hard.

The resulting erosion of the dish is shown in the profilometer measurement of the pellets, shown in Figure 6-4 and described in Table 6-2. The virgin punch created a dish 0.247 mm deep, which met design specifications. As the punch was reused, the dish became gradually shallower until the fifth pellet in the run, which at 0.097 mm deep was only forty percent of the original dish depth.

In an attempt to overcome this occurrence, an intermediate punch tip has been introduced between the punch and powder. The punch is then flat on both sides, with the punch tip being flat on one end and machined on the other. The material for this was chosen to be harder than graphite. Two choices were made; one with a higher electrical resistance than graphite and one with a low electrical resistance. A high resistance leads to the current diverging at the interface with the punch tip. This situation would effectively put less stress on the interface of the dish of the pellet. This material was the YSZ. For this process to be a beneficial addition to our sintering method the punch tips have to have a reusability of more than 6 while still producing satisfactory dishes.

Using YSZ punch tips, the first pellet was sintered at 1050C for 5 mins. This pellet came out so good that the temperature was decreased to 1000C for the 2nd test. A similar result was observed with 3rd pellet. The 4th pellet was sintered at 900C for 5mins. None of these sintering processes used added pressure (usually 40MPa). Pellets 1 and 4 are shown in Figure 6-5.

High density was not the original intent of this experiment but this sintering result has offered a means of achieving high theoretical density at a lower sintering temperatures and with less time needed for processing. It is believed that even higher density can be achieved at lower sintering temperatures with the application of pressure (40MPa) at the hold temperature. This result does not imply the actual temperature inside the die is in fact 100 degrees lower, but the temperature distribution changed quite significantly with the addition of the ceramic punch tips, allowing for a lower tooling temperature.

It was noticed that the even after cleaning the punch tips they still keep residual graphite spray, the amount increases with each successive test. After the 3rd pellet a graphite foil inclusion was noticed on both the punch tip and the pellet itself. The dish surface appears to be just as defined after the 4th test as it was after the 1st. The punch tips are shown in Figure 6-6. Profilometer measurements confirm that observation and are shown in Figure 6-7. The dish remains close to the ideal depth throughout the four pellet run. These measurements are described in Table 6-3. It is clear that the YZS punches did not wear like the graphite punches. The pellets are not quite as cosmetic as some of the pellet made with graphite punches but they are sufficient. The central

ring, present to previous pellet, is not only present but may be more prominent with the YSZ punch tips.

The B_4C punch tips could not be purchased externally. These were fabricated in house at UF. To fabricate the B4C punch tips, graphite punches with a dished end were fabricated. Then B4C powder was obtained and sintered with those graphite punches. This produced the goal punch tip shape in the B4C; however, there was not any quality control of this process so the actual dimension of the B4C punch tip are not known. The pellets made with the B4C punch tip were all high density (above 95% TD). The profilometer measurements for those pellets is shown in Table 6-4. The Profilometer measurements are shown in Figure 6-8. It is obvious the dish is a different shape than when produced with the graphite or YSZ punch tips, but the shape remains stable over the three pellets. These two studies show that the graphite's main drawback, when it comes to reliability, is its softness and tendency to wear away.

To further understand the effect the punch tips had on the SPS process, the temperature, voltage, displacement and power profiles of the YZS punch tips used to fabricate a pellet at 1050 C were compared with a typical graphite punch used for the same purpose. These profiles are shown in Figure 6-9. The temperature profiles mimic each other exactly. The Z-axis displacement and power profiles are also very similar and nearly identical. The only difference is the voltage profile. The ceramic YSZ requires more voltage to drive the current through the tooling. This is because the ceramic has a higher resistance. This difference is obvious when watching the process as the punches get very hot with the ceramic punch tip. This is because the higher contact resistance between the graphite punch and the ceramic punch tip as opposed to

just having a pure graphite punch and tip. The interesting bit is that the power output was still the same, indicating the current was lower for the ceramic punch tips. The same product was produced, but the environment was slightly different.

As stated above, the ceramic punch tips enabled full density pellets to be formed with a die temperature of only 900 C. This was interesting because with graphite punch tips, full density required 1050 C. The temperature, voltage, displacement and power profiles of the YZS punch tips during the 900 C run are compare to the 1050 C run in Figure 6-10. As shown, the temperature profiles follow each other, with the exception of the peak temperature of course. The voltage profiles follow similarly. With the lower temperature, the power profile shows the 900 C run required half as much power as the 1050 C run. The displacement profiles followed each other and the densification plateau occurs between 850 and 900 C. In the graphite run, the plateau occurs at 1050 C. The cause of this phenomena is unknown. It would seem either the temperature distribution in the tooling is different, or the current path is different. Whatever, the cause of this phenomenon, the pellet achieved full density at half the power requirement and without any tooling wear. A similar study with the B4C punch tips was not performed. B4C is of interest because it has a much lower resistivity than YSZ.

6.3 Conclusions

This study shows the large impact the tooling has. Every aspect of the tooling has a significant effect on the process and must be designed. The die dimensions allow for modifications if the rest of the tooling must meet certain requirements. The most important aspect of the tooling is the tooling material itself. Even the small punch tips, while achieving their initial goal of forming the pellet end, radically changed the current

and temperature gradients in the compact. These punch tips were far superior to graphite punch tips, at least in regards to wear resistance and reactivity with the UO_2. This complicates the process but allows for vast possibilities previous unexplored. Advanced tooling may considerably improve the process, even to the point of being more efficient than conventional sintering.

The most interesting change with the ceramic punch tips was the effect on the required sintering temperature. The YSZ punch tips led to a reduction in the required sintering temperature from 1050 C to 900 C. It was implied that this may even be as low as 800 C. The sintering temperature is of course the temperature at the die exterior. The power requirements were not significantly different for YSZ as compared to graphite, when the same temperature was achieved. This indicated the 900 C YSZ run required half the energy to get the same product. Further investigation is require to determine the nature of this result.

The most obvious requirement for commercialization of SPS is the removal of the graphite foil. A high conductivity barrier seems to be required to get a high density product; however, this is both clumsy and negatively impacts the pellet exterior. The work with other materials as a die material proved fruitless. The studies with the YSZ and B4C punch tips show other material can be used to interact with UO2 directly. Additional work is needed to determine a barrier between the powder and the die wall.

Graphite tooling may still be required in some capacity. Every die fabricated with a non-graphite material failed immediately. The graphite seems to be required for current flow and heat generation. It is suggested that the outermost portions of the die and punch remain graphite, while the inner portion, in contact with the powder, be

modified to a different material. This also makes sense economically, since graphite is cheap and easy to machine into the required shapes.

Table 6-1. Pellet density with varying die outer diameter

Die OD	Average Density (%TD)
~2”	98.1%
~1.5”	97.7%
~1”	96.6%
~0.5”	95.3%

Table 6-2. Comparison of dish depth in a five pellet run with graphite punches

Parameter	Goal Depth (mm)	1st Pellet (mm)	2ndPellet (mm)	3rd pellet (mm)	4th Pellet (mm)	5th Pellet (mm)
Dish Depth	0.254	0.247	0.221	0.198	0.172	0.097

Table 6-3. Comparison of dish depth in a four pellet run with YZX punches

Parameter	Goal Depth (mm)	1st Pellet (mm)	2ndPellet (mm)	3rd pellet (mm)	4th Pellet (mm)	5th Pellet (mm)
Dish Depth	0.254	0.245	0.244	0.246	0.244	N/A

Table 6-4. Comparison of dish depth in a three pellet run with B4C punches

Parameter	Goal Depth (mm)	1st Pellet (mm)	2ndPellet (mm)	3rd pellet (mm)	4th Pellet (mm)	5th Pellet (mm)
Dish Depth	0.254	0.262	0.266	0.257	N/A	N/A

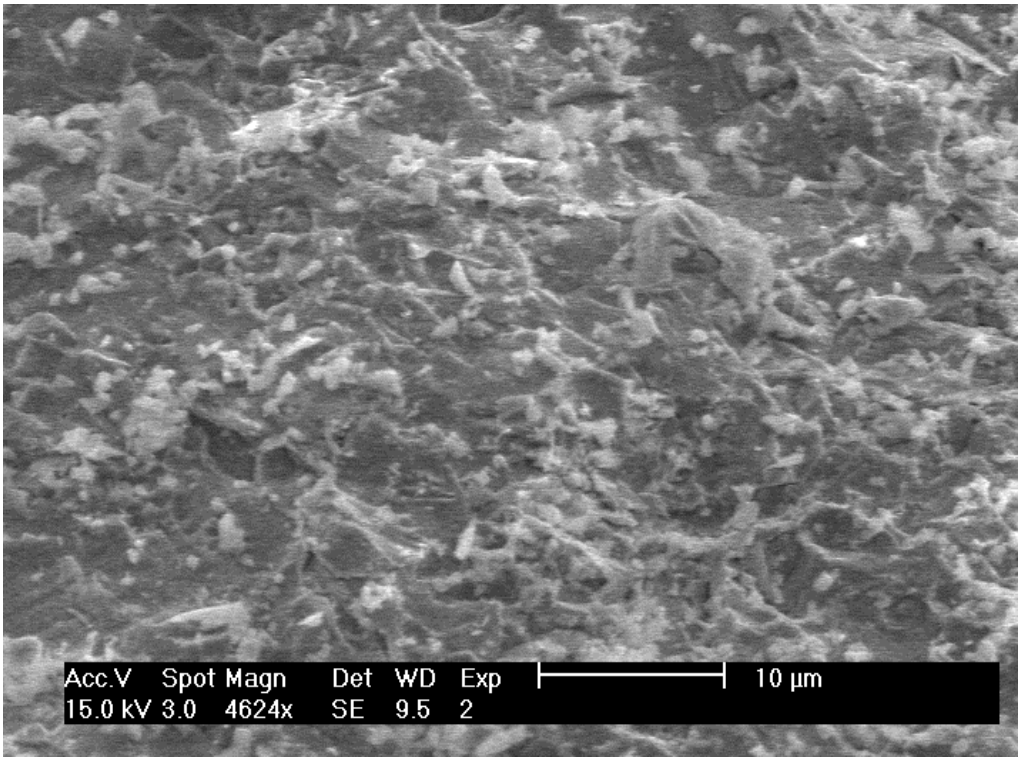

Figure 6-1. Fracture surface of pellet fabricated with Al_2O_3 spray showing Al_2O_3 coating fracture surface. Photo courtesy of the author.

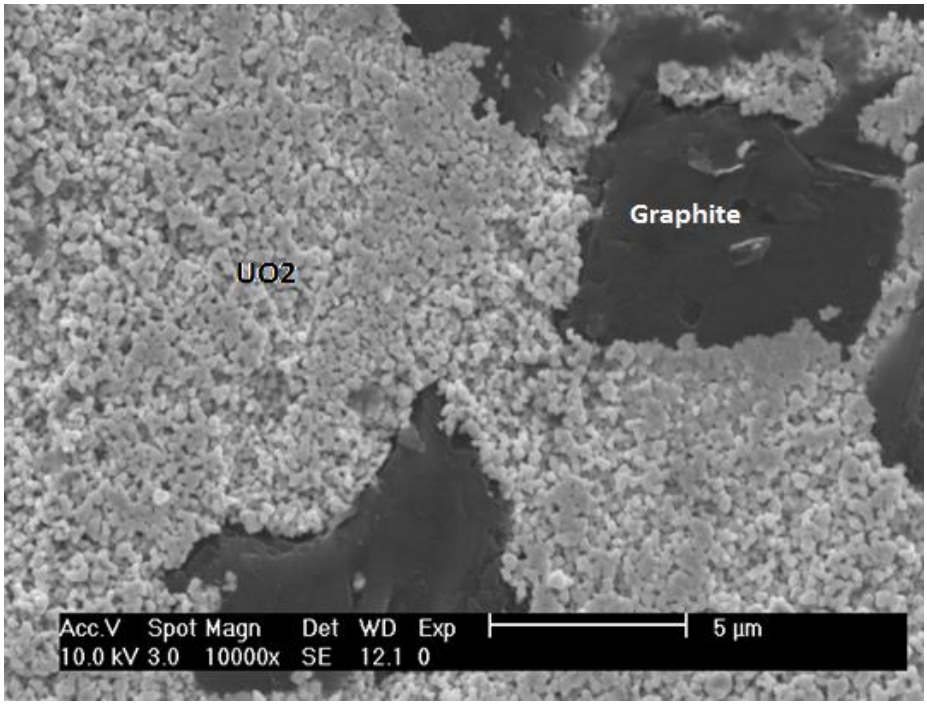

Figure 6-2. SEM image showing UO_2 powder inclusions on die interior surface. Photo courtesy of the author.

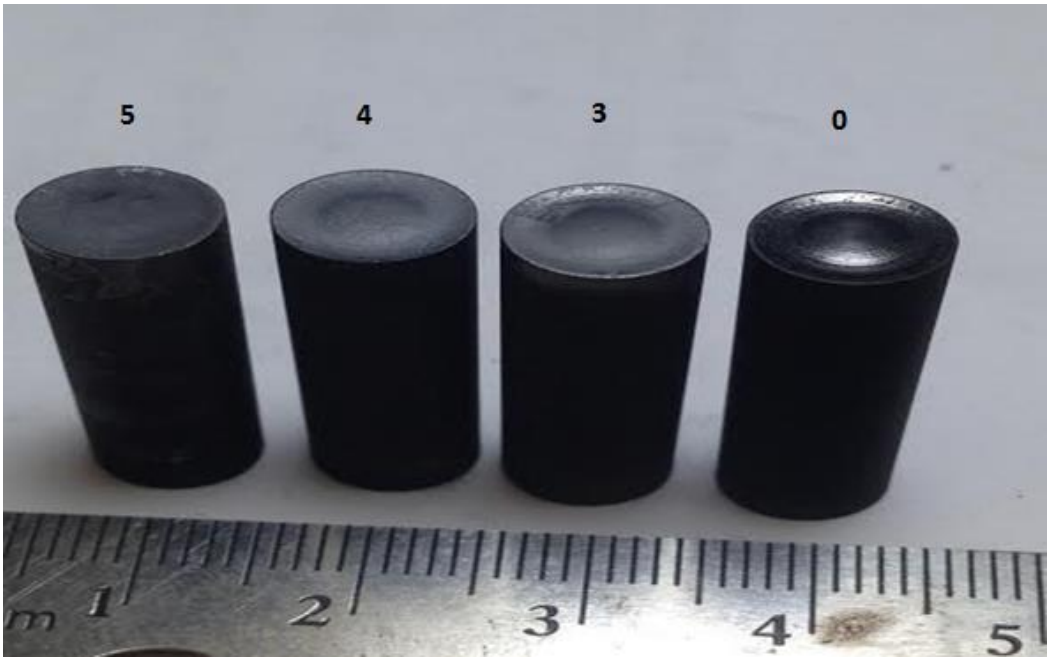

Figure 6-3. Images of the punch wear with usage. The number of times each punch was used is indicated on the top. Photo courtesy of the author.

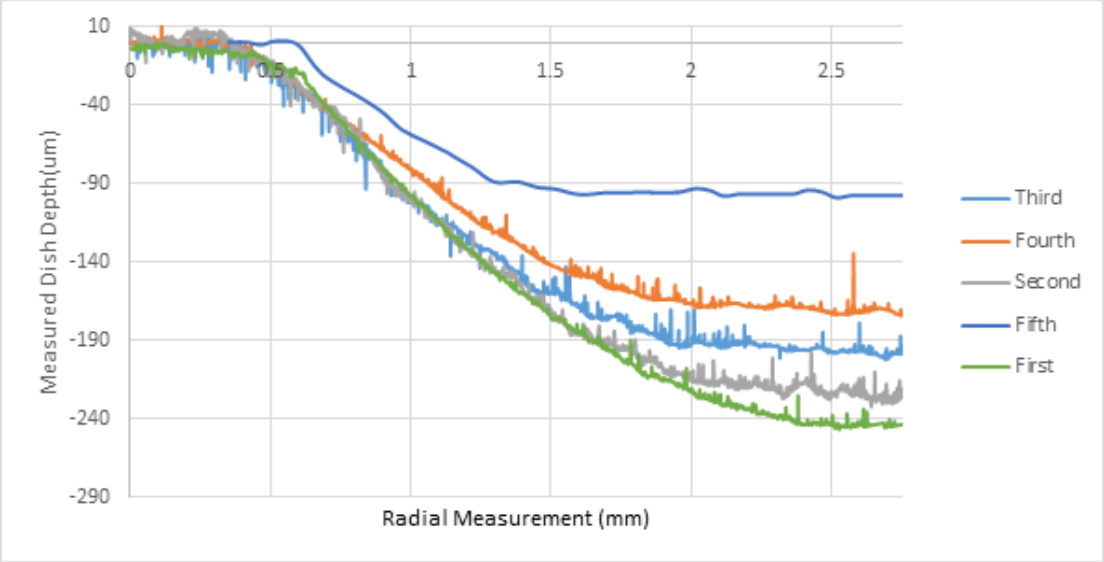

Figure 6-4. Comparison of dish depth from 1st pellet produced to 5th pellet showing tooling wear

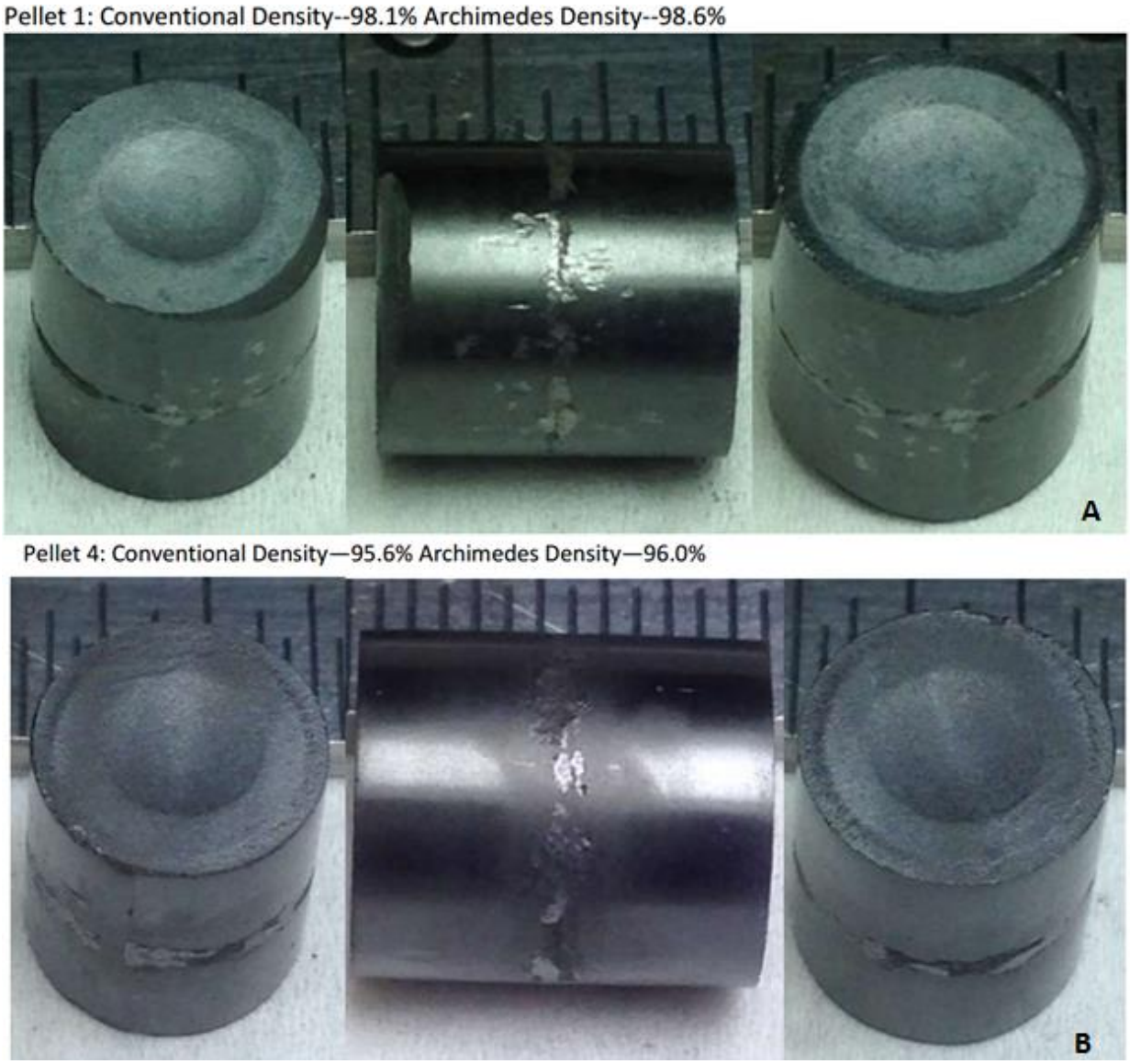

Figure 6-5. Pellets produced with YZX punch tip. A) First pellet produced. B) Fourth pellet produced. Photo courtesy of the author.

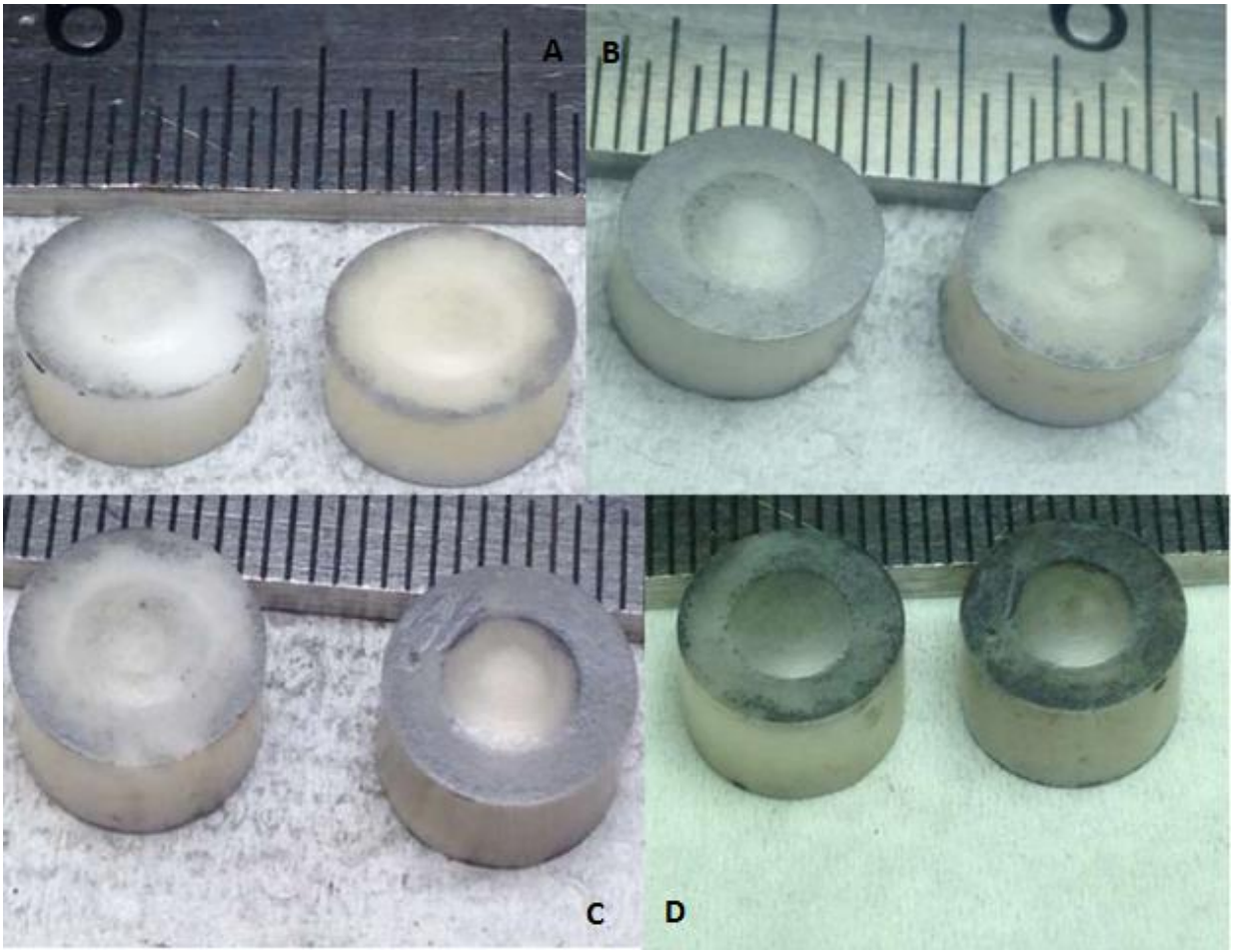

Figure 6-6. Punch tips after use. A) Pellet after first run. B) Pellet after second run. C) Pellet after third run. D) Pellet after fourth run. Photo courtesy of the author.

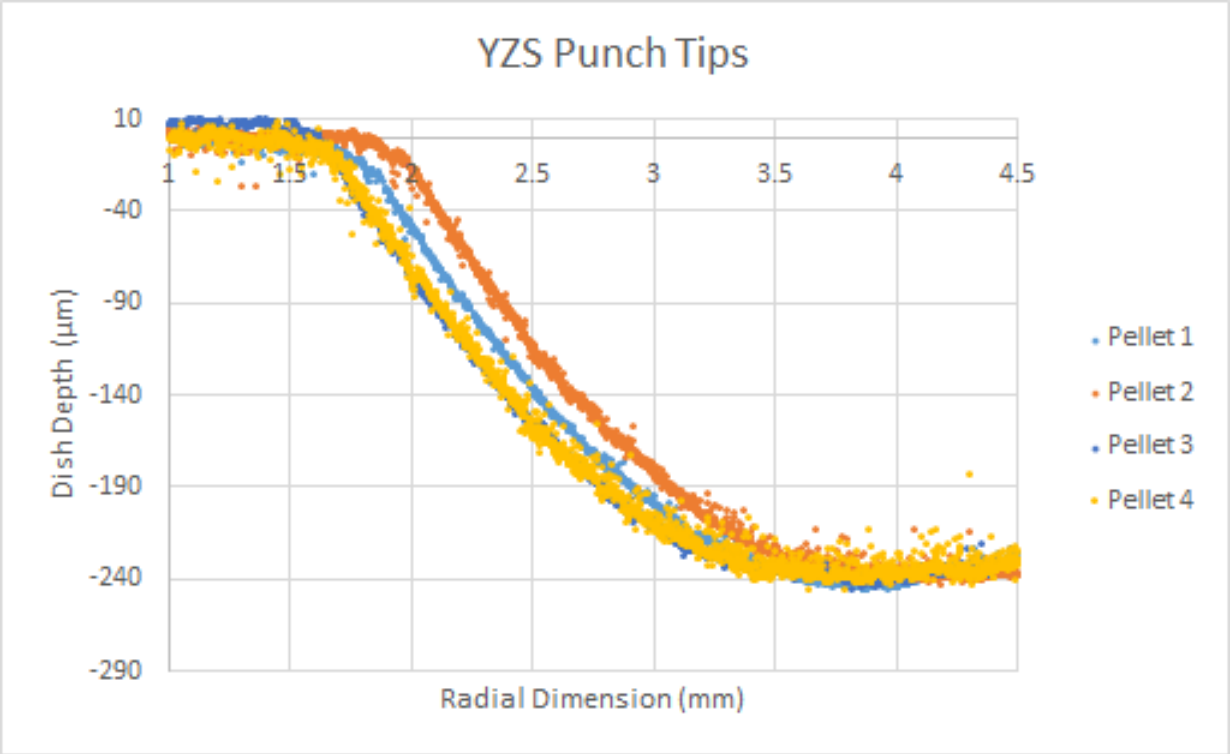

Figure 6-7. Comparison of dish depth from 1st pellet produced to 5th pellet showing tooling wear with YSZ punches

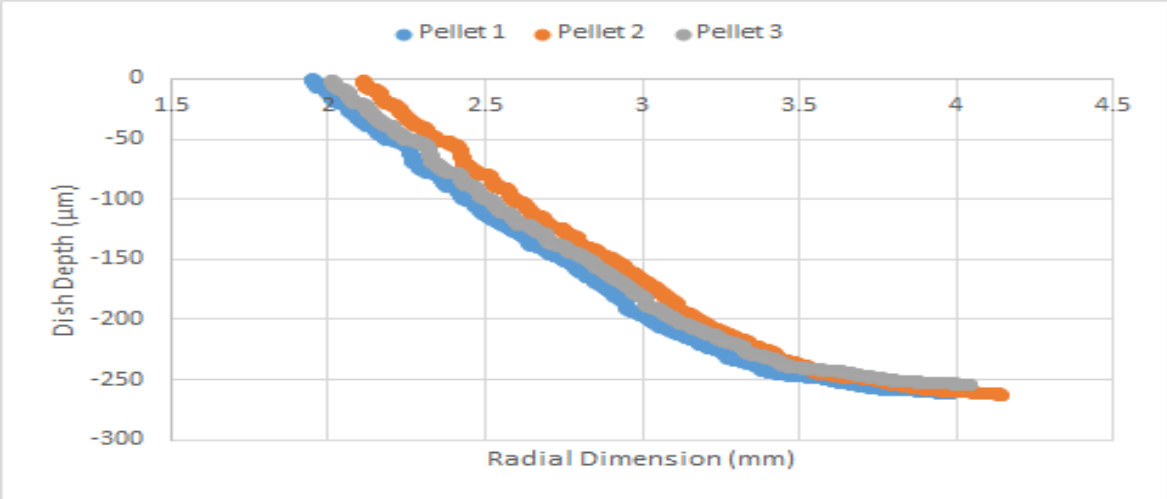

Figure 6-8. Comparison of dish depth from 1st pellet produced to 3rd pellet showing tooling wear with B4C punches

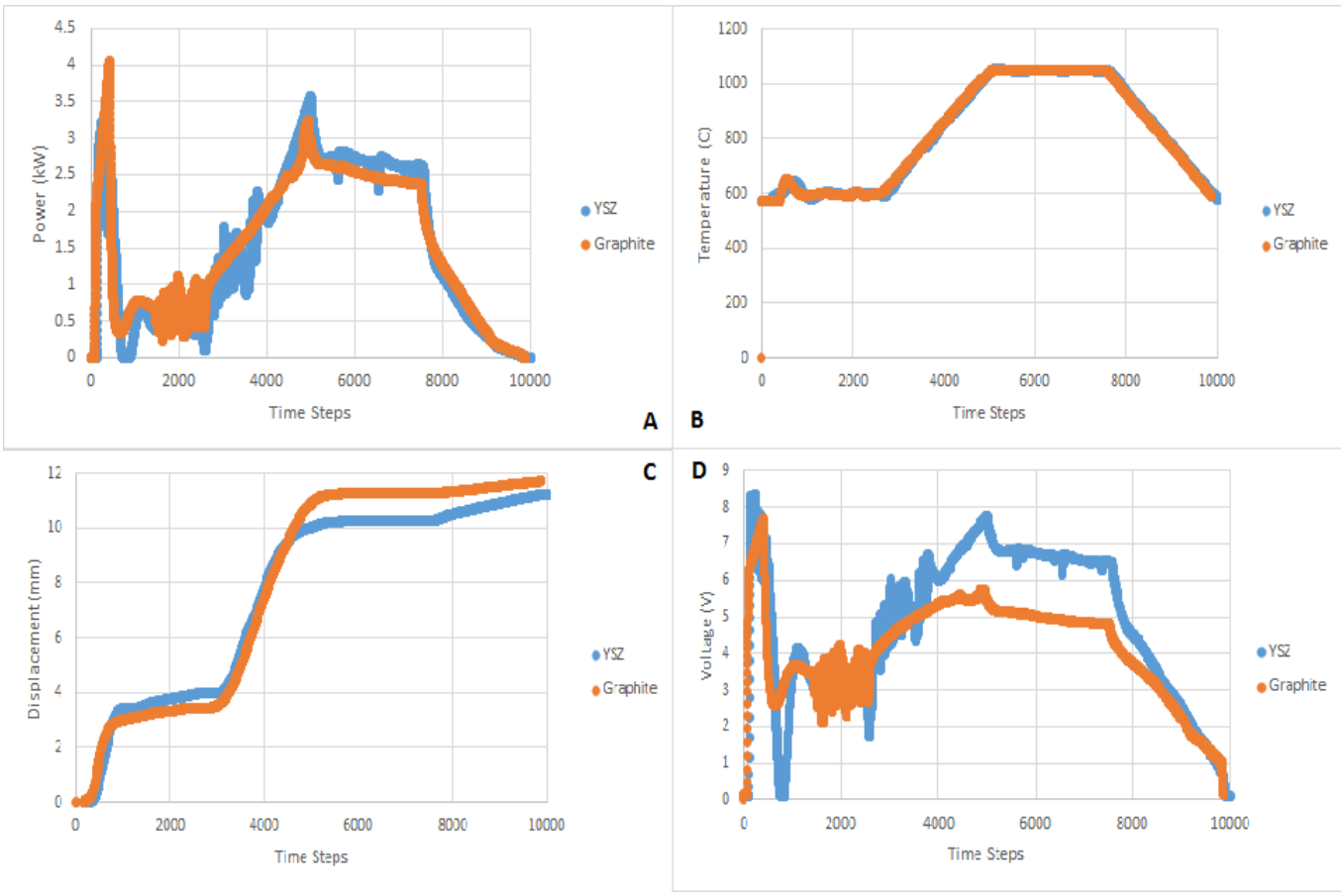

Figure 6-9. Profiles of SPS of the YSZ punch tips vs the graphite punch tips A) Power profile. B) Temperature profile. C) Displacement profile. D) Voltage profile.

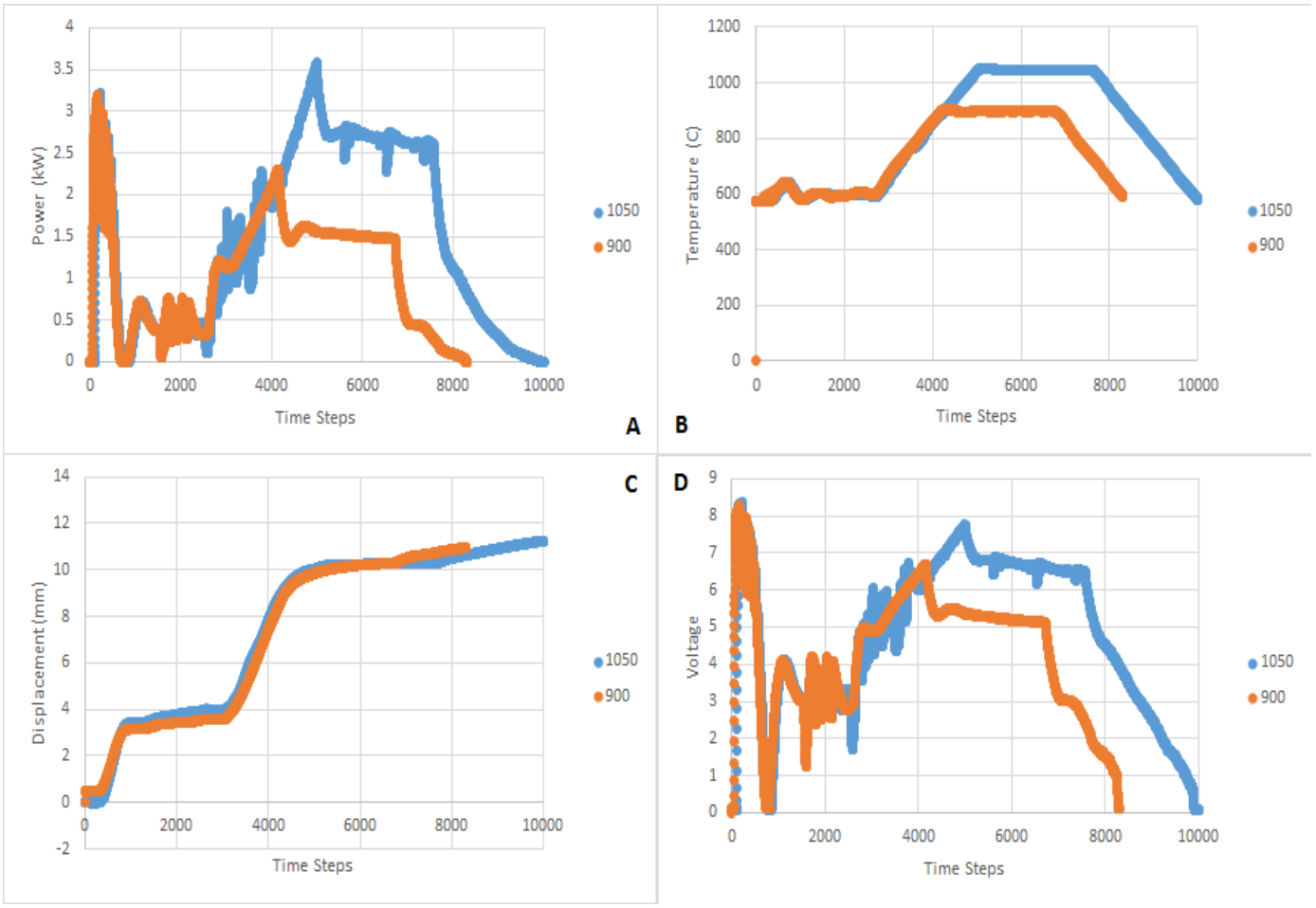

Figure 6-10. Profiles of SPS run of YSZ punch tips at 1050 C vs 900 C A) Power profile. B) Temperature profile. C) Displacement profile.

CHAPTER 7
SCALING UP PRODUCTION

7.1 Introduction

The commercial production of nuclear fuel is a large scale, twenty-four hour-a-day, mature process. A single fabrication facility produces 400 million pellets per year. While the results discussed above are encouraging, producing pellets one at a time, once per hour, would require over 45,000 SPS machines working 24 hours a day. Obviously, multiple pellets must be produced in a single production run. In the conventional process, pellets are pressed in batches of about 60, then loaded onto large containers and sent off to the furnaces. While the process to sinter any individual pellet is long (up to 17 hours), hundreds or thousands of pellets are being fabricated at any given time. Conversely, the SPS process sinters a single batch very fast (as little as five minutes), but the batch sizes have yet to be determined and will undoubtedly be smaller than the batches in the conventional process. To this researcher's knowledge, there are no published studies on fabricating multiple samples via SPS.

The most straightforward and easiest batch SPS method to implement is to continue to use a single die, but increase the number of pellets that can be loaded and sintered in that die. Alternative methods would instead use multiple dies within a single SPS machine. The use of multiple dies would make the application of pressure to the powder bodies much more complicated. This study focusses on increasing the number of pellets in single die and determining how many pellets can be produced in a single run of the Dr. Sinter SPS 1030. There are two obvious ways of increasing the number of pellets in a die: stack powder bodies in a single cavity (series production) and machine more cavities in the die (parallel production).

In this study these two methods were explored and then paired to determine if multiple commercial grade pellets could be successfully fabricated in a single SPS run. The pellets underwent the same qualification procedures used on the single UO_2 samples. The methods were compared and discuss. Then, a POC experiment was performed to test the maximum number of pellets the Dr. Sinter SPS 1030 could handle.

7.2 Experimental Procedures

All attempts at multiple pellet fabrication were performed using calcined depleted UO_2 powder with a nominal enrichment of 0.50 %, as supplied by Areva. The powder had a reported bulked density of 2.5 g/cm^3, a BET surface area of 3.11 m^2/g, and an average particle size of 2.4 microns. The grain size of the UO_2 was 100-400 nm. The O/M ratio of this powder was 2.11. This powder comes directly off the AREVA fuel line after U-235 was removed during the enrichment process. The powder contained no additional additives.

The process to fabricate two pellets in series was similar to fabricating a single pellet. The die length, punch length, and the powder loading procedure in the die were different. The die was made longer (105 mm) to accommodate two pellets and the punch lengths were extended to 40 mm, as shown schematically in Figure 7-1. A punch was first inserted on one end of the die and then the powder for one pellet was poured. A graphite spacer punch with mirrored pellet end profiles was then introduced. All surfaces of the graphite spacer are covered with graphite spray. This is done to prevent reaction between the powder and the spacer, and to decrease friction between the spacer and the die wall. Then the powder for the second pellet was poured and the upper punch was inserted. The die was then placed in the SPS machine.

The temperature profile used included a seven minute initial dwell time at 600 C to allow the pyrometer to calibrate. The die was then heating 100 C/min for 4.5 minutes to achieve a peak temperature of 1050 C. This temperature was held for 5 minutes while applying 40 MPa of pressure. The die was then cooled at 100 C/min for 4.5 minutes, followed by natural cooling for one hour. This process is the same as a single pellet except for the longer initial dwell time. To achieve this temperature profile, a larger current (1200 A) was needed than for the single pellet production. Both sintered pellets were then removed and characterized. While removing from the die, it was noticed than no additional pressure was required to remove the pellets. They basically just fell right out. In this manner, twelve pellets (6 batches of 2 each) were produced and characterized. Dies were reused for 3 batches each, making two dies required for the whole fabrication.

The die design was then modified to fabricate four pellets in each run. Four pellets were fabricated in parallel in a single run by using the larger die with four cavities shown in Figure 7-2(b). This die was 65 mm long with an outer diameter of 42 mm. The cavities' edges are 6.35 mm from the die exterior and 6.35 mm from the die central axis. 5.50 grams of UO_2 powder were placed in each of the four cavities. Eight punches (four on top and four at the bottom) were then used to fill the cavities and apply axial pressure to the powder. Graphite spray was applied to the tips of these punches. The typical graphite felt was placed around the die exterior.

The die was then placed in the SPS machine. The sintering parameters for this large die were slightly different than for the smaller die. First the dwell time, the hold at 600C to allow the pyrometer to calibrate, was 10 minutes. This is double the dwell time

used for a single die. The heating rate was kept at a constant 100 C/min. The die was heated for 4.5 minutes to 1050 C and held for 5 minutes with 40 MPa of applied pressure. To attain this pressure, an effective diameter and thus effective area of the punches had to be programmed into the SPS controller. This simply required telling the SPS controller the diameter of pressure application was twice as large as for a single cavity. The temperature was measured, as before, on the die exterior, not in the powder body. Twelve pellets in total were produced with the die shown in Figure 7-2(a).

To fabricate eight pellets in a single run, the series and parallel methods discussed above were combined as shown in Figure 7-2(b). This die has the same dimensions as the four pellet die except it is 110 mm long as opposed to the 65 mm length of the four pellet die. This die uses eight machined graphite punches, four graphite inserts, and a large thick graphite felt, which insulates the die. The standard pellet mass (5.5 g) was used. The loading process was to place a single punch in a single cavity, then pour 5.5 g of UO_2 powder into that cavity. This powder was compressed by hand via a metal punch to make room for the second powder body. After compressing the first powder body, the insert was placed into the die cavity. The second powder body followed the insert and a second punch was placed on top of the second powder body. This whole system was then compressed by hand and fastened with electrical tape. Then the other three cavities were filled with the same methods. The process of loading this die took around 30 minutes as opposed to the one minute it takes to fill a die for a single pellet. This was due to the awkward handling of the large die and the need to constantly secure the die before moving. An automated system would greatly reduce the loading time. After the four cavities were filled, a thick graphite

felt was wrapped around the die with a 1cm by 1cm hole in the felt. The hole is so the pyrometer can measure the die temperature. The sintering parameters were identical to the 4 pellet die as described above with the one exception that the peak temperature was 1150 C instead of the 1050 C. The higher temperature (1150 vs 1050) was chosen because preliminary work [43] suggested that this temperature provides the desired density in each pellet.

Finally, a large proof of concept batch was fabricated. The POC used the largest die that could fit in the Dr. Sinter SPS 1030 and 19 cavities were drill through the die. These cavities were filled with 5.5 g of UO_2 powder for a parallel production run of 19 pellets. The spacing between cavities was kept constant and identical to the four pellet die described above. A complete schematic is shown in Figure 7-3(b). This die (Figure 7-3a) required 38 machined graphite punches. The loading time for this die was over one hour and took two researchers.

The die was placed in the SPS furnace and the temperature was brought up to 600 C. The dwell time at 600 C was 10 minutes to ensure the temperature was measured correctly. The temperature was then increased to 1150 C in 5.5 minutes at 100 C/min. The die was then held at 1150 C for 5 minutes then allowed to cool naturally for 1 hour. No pressure was applied during the hold leaving the pressure on the pellets at around 1 MPa. This was done for safety reasons. The large die would require a much higher force to produce to 40 MPa typical of sintering UO_2. If there was some small contact deviation so that a single punch felt this whole force, then the entire die could fail. This was just a first step to prove so many pellets would be sintered. The density was expected to be less than previous pellets made. After sintering, the 19 pellets were

removed, cleaned and characterized. The die during sintering is shown in Figure 7-4. As shown, there is plenty of energy being lost due to radiation.

7.3 Results and Discussion

The twelve pellets produced as stacked doubles are described in Table 7-1. Consecutive pellets were made in a die with the odd numbered pellet on top in the die and the even number below it in the die.

Three pellets were at a lower density than the specifications, with two pellets under 92% TD. The reason for this results may be an increased friction with the die wall. There is twice as much powder in contact with the die wall in this fabrication scheme than in a single pellet fabrication, thus twice as much friction. Additionally, the graphite insert between the two powder compacts also appeared not to slide smoothly during powder packing due to stray UO_2 powder being lodged in the small space between the insert and the die wall. However, nine of the twelve pellets have met the specification. These twelve pellets all had the grey ring at their center.

There was a visible difference in the quality of the dish on two surfaces of a pellet made in this stacked configuration. The surfaces of the pellets that were in contact with the central insert were superior as compared to the other two surfaces that were in contact with the punches, (Figure 7-5). The surfaces in contact with the punches had small amounts of graphite in the dish. In the SPS process, the current flows through one punch into the die and down through the other punch. The heat produced is mostly through resistive heating throughout the punches and die. Neither the heating nor the radiative loss are uniform throughout the entire tooling assembly. These factors, along with the geometry variations along the tooling assembly, lead to temperature gradients in the tooling. These gradients are even more severe in the two pellet stacked

arrangement. Our research group is currently conducting a coupled electro-thermo-mechanical modeling of the SPS tooling process [43]and our preliminary modeling efforts have shown that the temperature gradient indeed exists across the specimen length and especially in the two-pellet configuration. A temperature gradient in the tooling is undesirable and can produce deleterious effects on the sintered samples.

The results of the four pellets fabricated in parallel in a single die are presented in Table 7-2. Once again, these pellets did not achieve adequate density, but they did display the desired dish and chamfer shape. The low density may be due to two reasons: (i) the maximum current available in the Dr. Sinter®1030 machine is 3000A and it was noticed during the fabrication that this value reached its limit and hence the maximum desired temperature could not be reached. (ii) It is also quite likely that, severe temperature gradients existed among the four pellets, resulting in uneven temperature distributions and possibly lower temperatures in the powder when compared to the single pellet production. Finally, the applied pressure on the four pellets was not sufficient to cause full densification. Furthermore, the pressure may not have been equally distributed to compress the four powder compacts equally. This would have led to reduced green pellet density prior to sintering and hence a lower final pellet density.

The surfaces of these pellets had no visible defects. The dish and chamfer geometry were visible on all pellets; however, the pellets had lower densities than the desired values. The parallel production leads to reduced density with the available amperage. These four pellets had the grey ring at their center.

The details of the eight pellets produced in series and parallel in a single die are described in Table 7-3. All pellets had a smooth surface finish and a clearly visible dish and chamfer. All pellets had the grey ring at their center. The pellets were produced with the desired length and diameter. The average density was low but within the acceptable range according to the specifications (Table 7-3). There is a loose correlation between pellet diameter and pellet density. Pellets 1 and 2 are both less dense and smaller than the other 6 pellets. Additionally, pellets 1 and 2 were produced in the same cavity. This cavity had a slightly smaller diameter than the other three cavities, due to a machining error. This led to the smaller diameters. It is unclear if this led to the reduced density in pellets 1 and 2. Other possibilities are temperature gradients within the larger die. The temperature distribution is expected to be more uneven than in the smaller dies. If cavity 1 was off-center, then it would have a lower temperature than the other three cavities. All pellets have a higher density than the four pellets produced in parallel but a lower density than pellets produced only in series. These pellets were sintered with a higher external die temperature than the pellets produced as singles (Table 7-1) or in series (Table 7-2), but still were less dense.

The 19 pellets fabricated in the 19 pellet die are briefly summarized in Table 7-4. It is clear the pellet are not dense. All pellets average 63.7 % TD. The die has three rings of pellets starting at the center. The interior ring is the single pellet in the center. The middle ring is the 6 pellets outside the interior ring. The exterior ring is the 12 pellets on the die exterior. There is not a large difference in the density of the pellets in any ring. This study took place with no added pressure. There was very little force compressing the powder and it shows. Without the pressure application, the SPS

process is not the same, obviously. 19 pellets could still be heated in parallel and there were sintered. They were not just green bodies. Future experiments should include the application of pressure.

The various profiles extracted from the SPS machine are edifying. The temperature profiles for the fabrication of one (single), two (double), 4 (quad), and 8 (Octo) pellets are compared in Figure 7-6. The eight pellet die was heated to 1150 C as opposed to the 1050 C of the other dies. Also the four and eight pellet dies had a longer startup time. These conditions are easily read from the figure. Everything else looks identical. This is of course because that is what the SPS controller does; it simply ensures the desired temperature profile by adding current until the desired temreapture is reached.

The voltage profiles found in Figure 7-7 begins to show the variation that occurs during the SPS process for the various die sizes. The initial voltage spike implies the relative resistance of each die. This is because the SPS controller does not have any input for die geometry etc. It simply uses a set punch diameter to calculate pressure. The voltage spikes for the stacked double die more than the other dies (Figure 7-7). This implies the stacked double die had a higher resistance than the other dies and required the higher voltage for current flow. The voltage profile is similar for each die but with variation based simply on magnitude and the startup time. The voltage during the process is required for heating up the compact and follows the expected trend of the larger the die the more required voltage to achieve the maximum temperature.

Figure 7-8 shows the electrical power profiles of the sintering of various dies. The plot is normalized on a per pellet basis. This means that the power output for the eight

pellet die was divided by eight so the power requirement on a per pellet basis is shown. The double die appears to have the lowest power requirement per pellet. This was not expected but may be somewhat skewed. The surface area to volume ratio of the four and eight pellet dies is smaller than for the single and double dies. This normally implies that the heating should be more efficient.

The SPS process is different due to the heating mechanism and the graphite felt insulation. First the insulation is only on the die exterior, not on the top and bottom of the die and not on the punches. The surface area of the punches for the four and eight pellet dies are four times as large as for the single and double dies. This implies a larger loss of radiative heat. Additionally, they have a much larger cross sectional area that radiates heat from the top and bottom of the die. This may be a root cause of those dies seemingly being less efficient that the double die. Finally the heating mechanism must be considered. The different cross sectional area and length of the dies will have an effect on current and temperature gradients in the tooling. This is visually proven due to the single and double die clearly showing the localized over heating problem in their punches. Those punches, two in total, get heat and glow a bright red, maybe even a full on white glow. This does not occur with the four and eight pellet die. Those pellets stay relatively dark for the entire run. This is due to the current density in the punches.

Figure 7-8 shows the displacement profiles for the various dies. The most obvious aspect of this figure is the relative displacement. The four and eight pellet dies experience less pressure during the startup. This is due to their punches having a larger cross sectional area to absorb the holding force of the machine. This leads to the enormous displacement of the eight pellet die. The four and eight pellet dies are

basically the same but with the eight pellet die having twice the magnitude. The single and double die behave differently. The double die has a very low displacement. This is due to two reasons. First the powder is loaded into this die and compacted so it fits. It is compacted tighter than for the single die so it presumably has a higher green density. Additionally, the double die follows the trend of the single die but plateaus quicker. This may be due to the central insert not gliding. If the insert gets jammed, the powder consolidation changes.

Figure 7-9 shows the temperature profiles for the single, four and large (19) dies. These were chosen to compare with the large die because they have all pellets in a single plane without stacking, so trends may be more visible without the complication of the pellets stacking. The large die barely reached its desired temperature of 1150 C. This was because the machine was at its capacity in terms of current. The die could not be heated any faster. From the plot it appears that a heating rate of 100 C/min was attainable until about 1000 C, at which time the radiative heat loss must have become too great. At this point the large die drifted down to a heating rate of about 50 C/min.

Figure 7-10 shows the electrical power profiles for the single, quad and large die, normalized on a per pellet basis. As shown, there doesn't appear to be any efficiency gained in the power requirements for the larger dies. This continues the trend from Figure 7-8. Expanding the die radius and adding cavities did not make the dies more efficient. This may be due to the same reasons stated above, namely a lack of insulation causing a large amount of radiative heat loss (Figure 7-4). The punches radiated a large amount of heat. Insulation could be added to the top and bottom surface of the die, but adding insulation to the punches may not be possible.

Figure 7-11 shows the voltage profile for the single, four pellet and large die. The voltage profile of the large dies differs from the other two dies. That voltage profile rises slower but stays high. This is because energy was constantly needed to keep the die hot. It was harder to achieve the desired heating rate so there was never an overheating that needed to be corrected by the machine.

Figure 7-12 shows the displacement profiles for the single quad and large dies. As shown, the large die never truly levels off. In fact it is still densifying even when the powder is cut. This is primarily due to the lack of pressure. The lack of pressure both required a greater amount of densification due to lower green density and would require greater densification rates to achieve full density or conventional sintering times (12 hours). Since the densification did level off, it is implied that temperature was not the driving force behind the low density pellets. This experiment should be repeated with added pressure.

7.4 Conclusions

The batch processing of pellets was partially successful, but did provide valuable information for further investigation. When producing eight pellets via parallel and series production, the success rate was 50%. This is most likely due to increased die wall friction, along with uneven temperature and pressure gradients in the die compacts, in addition to a limited power supply currently available in the SPS facility. Producing pellets in parallel will require a higher temperature and/or higher pressure to achieve full density. Application of pressure through the sintering process is suggested. This may require a novel approach to pressure application. Ensuring pressure is evenly applied to all powder compacts is not straight forward. Expanding dies radially did not lead to

more efficient use of power. This may be due to exaggerated radiative heat loss. The pellets made through the parallel production were lower in density but this is primarily due to pressure application.

Stacking pellets in series led to pellets of lower density. The pellets also were produced with a wide range of densities (standard deviation of over 2.0%). These results show that there are non-uniform temperatures and/or pressures within the die. The displacement curve for the double die showed a leveling off of densification before the single die. This may be due to the insert getting stuck. The double die did provide the greatest power benefit. This was counterproductive due to having a large surface area to volume ratio; however, the double die also has the greatest percentage of surface area covered by insulation. This implies the insulation and maybe not the double die is the cause of this efficiency. Further investigation should be conducted before the stacking production of pellets would be successful.

The large scale proof of concept showed many of the difficulties with scaling up the SPS process. The addition of so many punches (38 vs 2 for the single die) reduced any efficiency gains in power usage. The number of pellets made applying pressure complicated. Even if a single punch was out of alignment, massive pressures would destroy that punch. For this reason, no pressure was applied and the pellets could not densify. This experiment did show that the DR. Sinter SPS 1030 could heat this large die to 1100 C at 100C/min. It is theorized the full temperature of 1050 C or 1150C could be attained with the desired heating rate with added thermal insulation. The ability to fabricate full density pellets with this setup have yet to be proven.

Table 7-1. Statistics of pellets produced as stacked doubles

Pellet	Density % TD	Length (mm)	Diameter (mm)
Goal	96.5 ± 2.0	10.16 ± 1.27	8.1915 ± 0.0254
1	90.4	10.77	8.1940 ± 0.0038
2	97.0	9.93	8.1991 ± 0.0030
3	96.7	9.98	8.1966 ± 0.0064
4	95.4	10.11	8.2042 ± 0.0053
5	97.4	9.75	8.2017 ± 0.0043
6	96.4	9.50	8.2093 ± 0.0053
7	96.7	9.83	8.2017 ± 0.0038
8	91.8	10.34	8.1915 ± 0.0053
9	96.4	9.83	8.2042 ± 0.0038
10	96.7	9.53	8.1686 ± 0.0064
11	95.2	9.91	8.1940 ± 0.0124
12	93.0	10.16	8.1966 ± 0.0038
Avg	95.3 ± 2.3	9.98 ± 0.34	8.1964 ± 0.0069

Table 7-2. Density and dimensions of parallel produced pellets

Pellet	Density (% TD)	Length (mm)	Diameter (mm)
Goal	**96.5 ± 2.0**	**10.16 ± 1.27**	**8.1915 ± 0.0254**
1	93.8	10.35	8.1737 ± 0.0067
2	92.0	10.50	8.1670 ± 0.0039
3	94.0	10.21	8.1763 ± 0.0025
4	94.4	10.12	8.1763 ± 0.0044
Average	**93.5 ± 1.1**	**10.30 ± 0.17**	**8.1733 ± 0.0044**

Table 7-3. Pellets produced by combining series and parallel setup

Pellet	Density % TD	Length (mm)	Diameter (mm)
Goal	**96.5 ± 2.0**	**10.16 ± 1.27**	**8.1915 ± 0.0254**
1	92.6	10.35	8.1686 ± 0.0067
2	93.3	10.27	8.1678 ± 0.0059
3	95.3	10.01	8.1890 ±0.0025
4	95.6	9.96	8.1873 ± 0.0015
5	95.6	9.95	8.1830 ± 0.0053
6	94.5	10.03	8.1932 ± 0.0039
7	94.2	10.08	8.1890 ± 0.0051
8	94.7	10.07	8.1898 ± 0.0082
Average	**94.5 ± 1.1**	**10.09 ± 0.14**	**8.1835 ± 0.0049**

Table 7-4. Pellets produced by 19 pellet die

PELLET AREA	AVERAGE DENSITY
INTERIOR	63.1
MIDDLE	63.5
EXTERIOR	63.8
WHOLE	63.7

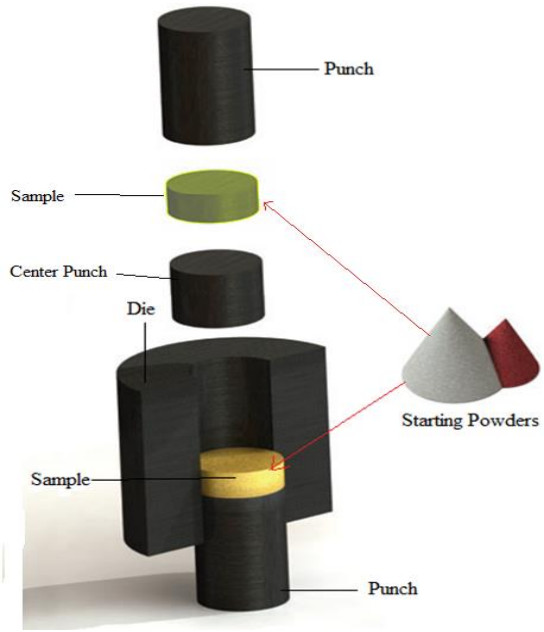

Figure 7-1. Schematic showing stacking powder samples in two pellet die

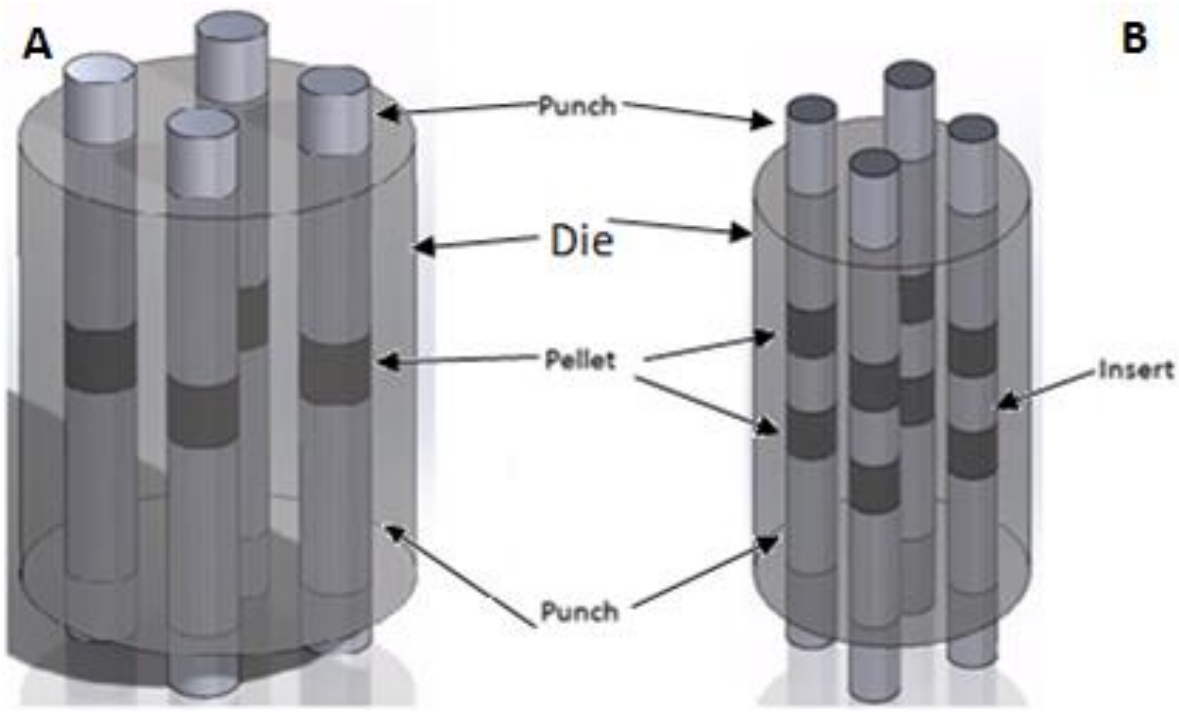

Figure 7-2. Schematic of the die geometry used to fabricate multiple pellets. A) Four pellet die. B) Eight pellet die.

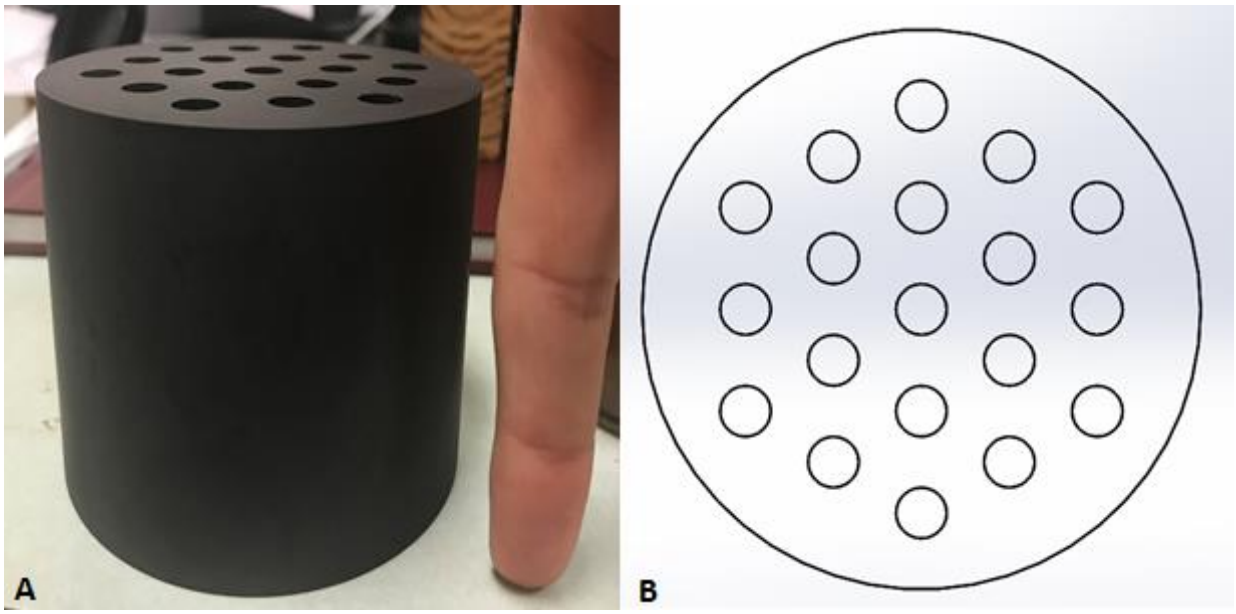

Figure 7-3. Die used to fabricate 19 pellets. A) Photograph B) Schematic. Photo courtesy of the author.

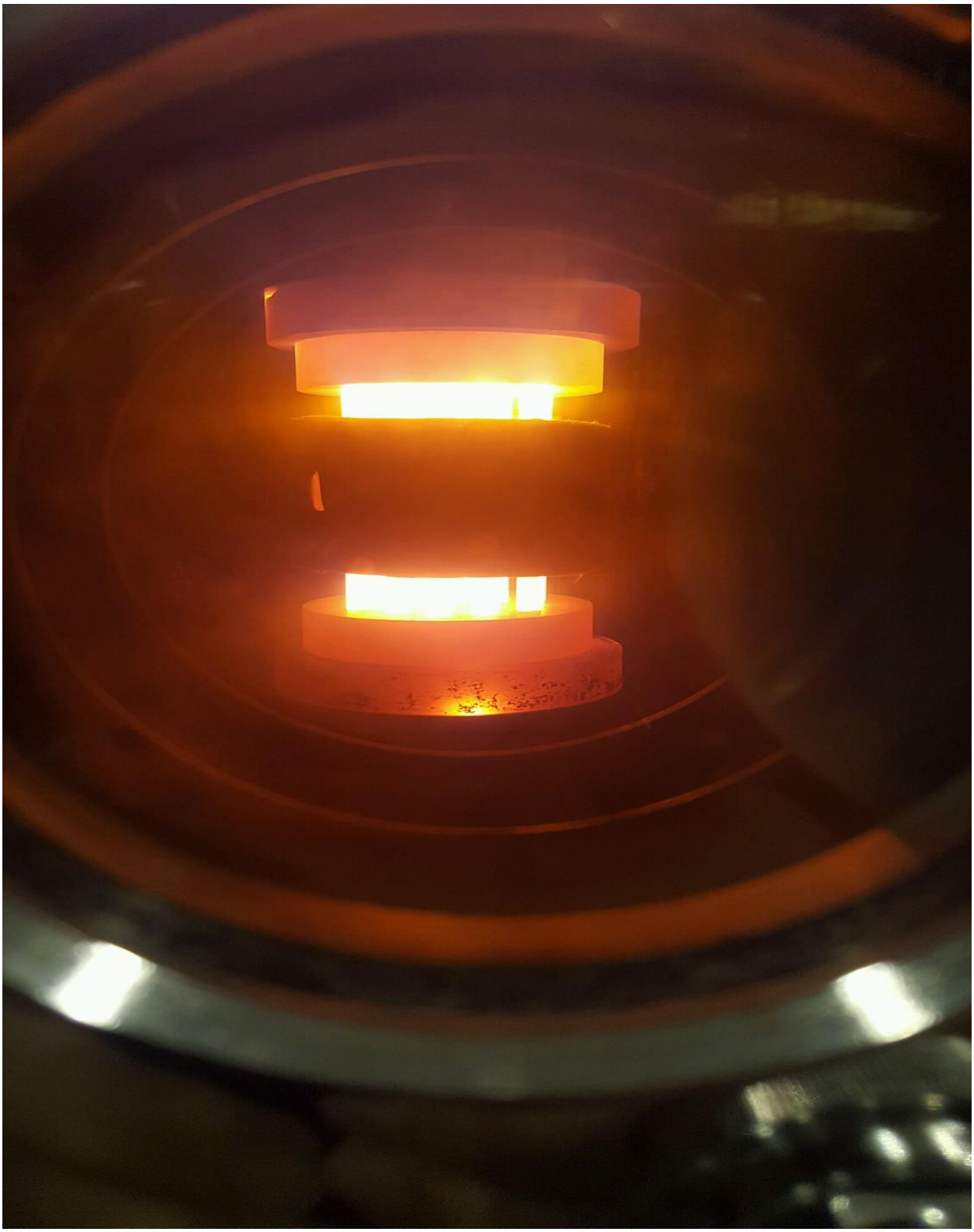

Figure 7-4. Sintering of 19 pellet die showing localized overheating of punches. Photo courtesy of the author.

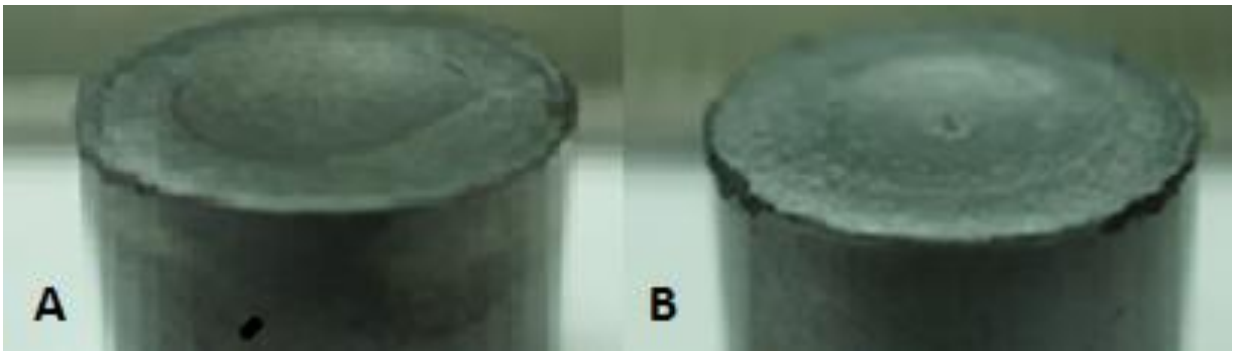

Figure 7-5. Stacked pellets as fabricated. A) Pellet edge in contact with punch showing some deformation. B) Pellet edge in contact with insert showing clear dish. Photo courtesy of the author.

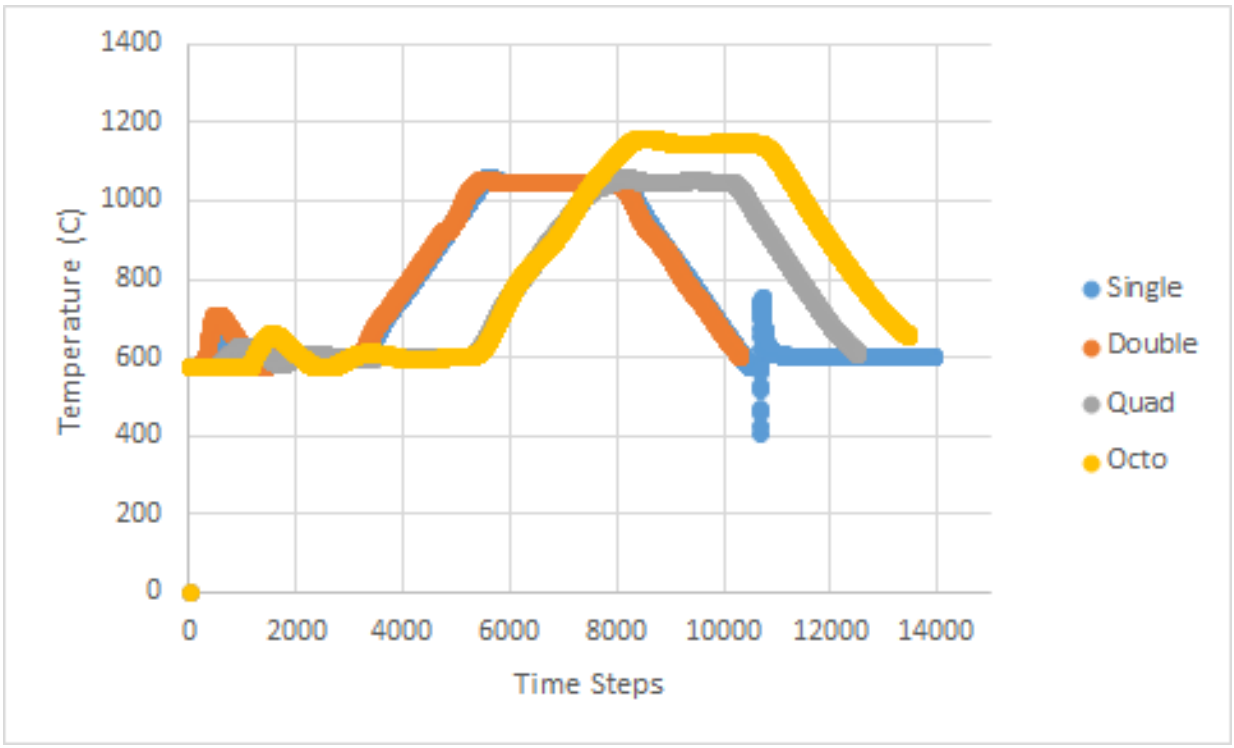

Figure 7-6. Temperature profiles for dies fabricating one (single), two (double), 4 (quad), and 8 (Octo) pellets.

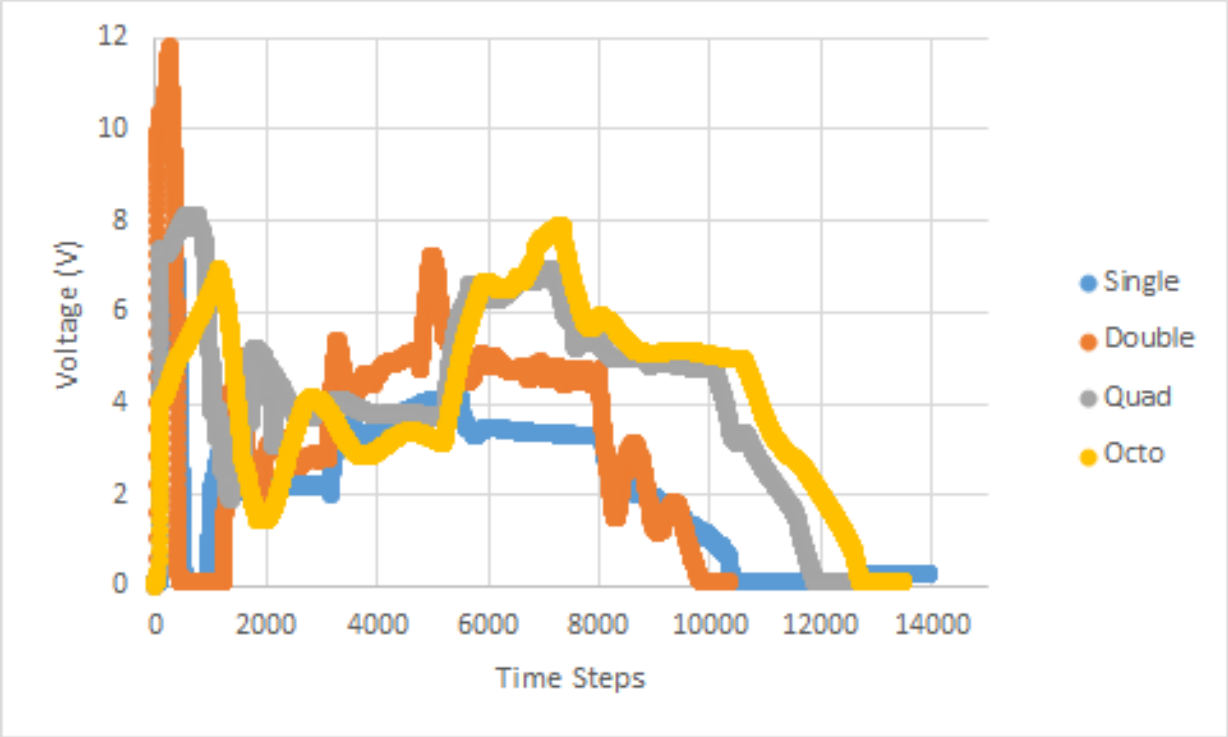

Figure 7-7. Voltage profiles for dies fabricating one (single), two (double), 4 (quad), and 8 (Octo) pellets.

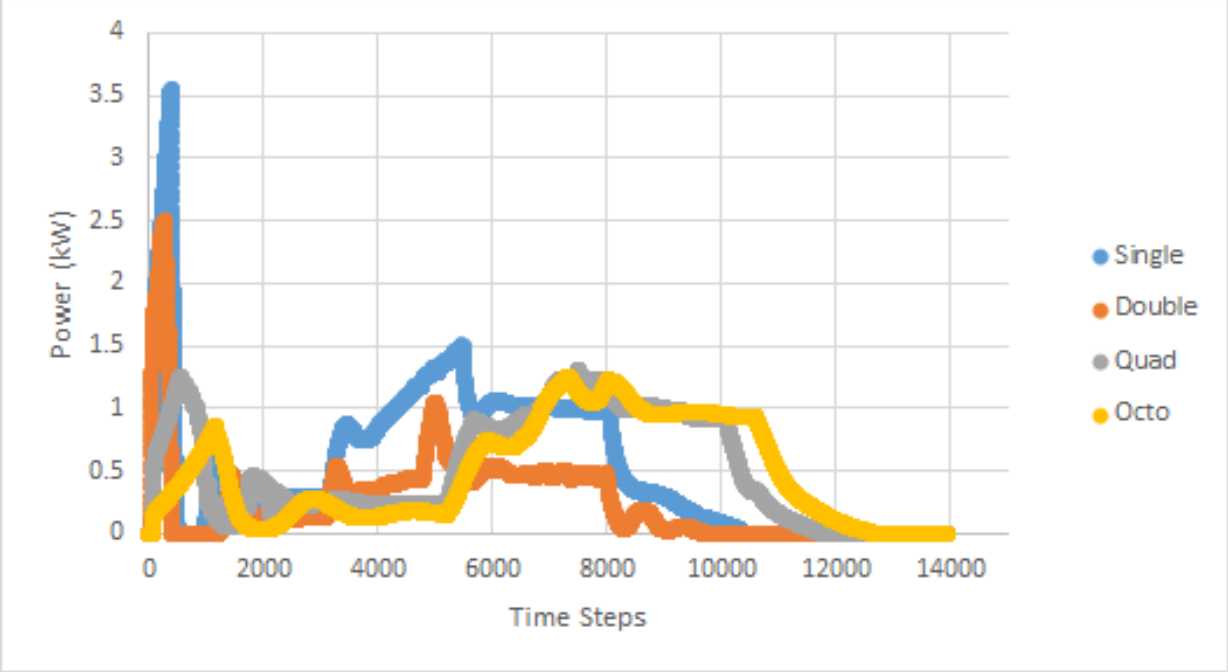

Figure 7-8. Electrical power profiles for dies fabricating one (single), two (double), 4 (quad), and 8 (Octo) pellets.

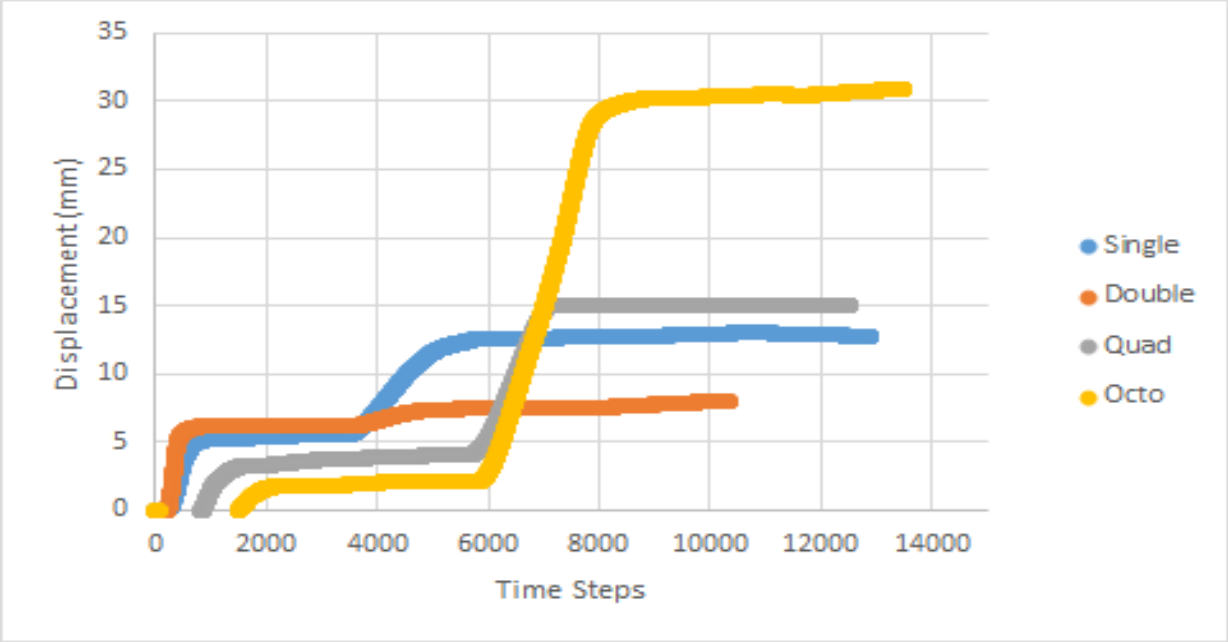

Figure 7-9. Z-axis displacement profiles for dies fabricating one (single), two (double), 4 (quad), and 8 (Octo) pellets.

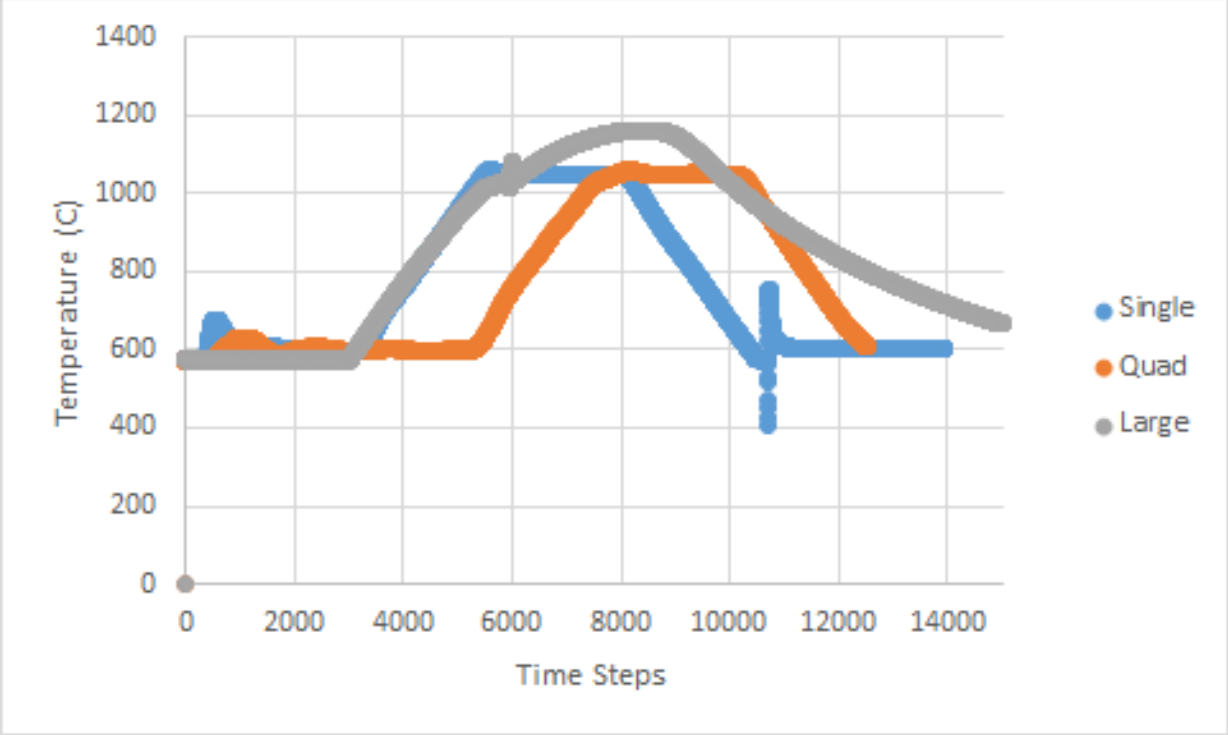

Figure 7-10. Temperature profiles for dies fabricating one (single), 4 (quad), and 19 (Large) pellets.

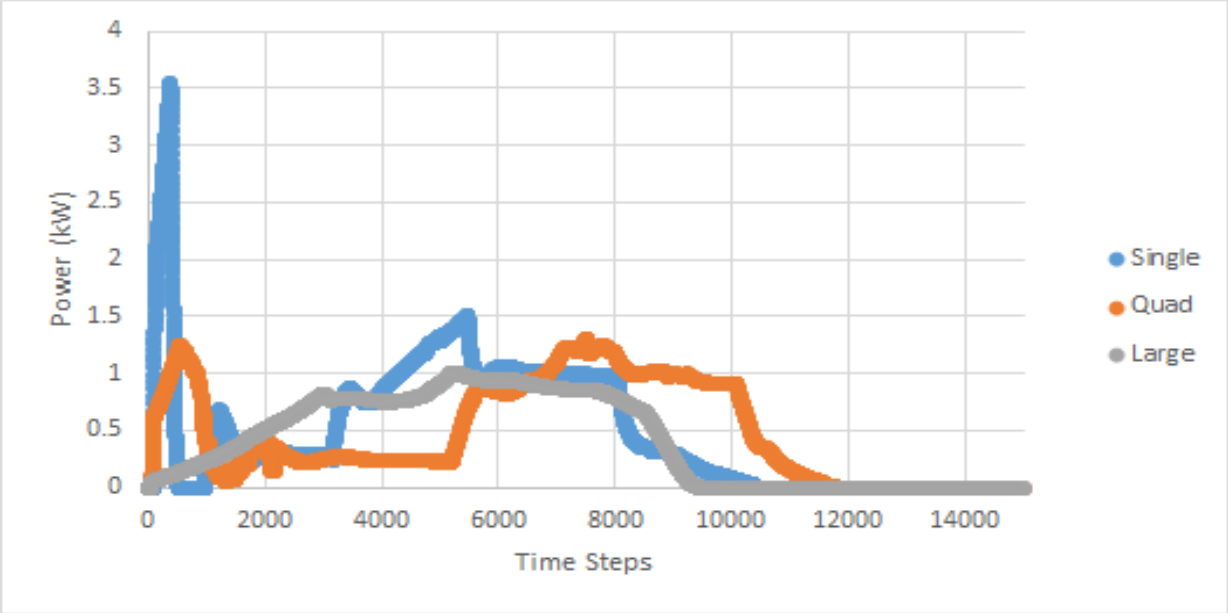

Figure 7-11. Electrical power profiles for dies fabricating one (single), 4 (quad), and 19 (Large) pellets.

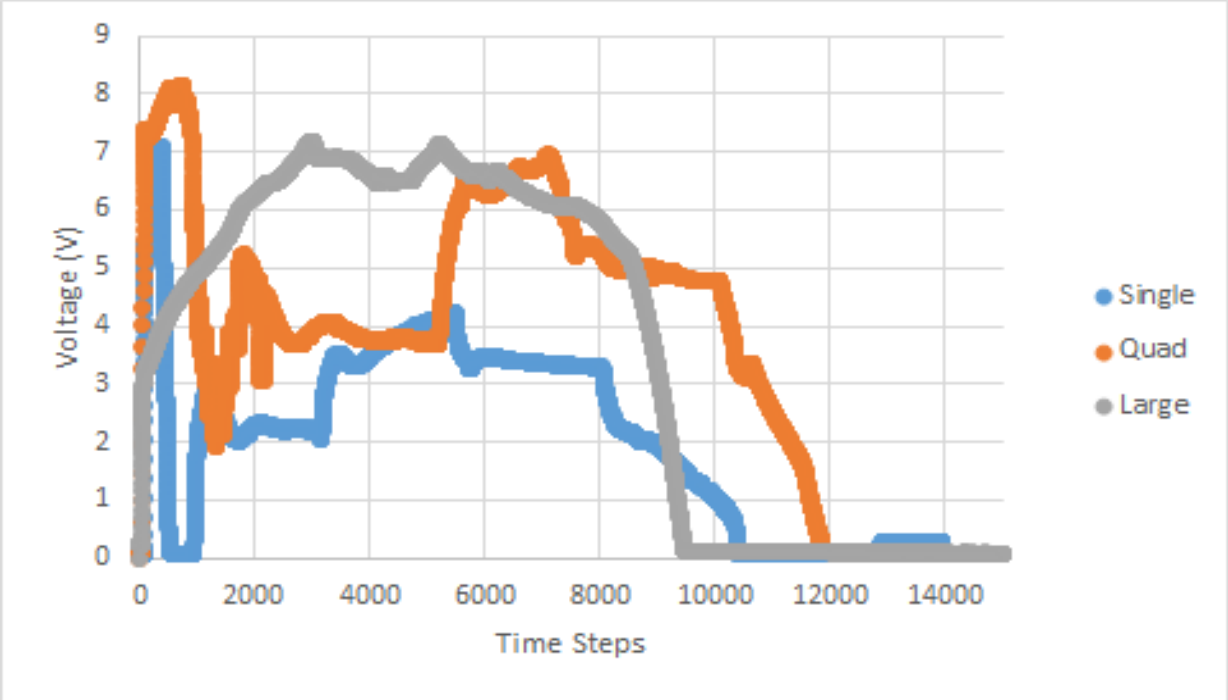

Figure 7-12. Voltage profiles for dies fabricating one (single), 4 (quad), and 19 (Large) pellets.

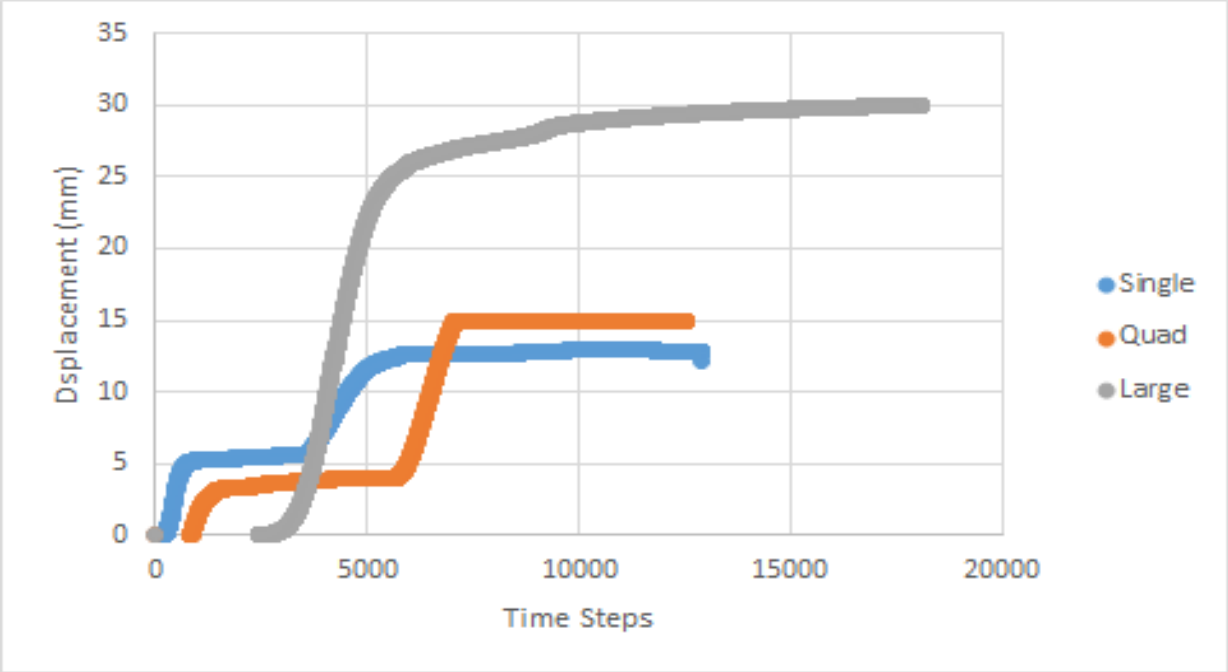

Figure 7-13. Z-axis displacement profiles for dies fabricating one (single), 4 (quad), and 19 (large) pellets.

CHAPTER 8
ATR PELLET PRODUCTION

8.1 Introduction

All lessons learned from the above studies were incorporated into another proof of concept pellet fabrication. In this production cycle, pellets would be produced for insertion into the Advanced Test Reactor at Idaho National Lab. This study was a partnership with Areva to place 4 pellet types into the ATR and irradiate them. In the future, post-irradiation examinations will be performed on the fuel to determine the reliability of the fuel, but for this particular work, the fabrication of the pellets is the only concern. The four pellet types produced were pure depleted UO_2 pellets labeled Blankets, pure enriched UO2 pellets labeled Base, 10% by volume SiC (w)/UO_2 pellets labeled SiC (w), and 10% by volume diamond/ UO_2 pellets labeled “Dia”. The composite pellets and the Base pellets used 4.95% enriched powder. These pellets must strictly pass all requirements previously stated. In addition, to prove fabrication of multiple pellets could be accomplished and to save time, all pellets were initially fabricated in the stacked arrangements explained earlier. This arrangement fabricates two samples per run. All other procedures are discussed below. Throughout the production cycle, all procedures were continuously reevaluated.

The ATR pellet production’s final goal was to irradiate six rodlets; two rodlets being Base pellets, two of Dia, and two of SiC (w). The rodlets were a stack of ten pellets. Each rodlet had a Blanket pellet on the top and bottom of the rodlet leaving the other eight pellets as Base, Dia, and SiC. This requires 16 Base pellets, 16 Dia pellets, 16 SiC pellets and 12 Blanket pellets. Areva wanted to keep a few extra pellets for

further testing and archive. It was decided that 20 pellets of each type would be fabricated. A total of 80 pellets should take 40 sintering runs during optimal conditions.

8.2 Experimental Procedures

The depleted UO_2 powder was the same powder used in the experiments earlier and was obtained through AREVA. The powder had a bulk density of 2.3 g/cm^3, a mean diameter of 2.4 µm, and a starting U/M ratio of 2.11. The powder was depleted UO_2 with an enrichment of less than 0.71%. The raw powder was stored at room temperature and pressure for period of time of over one year after being obtained from AREVA.

The 4.95% enriched UO2 powder was supplied by Areva Fuels. It contained trace amount of U-234. The U/M ratio was 2.038. The powder is straight off the Areva fuel fabrication line and was labeled “standard un-prepped dry conversion calcined UO_2” powder. The bulk density was 1.65 g/cc. No surface area or other metrological information was provided by Areva.

The SiC whiskers used in these experiments was obtained from Advanced Composite Materials, Inc. The whiskers had an average length of 11 µm, an average diameter of 0.65 µm, an aspect ratio of 15:1, and were reported to be greater than 98% pure. The whiskers were found to have trace amounts of Carbon (0.1 wt %) and SiO_2 (0.43 wt %). The diamond particles used were purchased from Advanced Abrasives Corporation. The particles were single crystals with a reported average diameter of 3 µm and a standard deviation of 0.475 µm.

The constituent powders were mixed through the use of a vibrational ball mill acting as a mixer. Powder batches totaling 20 grams were produced by loading raw UO_2 powder and the requisite additive powder into a zirconia vial; a mixing aid,

decafluoropentane, was also added to enhance facilitate mixing. Deca is a stable organic compound that does not react with UO_2, SiC or diamond. Additionally, Deca evaporates quickly at room temperature. Powders were mixed to attain a 10 % by volume fraction of the additive. The SiC/UO_2 mixture contained 19.37 grams of UO_2 and 0.69 grams of SiC. The diamond/UO_2 mixture contained 19.31 grams of UO_2 and 0.63 grams of diamond particles. The zirconia vial was then sealed via a rubber O-ring and a generous amount of electrical tape. The SiC and UO_2 were mixed in the mill for 60 minutes. Three steel balls were added to the UO_2/SiC mix to break up SiC agglomerates. The diamond and UO_2 powders were mixed for 180 minutes. Steel balls were not used to mix the diamond. After mixing, the mixed powders were removed and placed in paper cups and dried in a dry keeper from 24 hours.

The loading process was more strictly controlled to ensure no enriched UO_2 was lost. The mass of powder required was measured. The powder was loaded into the die using the glass funnel, as needed. The loading was performed over a tray to catch any spills. Next, the powder was compressed with the other punch, using moderate hand pressure. After loading the first powder mass, a clean steel punch was run through the die to remove any residual powder from the die wall. A cold press with the steel punch was to compact the first powder mass. Then, the insert was sprayed with graphite spray and added to the die. The mass of powder required to produce a second pellet was weighed and loaded into the die using the glass funnel, as needed. The cold press and metal punch was used to compact the second powder mass. The second punch was then inserted and the punch/ die compact was secured with electrical tape. The loaded dies were then transported for sintering.

Pellets were sintered according to the parameters listed in Table 8-1. Initial Base and Blanket pellets were sintered at 1050 C for 5 minutes with an applied pressure of 40 MPa. Dia and SiC (w) pellets were sintered at 1400 C for 5 minutes. Dia pellets had an applied pressure of 40 MPa while SiC had an applied pressure of 60 MPa. After sintering was completed, all pellets went through the rigorous pellet qualification plan as previously outlined. These parameters changed after preliminary pellets were fabricated.

The goal of the study was to produce at least 16 acceptable pellets of each pellet type. While each pellet was characterized, pellets were continuously fabricated until 20 acceptable pellets were produced or the required powder ran out. The study was continuously altered and these alterations are discussed below.

8.3 Results and Discussion

The Blanket pellets were the first pellets fabricated. The first pellet run was a disaster. The pellets were not loaded correctly and led to both pellets failing all tests. Additionally pellet 2 was lost before it could be characterized. Pellets 3-28 were fabricated in a more streamline process once the researchers mastered the loading process. 26 pellets were fabricated before it was determined that sufficient supply was attained. These pellets are described in Table 8-2. 18 of the 26 pellets passed the qualification tests. Three pellets were fabricated with a density of under 93%. These pellets were also longer than the rest. It is believed that the graphite insert failed to freely move during sintering of these pellets. In that case, one of the pellets does not receive pressure during the hold and fails to fully densify. Two pellets achieved high density but had surface flaws, which were deemed to be due to poor tooling maintenance. An additional three pellets fracture immediately upon removal from the die

and could not be characterized. Excluding pellets 1 and 2, which were associated with obvious human errors, the success rate was 70%.

The BASE pellets were undoubtedly less successful. Initial pellets fabricated via stacking produced pellets around 90% TD. Additionally, the loading process was judged to be too difficult and too much powder was being lost. This was acceptable for depleted UO2 but not for special nuclear material. For these reasons, the stacking setup was scraped and pellets were fabricated as singles. This decision also included all composite pellets. Fabricating Base pellets in the single pellet setup still did not initially produce high density pellets. Pellets were achieving only 92-93% TD. It appeared that the enrich powder sintered differently from the depleted powder. So for the rest of the study, the temperature was increased to 1100 C from 1050 C for BASE pellets. This worked out much better.

Twenty-four Base pellets were produced at 1100 C in the single pellets setup. They are described in Table 8-3. Twenty of the twenty-four pellets based all qualification testing. The four pellets that failed all failed for structural integrity issues. Pellets 15 and 23 had issues with the punch end reacting with the pellet. Pellet 1 and 16 had significant chipping. The average density of the BASE pellets was 96.7 % TD. This density is typical of depleted UO2 pellets but the Base pellets were sintered at 1100 C instead of 1050 C. Some property of the powder led to a required temperature increase of 50 C. No characterization studies were performed on the enriched powder at UF due to its status as special nuclear material. The Base pellets success rate was 83 %.

The 31 diamond pellets produced are described in Table 8-4. Of the 31 diamond pellets, only 15 passed pellet qualification for a success rate of 48%. The common

thread with the diamond pellets was a failure to reach the 94.5% minimum density. Ten pellets failed to reach this minimum. This ran counter to previous experiment with diamond mixed with depleted UO_2 powder. The enriched UO_2 powder was more difficult to sinter. The cause of this difficulty is unknown. After pellet 12, it was determined to start using graphite foil in attempt to get higher densities. This worked a small amount. The average density of the twelve pellets without foil was 93.8%. The average density of the 16 pellets with graphite foil was 94.9%. There were three pellet failures with the foil due to foil inclusions into the pellet exterior.

The SiC pellets were worse than the diamond pellets. The SiC pellets are described in Table 8-5. Twenty-eight pellets were produced but only nine passed pellet qualification. SiC pellets repeatedly could not achieve high density even though the graphite foil was used to produce all of them. The final eight pellets used an increased sintering temperature of 1450 C. This led to dense pellets but the punches became single use and many pellets require significant post processing to remove graphite from the dish. The average density of the first twenty pellets was 93.1%. The average density of the last eight pellets was 96.1% TD.

8.4 Conclusions

Previous work on depleted UO_2 powder did not match up with results on the enriched powder. Elementally these powders are indistinguishable. The isotopic difference should not have any effect on the sintering of the powder. The only clear difference is the M/M ratio. The depleted powder had a U/M ratio of 2.11; whereas, the enriched powder had a U/M ratio of 2.038. It is unknown if this would make such a large difference. In conventional sintering, hyperstoichiometric UO_2 sinters easier than 2.00

UO_2. Many fuel fabricators add U3O8 to their fuel to improve sinterability. There may be some morphological differences. The sintering process is highly dependent on the shape, contact and surface features of the powder particles. More invasive characterization of both powders should be performed in the future. This may actually be beneficial. Further powder processing may be able to reduce sintering temperatures in the future.

The loading process for stacking pellets proved to be very difficult in a more industrial setting. Automating that process would help, but a method to guarantee the insert glides freely must be uncovered. A process of pre-pressing the powder may prevent powder from falling in between the insert and the die wall; thus, allowing the insert to move freely. Conventional sintering uses cold pressing paired with sintering. The effect of pre-pressing the powder before insertion into the SPS furnace should be investigated.

Table 8-1. Planned ATR pellet sintering parameters.

Pellet Type	Peak Temperature	Pressure
Blanket	1050 C	40 MPa
Base	1050 C	40 MPa
Dia	1400 C	40 MPa
SiC	1400 C	60 MPa

Table 8-2. ATR Blanket pellet results

Pellet #	Diameter (in)	Length (in)	Mass (g)	Density (%TD)	D&C (Pass/Fail)
1					no insp
3	0.3226	0.424	5.5675	90.4	P
4	0.3228	0.391	5.5172	97.0	P
5	0.3227	0.393	5.5349	96.7	P
6	0.3230	0.398	5.5417	95.4	F
7	3.3223	0.384	5.4507	97.4	P
8	0.3231	0.374	5.2662	96.4	P
9	0.3229	0.387	5.4502	96.7	P
10	0.3225	0.407	5.4316	91.8	P
11	0.3229	0.387	5.4329	96.4	P
12	0.3224	0.375	5.2446	96.7	P
13	0.3223	0.390	5.3990	95.2	P
14	0.3227	0.403	5.4599	93.0	P
15					no insp
16					no insp
17	0.3230	0.384	5.4467	97.3	P
18	0.3221	0.386	5.3746	96.9	P
19	0.3226	0.383	5.4366	97.6	P
20	0.3231	0.384	5.4401	97.1	P
21	0.3224	0.398	5.6135	97.1	P
22	0.3221	0.384	5.4280	97.4	P
23					no insp
24	0.3233	0.388	5.5162	97.3	P
25	0.3231	0.386	5.4558	96.9	P
26	0.3230	0.385	5.4565	97.2	P
27	0.3235	0.377	5.3829	97.4	F
28	0.3222	0.380	5.3551	97.1	P

Table 8-3. ATR Base pellet results

Pellet #	Diameter (in)	Length (in)	Mass (g)	Density (%TD)	D&C (Pass/Fail)
BE01			5.4046		no insp
BE02	0.3226	0.391	5.4629	96.2	P
BE03	0.3232	0.386	5.4527	96.7	P
BE04	0.3233	0.383	5.4396	97.1	P
BE05	0.3231	0.380	5.4462	97.1	P
BE06	0.3227	0.386	5.4389	96.9	P
BE07	0.3228	0.385	5.4495	97.1	P
BE08	0.3229	0.388	5.4493	96.5	P
BE09	0.3229	0.386	5.4562	97.1	P
BE10	0.3231	0.382	5.3966	96.9	P
BE11	0.3231	0.382	5.4065	96.9	P
BE12			5.4290		no insp
BE13	0.3226	0.390	5.4439	96.0	P
BE14			5.4800		F
BE15	0.3230	0.385	5.4188	96.4	P
BE16	0.3230	0.388	5.4685	96.6	P
BE17			5.2522		P
BE18	0.3231	0.388	5.4370	96.0	P
BE19	0.3226	0.344	4.8309	96.4	P
BE20	0.3225	0.382	5.3922	97.1	P
BE21	0.3227	0.386	5.4477	97.1	P
BE22	0.3230	0.386	5.4702	97.1	P
BE23	0.3225	0.385	5.4173	96.9	P
BE24	0.3230	0.390	5.4585	96.1	P

Table 8-4. ATR Diamond pellet results

Pellet #	Diameter (in)	Length (in)	Mass (g)	Density (%TD)	D&C (Pass/Fail)
1	0.3230	0.389	5.014	94.7	P
2	0.3234	0.393	4.9634	92.7	P
3	0.3229	0.385	4.9261	94.1	P
4			4.7335		no insp
5	0.3218	0.407	5.1626	94.1	P
6	0.3226	0.396	5.1372	95.5	P
7	0.3232	0.399	5.14	94.7	P
8	0.3234	0.401	5.1987	95.1	P
9	0.3230	0.400	5.1591	94.8	P
10	0.3227	0.405	5.1217	93.1	P
11	0.3233	0.409	5.0841	91.2	P
12	0.3231	0.404	5.0886	92.5	P
13	0.3203	0.388	5.003	96.3	P
14	0.3221	0.385	4.9703	95.6	P
15	0.3222	0.385	4.9007	94.2	P
16			5.0391		no insp
17	0.3234	0.385	5.015	95.6	P
18	0.3222	0.388	4.9929	95.1	P
19	0.3223	0.385	5.0113	96.1	P
20	0.3234	0.391	5.1256	96.1	P
21	0.3223	0.392	5.0634	95.3	P
22	0.3229	0.386	4.8735	93.0	P
23			5.1069		no insp
24	0.3227	0.376	4.8417	94.9	P
25	0.3225	0.402	5.0309	92.4	P
26	0.3224	0.386	4.9399	94.4	P
27	0.3229	0.379	4.9082	95.3	P
28	0.3231	0.384	4.9774	95.4	P
29	0.3195	0.372	4.6768	94.6	no insp
30	0.3228	0.375	4.8445	95.2	P
31	0.3218	0.380	4.8325	94.2	no insp

Table 8-5. ATR SiC pellet results

Pellet #	Diameter (in)	Length (in)	Mass (g)	Density (%TD)	D&C (Pass/Fail)
1	0.3212	0.401	4.9881	92.7	P
2	0.3227	0.401	4.9922	92.0	P
3	0.3207	0.404	4.9769	92.2	P
4	0.3209	0.388	4.8369	93.0	P
5	0.3218	0.388	4.9899	95.7	P
6	0.3226	0.401	5.0256	92.6	P
7	0.3226	0.384	4.9530	95.4	P
8	0.3220	0.395	5.0625	95.1	P
9	0.3279	0.403	5.0999	90.7	P
10	0.3227	0.396	5.0720	94.6	P
11	0.3213	0.392	5.0315	95.6	P
12	0.3226	0.395	5.0413	94.3	P
13	0.3212	0.400	4.9250	91.8	P
14	0.3231	0.409	5.1347	92.4	P
15	0.3222	0.398	5.0158	93.5	P
16	0.3231	0.404	5.0774	92.7	P
17	0.3240	0.400	4.9994	91.6	P
18	0.3228	0.403	5.0563	92.6	P
19	0.3211	0.406	4.9887	91.6	P
20	0.3225	0.392	4.9014	92.4	P
21	0.3234	0.379	4.9683	96.5	P
22	0.3232	0.373	4.8889	96.5	P
23	0.3231	0.377	4.9371	96.7	P
24	0.3183	0.380	4.6631	93.2	P
25	0.3230	0.365	4.7662	96.4	P
26	0.3231	0.365	4.7873	96.6	P
27	0.3225	0.370	4.8102	96.3	P
28	0.3223	0.365	4.7427	96.2	P

CHAPTER 9
ECONOMIC CONSIDERATIONS

9.1 Introduction

The commercial fabrication of pure UO2 pellets has been optimized over the past sixty years. As previously stated, the process includes producing the UO2 powder from feedstock, forming dense pellets from UO2 the powder, and loading pellets into a fuel assembly made up of long, thin fuel rods. The SPS process only affects the middle step: forming dense UO2 pellets from the powder. To form pellets from the UO2 powder, a four step process is applied. The first step is conditioning the UO2 powder for pressing and firing by adding lubricants, pore formers and other additives. The second step is pressing the conditioned powder into pellet form with a high pressure press. These pressed pellets are called green pellets. The third step involves firing the green pellets into fully dense pellets through heating them through a series of furnaces. In the fourth step, the fully dense pellets are post-processed via centerless grinding to ensure pellets meet the dimensional requirements. The SPS process can interrupt all four of these of these steps with as few as a single step: step 3.

The SPS process intrinsically is simply the firing process. A powder is heated and forms a dense compact. In SPS, the pressing process can be incorporated into the firing process. Pellets do not need to undergo centerless grinding due to the pellets consolidating into tighter dimensional ranges. Additionally, if optimized, post-processing can be drastically reduced or even eliminated. Finally, all work done during this study used unconditioned powder, so that step could hypothetically be removed as well. It has been theorized that conditioning the powder would still be useful. The experiments with enriched UO2 powder showed that powder behaved differently than the depleted

UO2. It is expected that processing the powder before sintering would improve the product but is not strictly necessary.

The major economic consideration of SPS is the costs associated with firing. These costs can be further broken up into capital costs and production costs. Capital costs are the cost of the SPS furnaces and associated equipment. Since all major fuel fabricators have large factories already, it is not expected that any capital costs except for the new furnaces are required. The production costs include the energy required to power the SPS furnaces, the tooling used in the SPS process, and personnel and maintenance costs. These are the focus of this study.

It is not expected that SPS would provide a financial incentive over conventional sintering of commercial grade UO2. This is primarily due to the long history of optimizing the conventional sintering process, the capital costs already spent and the associated technical expertise the industry has acquired. During these studies, UO2 was used as a base material because it has been the standard material used in the nuclear fuel industry. Any future material sintered via SPS may have its own unique characteristics, but the general process is not expected to change much.

9.2 Capital Costs

There are a variety of larger scale SPS furnaces available on the market currently. The largest available standard SPS machine from FUJI is a machine with a capacity of 45,000 amps and 6,000 kN. The cost of this machine, off the shelf, is $3 million. This machine (Figure 9-1) is very similar to the Dr. Sinter 1030 located at UF. Any high volume manufacturing would require the tunnel type system (Figure 9-2). The tunnel systems are all custom made but a single line with the large furnace shown in

Figure 9-2 would cost around $5 million. This is for a single furnace, along with a loading and pre-heating stage and a cooling chamber. This system would load dies with an automated system. Such as system would heat the powder to a prescribed temperature conventionally, then send the compact to the SPS furnace. After firing in the SPS furnace, the compact is immediately sent to the cooling chamber to cool naturally. This would make the time the compact is in the SPS furnace about 10 minutes. The SPS furnace would be the bottle neck in this process.

The Dr. Sinter 1030 here at UF has a maximum capacity of 3000 amps. This much larger furnace is capable of driving 45,000 amps through a die or series of dies. Taking this scaling factor and assuming that requisite insulation could ensure the die could maintain the require temperature, 285 pellets could be sintered in this large furnace in a single run. This number may be increased with a different set up. It is not suggested to have a single die of 285 pellets but a series of dies either stacked or in parallel. But with 285 pellets sintered in ten minutes, a single machine would have a production rate of 1710 pellets per hour. To achieve the industry required 45000 pellets per hour, 27 machines would be needed. Assuming some of these machines may require maintenance, 30 running SPS furnaces would meet this requirement. 30 furnaces would cost $150 million. There could be added efficiency in the cooling chamber setup or the loading setup. Since the SPS furnace is the limiting step, perhaps only one loading line or one cooling chamber would be required for every two to four furnaces. Even with the best case scenario, this is a capital cost of $100 million under ideal conditions.

While it is unclear if the capacity of a single machine could be increased beyond 285 pellets, there was some indication of such possibilities in the earlier work. The ceramic punch tips seemed to cut the energy requirements of a single pellet in half. Also the added thermal insulation may make a higher capacity possible; however, these efficiencies may just make each furnace require less energy but not increased pellet capacity. This all assumes that all the pellets are pure UO2 and will meet specifications. The ceramic composite pellets require a higher temperature, thus each machine would have a lower capacity. This may not be a drastic effect depending on the pre-processing of the composite powder and the actual sintering conditions. Then again the added temperature could reduce the capacity by as much as two-fold leading to a capital cost of $300 million. Any even more exotic material, would obviously change the capacity of each furnace.

There are newer hybrid heating systems being built. These systems use an external heating source in addition to joule heating via the electrical current. No work has been performed on UO2 for these systems, so it is not known if these would produce the same products.

9.3 Production Costs

The production costs associated with SPS fabrication have two main costs: materials costs and tooling costs. The materials costs are the costs of the powder materials being sintered. This may be limited to just raw UO2 power as currently produced in all fuel fabrication plants or may include additives such as burnable poisons, pore formers and any other desired additions. UO2 is comparatively cheap.

This is one advantage of the SP process, in that it does not require any pre-processing of powder. Pre-processing may be desirable but it is unnecessary. SPS will not replace conventional sintering for the production of the current UO2 fuel. The industry is too far ahead in terms of both optimizing the process and capital investment. Since, any future commercial use of SPS for the fuel industry would be for a composite material of exotic material not yet used, predicting the materials costs is just guesswork.

The tooling cost for this work was the major expense. Custom machined graphite punches cost about $50 each. Standard dies cost about $100 each. The large 19 pellet die cost about $500. The major cost for these tools were paying a machinist to custom produce the punch tips. These prices are obvious high and unsustainable if tooling is constantly replaced. If you take into account the fact that during composite pellet production, typically punches were single use or at best use twice, it cost between 100 and 200 dollars to make single composite pellet. Commercial pellet production is on the order of hundreds of dollars per kilogram of UO2. That's over 200 times more expensive to make a composite pellet than a commercial UO2 pellet conventionally.

The most obvious cost savings would be from improved materials. The YSZ punch tips were custom made and very expensive. The YSZ punch tips cost $500 per pair of punch tips. But these punch tips did not wear out. They could be reused many times. Of course purchasing something like that in commercial quantities would be vastly cheaper. YZS can be purchased for under $100 per kilogram. Punch tips weigh 1-2 grams. YSZ is certainly less expensive than B4C, although B4C may eventually prove to be more desirable. The conventional process is not foreign to these types of materials. A tungsten carbide punch tip is used during the pressing of conventional

pellets. The major cost for all these materials is the machining or forming them with the desired pellet end geometry. A cost reduction to $25 per pair seems conservative. This would still require flat UO2 punches but those are cheaper and last through multiple runs. The major tooling consideration would then be the wear of the die which depends on whatever barrier is used between the powder and the die body. Buying multiple dies provides a large price reduction.

The 19 pellet die cost about $500 but it was custom made. This too could be acquired in bulk possibly for as low as $50. The estimate cost of a whole compact, a 19 pellet die, 38 flat graphite punches and 19 YSZ pairs of punch is about $500. These punches and dies could conservatively survive 20 fabrication runs. That would make the tooling cost $25 per run or about $1 per pellet. One kilogram of UO2 is about 200 pellets. So the tooling costs alone, in this highly speculative case, already approach the current cost of UO2.

The other production cost is the actual electricity requirements. Scaling electrical requirements is also quite difficult to do with any certainty. For the 19 pellet die, 0.11 kWh per pellet was required. Compared to fabricating a single pellet which required 0.22 kWh to sinter. These numbers are skewed because they only include certain parts of the heating cycle, namely the rise from 600C and the hold at the peak temperature. Also the 19 pellet die could be insulated better which reduce these requirements. If the preloading stage heated the powder to 600 C, this part could be skip and the SPS furnace would only be heating the powder up from 600 C and holding at peak temperature. A reduction in required power to 0.05 kWh per pellet is not out of the question. At the current rate of $0.12 per kWh, the electrical cost would be $1.20 per

kilogram of UO2. This appears to be much smaller than the potential tooling costs of the SPS process. This is not unexpected since one of the overall benefits of SPS should be increased efficiency.

9.4 Conclusions

The economics of large scale SPS production are highly speculative. A complete large scale proof of concept is required to show the maximum number of pellets that can be fabricated with the largest available furnace. The trend implied by this research would be around 285 pellets in a 45,000 amp machine. Further optimization of materials and tooling structure may be able to drive that number closer to 500 pellets. These optimizations would be highly dependent on the material being sintered. A large production line with a single SPS furnace costs around $5 million. The actual automation of loading pellet quantity powder into dies has not been achieved currently. If the die remained in s ingle or possibly a double layer of pellets, the automation would be trivial.

The largest cost uncertainty is in the tooling costs. Since no set of tooling meets all the requirements of the nuclear industry yet, this would be determined by the specific material system. Separating as many part s as possible seems like an efficient idea. Punch tips could be replaced without replacing the punch body. The current costs of nuclear grade powder are well known but punch and die costs are not. Producing commercial quantities of the tooling is not currently available but the materials are not so foreign as to inhibit the possible of SPS for commercial production. B4C is the only material that would be difficult to acquire and this is only due to the pellet end geometry requirement. Most of these tooling concerns would be greatly minimized if flat pellets

could be produced. Stacking of flat pellets would be much simpler than optimized pellets. Any future material that did not require such a detailed geometry would be a better candidate for the use of SPS.

The power requirements are also highly speculative. An electricity cost of $1.00 per kilogram of UO2 is proposed. This may be higher or lower an order of magnitude depending on the specific requirements.

Figure 9-1. Dr. Fuji Dr. Sinter largest standard furnace with a capacity of 45000 amps and 6000kN. Reproduced with permission from FUJI ELECTRONIC INDUSTRIAL CO., LTD. (Kawasaka, Japan, 2010).

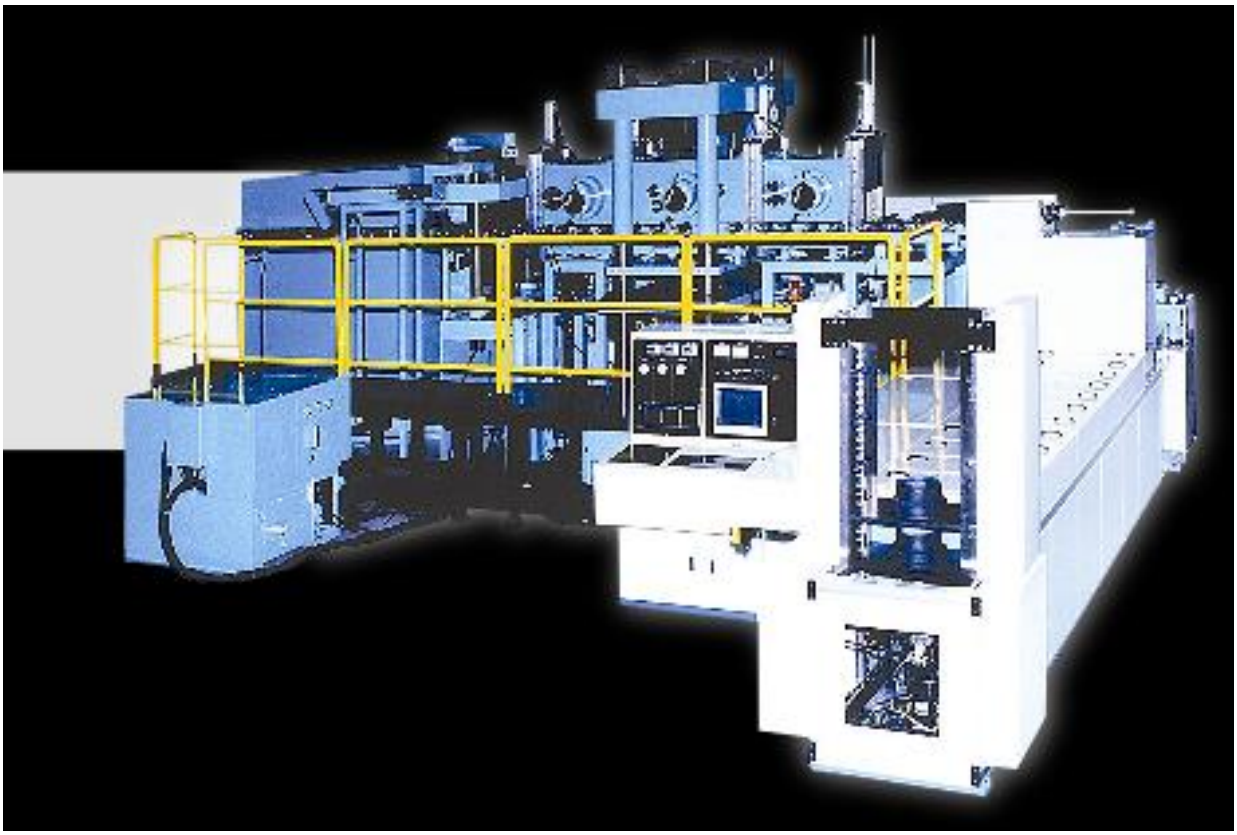

Figure 9-2. Dr. Fuji Dr. Sinter example tunnel furnace with pre-sintering and cooling areas. Reproduced with permission from FUJI ELECTRONIC INDUSTRIAL CO., LTD. (Kawasaka, Japan, 2010).

CHAPTER 10
CONCLUSIONS AND FUTURE WORK

While the feasibility of SPS for production of commercial grade fuel pellets has been shown, further improvements must be made for scale-up to manufacture 400 million of pellets per year, which is about to ~45,000 pellets/hour for 24 hour operation. It is also essential to further explore new die-design configurations and materials to accommodate thousands of pellets in each run.

New tooling materials must be developed to ensure that the dies can be used without unacceptable wear. While graphite is the material of choice based on electrical properties, its wear properties have been found to be insufficient to meet the rigorous industrial demands. YSZ and B4C both show some promise as punch tip replacements. These new materials show that other materials can be integrated into the established graphite tooling to achieve more desirable results. These materials should also be tested with the composite materials to determine if more desirable results can be achieved.

The composite pellets proved more difficult than pure UO2. This is primarily due to the higher sintering temperatures required, along with the incapability of graphite tooling at these elevated temperatures. The pellets can still be fabricated and were produced at a level high enough to be accepted for entry into the ATR. The further scaling of composite pellet fabrication requires new materials in contact with the powder. B4C or YSZ may make this possible.

Finally, to further assess the economic viability, a larger scale proof-of-concept should be explored to determine the maximum number of pellets that can be successfully produced within a single run. An example was performed showing

temperature could be achieved with a 19 pellet die in the Dr. Sinter 1030. These pellets were of poor density but the electrical and thermal aspects of the process were successful. Further scaling requires optimized pressure application and further finite element work to determine thermal and electrical gradients within the SPS compact.

REFERENCES

1. Carbajo, Juan J., et al., "A review of the thermophysical properties of MOX and UO 2 fuels." *Journal of Nuclear Materials* 299.3 (2001): 181-198.

2. Crossland, Ian, ed. *Nuclear fuel cycle science and engineering*. Elsevier, 2012.

3. Arborelius, Jakob, et al., "Advanced doped UO2 pellets in LWR applications." *Journal of Nuclear Science and Technology* 43.9 (2006): 967-976.

4. Ge, Lihao, "Processing of uranium dioxide nuclear fuel pellets using spark plasma sintering." (2014).

5. Yeo, S., et al., "Enhanced thermal conductivity of uranium dioxide–silicon carbide composite fuel pellets prepared by Spark Plasma Sintering (SPS)." *Journal of Nuclear Materials* 433.1 (2013): 66-73.

6. Chen, Zhichao, et al., "Spark plasma sintering of diamond-reinforced uranium dioxide composite fuel pellets." *Nuclear Engineering and Design* 294 (2015): 52-59.

7. Cartas, Andrew R, "An evaluation of UO2-CNT composites made by SPS as an accident tolerant nuclear fuel pellet and the feasibility of SPS as an economical fabrication process for the nuclear fuel cycle." (2014).

8. Cochran R, Tsoulfanidis N. The Nuclear Fuel Cycle: Analysis and Management. La Grange Park, Ill. : American Nuclear Society, 1999.; 1999.

9. Carter, Ralph E. "Process for preparing sintered uranium dioxide nuclear fuel." U.S. Patent No. 3,927,154. 16 Dec. 1975.

10. Munir, Z. A., et al., "The effect of electric field and pressure on the synthesis and consolidation of materials: a review of the spark plasma sintering method." *Journal of Materials Science* 41.3 (2006): 763-777.

11. Tokita, Masao, "Industrial applications of advanced spark plasma sintering." *American Ceramic Society Bulletin* 85.2 (2006): 32-34.

12. Z. A. Munir, D. V. Quach, M. Ohyanagi, in *Sintering: Mechanisms of Convention Nanodensification and Field Assisted Processes* (Eds: R. Castro, K. van Benthem), Springer, Berlin/Heidelberg 2012, pp. 137–158, Ch. 7.

13. T. Mizuguchi, S. Guo, Y. Kagawa, *Ceram. Int.* 2010, **36**, 943.

14. A. Krell, T. Hutzler, J. Klimke, *J. Eur. Ceram. Soc.* 2009, **29**, 207.

15. Y. Kodera, C. L. Hardin, J. E. Garay, *Scr. Mater.* 2013, **69**, 149.

16. N. Frage, S. Kalabukhov, N. Sverdlov, V. Kasiyan, A. Rothman, M. P. Dariel, *Ceram. Int.*2012, **38**, 5513.

17. G. Spina, G. Bonnefont, P. Palmero, G. Fantozzi, J. Chevalier, L. Montanaro, *J. Eur. Ceram. Soc.* 2012, **32**, 2957.

18. E. H. Perilla, Y. Kodera, J. E. Garay, *Mater. Sci. Eng. B* 2012, **177**, 1178.

19. H. Zhang, B. N. Kim, K. Morita, H. Yoshida, K. Hiraga, Y. Sakka, *J. Am. Ceram. Soc.* 2011, **94**, 3206.

20. R. Chaim, Z. Shen, M. Nygren, *J. Mater. Res.* 2004, **19**, 2527.

21. K. Morita, B. N. Kim, H. Yoshida, K. Hiraga, *J. Am. Ceram. Soc.* 2009, **92**, 1208.

22. G. Bonnefont, G. Fantozzi, S. Trombert, L. Bonneau, *Ceram. Int.* 2012, **38**, 131.

23. U. Anselmi-Tamburini, G. Spinolo, F. Maglia, I. Tredici, T. B. Holland, A. K. Mukherjee, in *Sintering: Mechanisms of Convention Nanodensification and Field Assisted Processes* (Eds: R. Castro, K. van Benthem), Springer, Berlin/Heidelberg 2012, pp. 159–193, Ch. 8.

24. Olevsky, Eugene A., et al. "Fundamental aspects of spark plasma sintering: II. Finite element analysis of scalability." *Journal of the American Ceramic Society* 95.8 (2012): 2414-2422.

25. Guillon, Olivier, et al. "Field-assisted sintering technology/spark plasma sintering: mechanisms, materials, and technology developments." *Advanced Engineering Materials* 16.7 (2014): 830-849.

26. A. Becker, S. Angst, A. Schmitz, M. Engenhorst, J. Stoetzel, D. Gautam, H. Wiggers, D. E. Wolf, G. Schierning, R. Schmechel, *Appl. Phys. Lett.* 2012, **101**, 013113

27. Fang, Zhigang Zak, ed. *Sintering of Advanced Materials*. Elsevier, 2010.

28. M. Beekman, M. Baitinger, H. Borrmann, W. Schnelle, K. Meier, G. S. Nolas, Y. Grin, *J. Am. Chem. Soc.*2009, **131**, 9642.

29. Angerer, P., et al. "Residual stress of ruthenium powder samples compacted by spark-plasma-sintering (SPS) determined by X-ray diffraction." *International Journal of Refractory Metals and Hard Materials* 27.1 (2009): 105-110.

30. Chen, Zhichao, et al., "Master sintering curves for UO 2 and UO 2–SiC composite processed by spark plasma sintering." *Journal of Nuclear Materials* 454.1 (2014): 427-433.

31. Wangle, T., et al., "Simulated UO 2 fuel containing CsI by spark plasma sintering." *Journal of Nuclear Materials* 466 (2015): 150-153.
32. O'Brien, R. C., and N. D. Jerred. "Spark Plasma Sintering of W–UO 2 cermets." *Journal of Nuclear Materials* 433.1 (2013): 50-54.

33. Johnson, Kyle D., et al. "Spark plasma sintering and porosity studies of uranium nitride." *Journal of Nuclear Materials* 473 (2016): 13-17.

34. Hennecke JFA, Scherff HL: Carbon monoxide equilibrium pressures and phase relations during the carbothermic reduction of uranium dioxide. *Journal of Nuclear Materials* 1971, 38(3):285-291.

35. Biasetto L, Zanonato P, Carturan S, Bernardo PD, Colombo P, Andrighetto A, Prete G: Developing uranium dicarbide–graphite porous materials for the SPES project. *Journal of Nuclear Materials* 2010, 404(1):68-76.

36. Gossé S, Guéneau C, Alpettaz T, Chatain S, Chatillon C, Le Guyadec F: Kinetic study of the UO2/C interaction by high-temperature mass spectrometry. *Nuclear Engineering and Design* 2008, 238(11):2866-2876.

37. Carvajal Nuñez U, Martel L, Prieur D, Lopez Honorato E, Eloirdi R, Farnan I, Vitova T, Somers J: Coupling XRD, EXAFS, and 13C NMR to Study the Effect of the Carbon Stoichiometry on the Local Structure of UC1±x. *Inorganic Chemistry* 2013, 52(19):11669-11676.

38. Gossé S, Guéneau C, Chatillon C, Chatain S: Critical review of carbon monoxide pressure measurements in the uranium–carbon–oxygen ternary system. *Journal of Nuclear Materials* 2006, 352(1–3):13-21.

39. Giuntini, Diletta, et al. "Localized overheating phenomena and optimization of spark-plasma sintering tooling design." *Materials*6.7 (2013): 2612-2632.

40. Wei, Xialu, et al. "Experimental investigation of electric contact resistance in spark plasma sintering tooling setup."*Journal of the American Ceramic Society* 98.11 (2015): 3553-3560.

41. ASTM E112-13 Standard Test Methods for Determining Average Grain Size, ASTM International, West Conshohocken, PA, 2013

42. Standard Specification for Sintered Uranium Dioxide Pellets, ASTM C776-06 (2006).

43. Bijan Nili, et al., "Coupled Electro-Thermo-Mechanical Simulation for Multiple Pellet Fabrication using Spark Plasma Sintering" Journal of Manufacturing Science and Engineering (submitted, 2017)

BIOGRAPHICAL SKETCH

Timothy Ironman, born 1986, received his B.S. (2009) and M.Eng (2010) degrees in materials science and engineering from Cornell University. Timothy's research focusing on nuclear fuels advanced manufacturing and advanced materials. In the fall of 2017, he received his doctorate in nuclear engineering sciences under the guidance of Professor James Tulenko. He is the son of Paul and Felicia Ironman. He has an older sister, Kerrie and an older brother, Sean.